AD-A081 531 NIELSEN ENGINEERING AND RESEARCH INC MOUNTAIN VIEW CALIF F/G 20/4
DEVELOPMENT OF PERTURBATION PROCEDURES FOR NONLINEAR INVISCID A--ETC(U)
JAN 80 D NIXON F49620-79-C-0054
UNCLASSIFIED NEAR-TR-214 AFOSR-TR-80-0129 NL

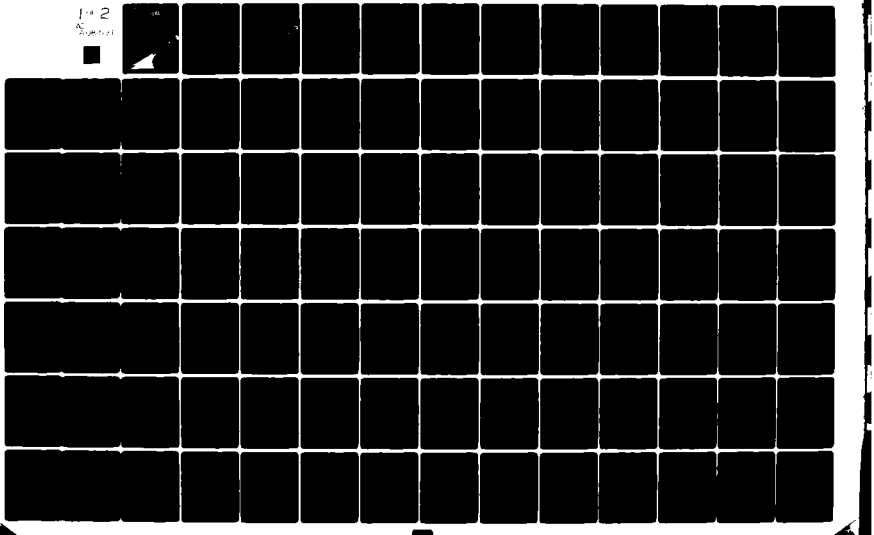

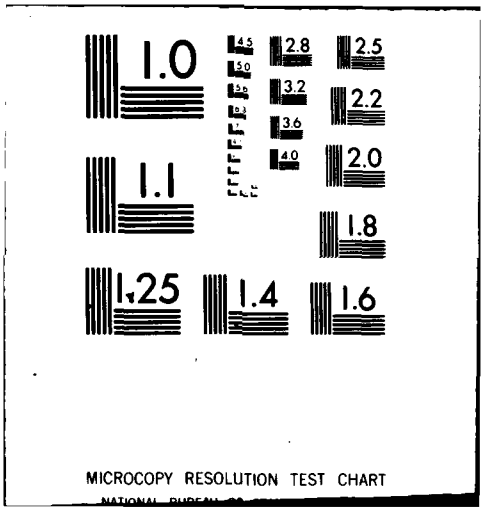
1.0
1.1
1.25
1.4
1.6
1.8
2.0
2.2
2.5
2.8
3.2
3.6
4.0
4.5
5.0
MICROCOPY RESOLUTION TEST CHART

AFOSR-TR- 80-0129

LEVEL II

5

AD A081531

DTIC
ELECTE
MAR 5 1980
S D
C

DDC FILE COPY

80 3 3 010

Approved for public release;
distribution unlimited.

NIELSEN ENGINEERING
AND RESEARCH, INC.

OFFICES: 510 CLYDE AVENUE / MOUNTAIN VIEW, CALIFORNIA 94043 / TELEPHONE (415) 968-9457

UNCLASSIFIED
SECURITY CLASSIFICATION OF THIS PAGE (When Data Entered)

ADA081531

REPORT DOCUMENTATION PAGE		READ INSTRUCTIONS BEFORE COMPLETING FORM
1. REPORT NUMBER **AFOSR-TR- 80-0129**	2. GOVT ACCESSION NO.	3. RECIPIENT'S CATALOG NUMBER
4. TITLE (and Subtitle) DEVELOPMENT OF PERTURBATION PROCEDURES FOR NONLINEAR INVISCID AND VISCOUS FLOWS		5. TYPE OF REPORT & PERIOD COVERED INTERIM 01 Apr 79-30 Sep 79 6. PERFORMING ORG. REPORT NUMBER NEAR TR 214
7. AUTHOR(s) DAVID NIXON		8. CONTRACT OR GRANT NUMBER(s) F49620-79-C-0054
9. PERFORMING ORGANIZATION NAME AND ADDRESS NIELSEN ENGINEERING & RESEARCH, INC. 510 CLYDE AVENUE MOUNTAIN VIEW, CALIFORNIA 94043		10. PROGRAM ELEMENT, PROJECT, TASK AREA & WORK UNIT NUMBERS 61102F 2307A1
11. CONTROLLING OFFICE NAME AND ADDRESS AIR FORCE OFFICE OF SCIENTIFIC RESEARCH/NA BLDG 410 BOLLING AIR FORCE BASE, D C 20332		12. REPORT DATE JANUARY 1980 13. NUMBER OF PAGES 103
14. MONITORING AGENCY NAME & ADDRESS(if different from Controlling Office)		15. SECURITY CLASS. (of this report) UNCLASSIFIED 15a. DECLASSIFICATION/DOWNGRADING SCHEDULE

16. DISTRIBUTION STATEMENT (of this Report)

Approved for public release; distribution unlimited.

17. DISTRIBUTION STATEMENT (of the abstract entered in Block 20, if different from Report)

18. SUPPLEMENTARY NOTES

19. KEY WORDS (Continue on reverse side if necessary and identify by block number)

TRANSONIC FLOW
PERTURBATION METHODS

20. ABSTRACT (Continue on reverse side if necessary and identify by block number)

The perturbation theory for transonic flow is further developed for two and three dimensional problems. The physical perturbation theory, in which the perturbation parameter is a physical quantity, is applied to solutions of the Navier-Stokes equations in two dimensions. The mathematical perturbation theory, in which the perturbation parameter is a measure of the difference between approximate and exact solutions, is applied both to the three dimensional potential flow problems and to the two dimensional Navier Stokes equations. The strained coordinate technique is used to treat changes in location of any shock

DD FORM 1473

Unclassified

TECHNICAL REPORT

DEVELOPMENT OF PERTURBATION PROCEDURES FOR NONLINEAR INVISCID AND VISCOUS FLOWS

by

David Nixon

NEAR-TR-214
January 1980

Prepared under Contract No. F49620-79-C-0054

for

AIR FORCE OFFICE OF SCIENTIFIC RESEARCH
Bolling Air Force Base
Washington, DC 20332

by

NIELSEN ENGINEERING & RESEARCH, INC.
510 Clyde Avenue, Mountain View, CA 94043
Telephone (415) 968-9457

TABLE OF CONTENTS

1

DEVELOPMENT OF PERTURBATION PROCEDURES FOR NONLINEAR INVISCID AND VISCOUS FLOWS

by David Nixon

ABSTRACT

The perturbation theory for transonic flow is further developed for two and three dimensional problems. The physical perturbation theory, in which the perturbation parameter is a physical quantity, is applied to solutions of the Navier-Stokes equations in two dimensions. The mathematical perturbation theory, in which the perturbation parameter is a measure of the difference between approximate and exact solutions, is applied both to the three-dimensional potential flow problems and to the two-dimensional Navier-Stokes equations. The strained coordinate technique is used to treat changes in location of any shock waves or large gradients.

1. INTRODUCTION

A series of papers recently published (refs. 1, 2, and 3) concern the development of a perturbation method for transonic flow problems. A basic problem in transonic flow perturbations is the treatment of possible movement of discontinuities (shock waves) which can make the perturbation invalid. A means of solving this problem, using a strained coordinate method, has been derived (ref. 1). The location of the discontinuities in this strained coordinate system remain the same throughout the perturbation, leading to a final linear perturbation equation for the perturbed unknowns. The final solution is not linear because of the transformation from the strained coordinate system to the physical coordinate system. However, since the perturbation equation is linear, the principle of superposition can be

used, and the effect of several different types of perturbations can be easily, and inexpensively, estimated.

The most common application (ref. 2) of the method has been concerned with extrapolating transonic flow solutions. For example, given two transonic flow solutions for the same airfoil and Mach number, but at two different angles of attack, then the pressure distribution for any other angle of attack can be found by simple proportion and the use of the strained coordinate transformation. Applications of this technique to two-dimensional, multi-parameter flow solutions and to three-dimensional, multi-shock problems are reported in references 1 and 2. These examples are concerned with the physical perturbation quantities, such as angle of attack, profile geometry changes, etc.

More recently the concept of "mathematical perturbations" has been discussed (ref. 3) in which the perturbation quantities characterize the difference between solutions of a subset of the full potential equation, namely the transonic small-disturbance (or TSD equation), and the potential equation itself. The results of this type of perturbation solution indicate that such a general type of correction for various subsets of equations is feasible.

For the present work the perturbation theory is concerned with solutions of the Navier-Stokes equations. In particular, three specific problems are investigated. In two dimensions the application of the physical perturbation theory to the Navier-Stokes equations is investigated. Also the application of the mathematical theory to solutions of the transonic small-disturbance theory and the Navier-Stokes equations are considered. The extension of the mathematical perturbation theory to three-dimensional flow is also considered. In all cases the strained coordinate technique[1] is employed to treat shock waves or rapid gradients in the solutions.

First consider the physical perturbations of the Navier-Stokes equations. The first step in deriving a perturbation

equation is to write the governing equations and their associated boundary conditions in such a form that only the basic equations or the boundary conditions contain the perturbation parameter, otherwise the correct parameter to use may not be obvious. In the previous work for the TSD equation (ref. 2) the perturbation parameter is contained only in the boundary conditions. For the Navier-Stokes equations the perturbation parameter appears only in the set of equations, if these are written in a general body conforming curvilinear coordinate system and the variables non-dimensionalized with respect to free-st·eam quantities. Both attached flows and flows with shock induced separation are considered.

The basic physical principle behind the "physical" perturbation theory is that, relative to certain physical features of the problems, for example the geometric confines of the airfoil and the shock location, the physical processes throughout the perturbation are in some sense similar. For instance, if two solutions are known (the base and calibration solutions) and have shock induced separation then an interpolated solution will also have shock induced separation. Examples with attached flow and with separated flow are calculated with satisfactory results. However, in contrast to the earlier potential equation work[1,2], it is found in the present case that the base and calibration solutions should not be too close, otherwise numerical inaccuracies in the Navier-Stokes solution can dominate the perturbation quantities.

The second type of perturbation problem considered here is the mathematical perturbation correction technique. In the present case the basic aim is to correct transonic small-disturbance theory to give results typical of solutions of the Navier-Stokes equations. As described fully in reference 3, the idea is to determine a correction between the two types of equations by considering the numerical results for both equations for some case. This correction is then applied to the TSD solution of other near-by cases. A nearby case is assumed to mean an example

with a similar pressure distribution to the correction example. The basic assumptions behind this idea are, firstly, that a flow is characterized by its surface pressure distribution and, secondly, that those physical features modeled by the Navier-Stokes equations and not by the TSD equations (e.g., viscous effects) for the correction example are also present in the near-by cases. To a large extent the validity of the assumption is to be determined by numerical experiment.

A basic feature of all perturbation methods is that the perturbation variables and their derivatives are of the same order of magnitude. In the course of investigation of the correction technique it was found that the shock movement due to a change in some parameter, e.g., angle of attack, was much greater for the TSD equation than for either Navier-Stokes equations or the Euler equation. This is due to the larger shock strength associated with the TSD equation. Consequently an additional perturbation, within the confines of small-disturbance theory, is added such that the difference in shock strength between, say, the Euler and TSD equations is the same as for the correction case.

The third part of the present work is the extension of the mathematical perturbation correction technique (ref. 3) for inviscid three-dimensional flow. To a large extent this is a straightforward development of the work reported in reference 3. Both corrections for grid size, the use of the transonic small-disturbance equation, and a combination of both are investigated.

2. BASIC PRINCIPLES OF THE PERTURBATION THEORY

2.1 General Concepts

It is usually assumed in perturbation theory that the form of the perturbation parameter characterizing the disturbance is known or can be easily found. For example, in the earlier work

(refs. 1 and 2) on the perturbation theory, the transonic small-disturbance equation was written in an invariant form and the "natural" perturbation parameters were easily discernible from a study of the boundary conditions. An example of such a "natural" parameter is that, for changes in Mach number, M_∞, the parameter is

$$\Delta\left[\frac{M_\infty^2}{(1 - M_\infty^2)^{3/2}}\right]$$

where "Δ" denotes an increment. One problem that arose in previous work (ref. 4) was to determine the precise nature of a Mach number perturbation for the full potential equation, since this equation cannot be written in a Mach number invariant form. In practice, the small-disturbance perturbation parameter, given above, was used for Mach number variations.

In the present work, the strained coordinate perturbation theory is to be extended to treat the Navier-Stokes equations. It is unlikely that these equations can be written in a form independent of the freestream conditions and consequently, as in the case of the earlier full potential equation problems, the choice of the "natural" perturbation parameter for a perturbation in freestream quantities may not be obvious. Accordingly, it is proposed to write the Navier-Stokes equations in a form where the boundary conditions are invariant, and then examine the transformed equations to determine the correct choice of perturbation parameters. A further simplification is to use the thin-layer (ref. 5) approximation to the Navier-Stokes equations. This letter assumption is consistent, since these are the equivalent equations solved in most computer codes, whether explicitly coded or not.

The steady thin-layer Navier-Stokes equations for two dimensions can be written (ref. 6) in a general curvilinear coordinate system as

$$\frac{\partial E}{\partial \xi} + \frac{\partial F}{\partial \eta} = R_e^{-1} \frac{\partial S}{\partial \eta} \tag{1}$$

where R_e is the Reynolds number, (ξ,η) are the computational coordinates which are functions of Cartesian coordinates (x,y) with a transformation Jacobian J, given by

$$J = \xi_x \eta_y - \xi_y \eta_x = 1/(x_\xi y_\eta - x_\eta y_\xi) \tag{2}$$

The transformation metrics are given by

$$\begin{aligned} \xi_x &= J y_\eta & \eta_x &= -J y_\xi \\ \xi_y &= -J x_\eta & \eta_y &= J x_\xi \end{aligned} \tag{3}$$

The vectors E, F, S are defined as follows:

$$E = J^{-1} \begin{pmatrix} \rho U \\ \rho u U + \xi_x p \\ \rho v U + \xi_y p \\ (\rho e + p) U \end{pmatrix} \qquad F = \begin{pmatrix} \rho V \\ \rho u V + \eta_x p \\ \rho v V + \eta_y p \\ (\rho e + p) V \end{pmatrix} \tag{4}$$

and

$$S = J^{-1} \begin{pmatrix} 0 \\ \mu(\eta_x^2 + \eta_y^2) u_\eta + \frac{\mu}{3} \eta_x (\eta_x u_\eta + \eta_y v_\eta) \\ \mu(\eta_x^2 + \eta_y^2) v_\eta + \frac{\mu}{3} \eta_y (\eta_x u_\eta + \eta_y v_\eta) \\ \kappa P_r^{-1} (\gamma-1)^{-1} (\eta_x^2+\eta_y^2) \frac{\partial (a^2)}{\partial \eta} + \frac{\mu}{2} (\eta_x^2+\eta_x^2) (u^2+v^2)_\eta \\ \quad + \frac{\mu}{3} (\eta_x u + \eta_y v)(\eta_x u_\eta + \eta_y v_\eta) \end{pmatrix} \tag{5}$$

where U,V are contravariant velocities related to the Cartesian velocities u,v by

$$\begin{aligned} U &= \xi_x u + \xi_y v \\ V &= \eta_x u + \eta_y v \end{aligned} \tag{6}$$

ρ, p, e are the density, pressure and internal energy, respectively. P_r is the Prandtl number, κ is the conductivity, and a is the speed of sound of the gas. The pressure is related to e, ρ, u, v by

$$p = (\gamma-1)\ \rho e - \frac{1}{2}\rho(u^2 + v^2) \tag{7}$$

where γ is the ratio of specific heats.

The computational coordinates ξ,η are chosen such that the surface $\eta(x,y) = 0$ represents the body surface. The boundary conditions are the tangency and no-slip conditions and therefore,

$$\begin{aligned} V &= 0 \\ U &= 0 \qquad \text{on } \eta = 0 \end{aligned} \tag{8}$$

The far-field boundary conditions are that free-stream conditions, denoted by the subscript ∞, prevail.

If the reference quantities are taken to be free-stream conditions, then the basic equations, eq. (1), can be nondimensionalized to give

$$\frac{\partial \bar{E}}{\partial \xi} + \frac{\partial \bar{F}}{\partial \eta} = R_e^{-1}\ \frac{\partial \bar{S}}{\partial \eta} \tag{9}$$

where

$$E = J^{-1}\begin{pmatrix} \bar{\rho}\bar{U} \\ \bar{\rho}\bar{u}\bar{U} + \xi_x \bar{p}\ \dfrac{1}{\gamma M_\infty^2} \\ \bar{\rho}\bar{v}\bar{U} + \xi_y \bar{p}\ \dfrac{1}{\gamma M_\infty^2} \\ [\bar{\rho}\bar{e} + \bar{p}(\gamma-1)]\bar{U} \end{pmatrix} \tag{10a}$$

$$\bar{F} = \begin{pmatrix} \bar{\rho}\bar{V} \\ \bar{\rho}\bar{u}\bar{V} + \eta_x \bar{p}\,\frac{1}{\gamma M_\infty^2} \\ \bar{\rho}\bar{v}\bar{V} + \eta_y \bar{p}\,\frac{1}{\gamma M_\infty^2} \\ [\bar{\rho}\bar{e} + \bar{p}(\gamma-1)]\bar{V} \end{pmatrix} \tag{10b}$$

$$\bar{S} = J^{-1} \begin{pmatrix} 0 \\ \mu(\eta_x^2 + \eta_y^2)\bar{u}_\eta + \frac{\mu}{3}\eta_x(\eta_x \bar{u}_\eta + \eta_y \bar{v}_\eta) \\ \mu(\eta_x^2 + \eta_y^2)\bar{v}_\eta + \frac{\mu}{3}\eta_y(\eta_x \bar{u}_\eta + \eta_y \bar{v}_\eta) \\ \kappa P_r^{-1}\gamma(\eta_x^2 + \eta_y^2)\frac{\partial \bar{a}^2}{\partial \eta} + \frac{\mu}{2}\gamma(\gamma-1)M_\infty^2(\eta_x^2 + \eta_y^2)(\bar{u}^2 + \bar{v}^2)_\eta \\ \quad + \frac{\mu}{3}\gamma(\gamma-1)M_\infty^2(\eta_x \bar{u} + \eta_y \bar{v})(\eta_x \bar{u}_\eta + \eta_y \bar{v}_\eta) \end{pmatrix} \tag{10c}$$

where $\bar{u} = u/u_\infty$, $\bar{v} = v/u_\infty$, $\bar{V} = V/U_\infty$, $\bar{U} = U/U_\infty$, $\bar{\rho} = \rho/\rho_\infty$, $\bar{p} = p/p_\infty$, $\bar{e} = e/e_\infty$, $\bar{a} = a/a_\infty^2$, and use has been made of the perfect gas equation

$$p/\rho = RT$$

and the sonic velocity relation

$$a^2 = \gamma RT$$

The pressure relation, eq. (7), can be written in the form

$$\bar{p} = (\gamma-1)\left[\frac{\bar{\rho}\bar{e}}{\gamma-1} - \frac{1}{2}\frac{\bar{\rho}(\bar{u}^2 + \bar{v}^2)M_\infty^2}{\gamma}\right] \tag{11}$$

The boundary conditions for the set of equations, eqs. (9), (10), (11), are the tangency and no-slip conditions, eq. (8), together with the far-field conditions

$$\bar{\rho} = \bar{p} = \bar{e} = \bar{u} = \bar{v} = 1 \tag{12}$$

It can be seen then that, with the exception of changes in M_∞, the basic equation set and its boundary conditions are independent of the free-stream conditions. Changes in geometry are transmitted through the changes in the metrics $\xi_x, \xi_y, \eta_x, \eta_y$ and the Jacobian J.

The system of equations, eqs. (9)-(11), can be written in the form

$$L(\bar{\rho}, \bar{p}, \bar{e}, \bar{u}, \bar{v}, M_\infty^2, m) = 0 \tag{13}$$

where m denotes the metric terms. Now consider a perturbation about some state or geometry denoted by a subscript o, and that the perturbation quantities, denoted by the subscript 1, are characterized by the parameter . First consider changes in geometry. An expansion of eq. (13) for m then gives

$$\Delta m \frac{L[\bar{\rho}_o, \bar{p}_o, \bar{e}_o, \bar{u}_o, \bar{v}_o, M_\infty^2, m_o]}{\partial m} + \varepsilon L[\bar{\rho}_1, \bar{p}_1, \bar{e}_1, \bar{u}_1, \bar{v}_1, M_\infty^2, m_1] = 0 \tag{14}$$

where $\bar{L}[\ ]$ is a linear operator, related to L[ ] and which depends on the zeroth order quantities. It can be seen from eq. (14) that the natural choice of perturbation parameter is Δm, i.e., the change in the geometry characteristics. If the general curvilinear coordinate system is related by a set of linear differential equations to the Cartesian variables, then Δm is simply a change in angle of attack, say, or a change in thickness ratio. Hence, if two solutions are known for two cases that differ by a one parameter variation then the solution for any other value of this parameter can be found by simple proportion.

A similar analysis to the above but for Mach number variations indicates that the correct parameter to use for Mach number changes is ΔM_∞^2. This is in contrast to the earlier small-disturbance result in Section 2, above.

Transonic small-disturbance theory can be regarded as a subset of the Navier-Stokes equations and a question arises regarding the relationship of these two different Mach number perturbation parameters, since for certain flows the small disturbance theory should be a close approximation to the Navier-Stokes equations. In the type of interpolation used in previous work, and also in the present work, the perturbation parameter ε appears in a combination, $\varepsilon/\varepsilon_o$, where ε_o is some known value of ε. In Table 1 the effect of changing the parameter for different Mach number is shown. Two different base and calibration Mach numbers (which gives ε_o) are used in the computations, namely 0.8 and 0.83, and 0.8 and 0.85. It can be seen that, while the values of ε for both theories differ greatly, the ratio $\varepsilon/\varepsilon_o$ for both forms of ε is in good agreement. This indicates that the small-disturbance perturbation is not inconsistent with the present work.

2.2 The Strained Coordinate Method

The interpolation procedure outlined above is only valid for smooth functions. A device for treating discontinuous functions using a strained coordinate system has been derived in previous papers (refs. 1 and 3) and a brief outline is given below. Because of the applicability to section 4 of this report, a more complete version of the idea is given here than is warranted by the simple interpolation used in this example.

The perturbation method outlined in the previous section requires that the changes due to the correction are small. In cases containing discontinuities which can alter location during the perturbation, the changes are not small in the region traversed by the discontinuity. A means of treating the problem of perturbations in discontinuous transonic flow has been described by Nixon (ref. 1); an outline is given below.

Briefly, the idea is that the problem is reformulated in a strained coordinate system in which the discontinuity remains at the same location throughout the perturbation and hence the difficulties associated with moving discontinuities do not arise explicitly. The required straining is then found as part of the solution. The basic equations in this strained coordinate system are then perturbed about some known solution to give a linear equation for the perturbation quantities similar to those discussed in the previous section. Once the solution of the linear perturbed equation is known, the total perturbed solution in the physical coordinates is then obtained. The major restriction is that the discontinuities must not be lost or generated during the perturbation.

The technique described above was originally developed to treat the discontinuities which can invalidate a perturbation analysis. However, the technique can also be applied to increase the range of application of a valid perturbation analysis. An example from transonic airfoil theory concerns the pressure distribution around an airfoil when shock waves are present; such a pressure distribution is sketched in figure 1. The solid and dashed lines denote two nearby solutions for the pressure distribution. The solution shock waves are captured, that is, the expected discontinuity is smeared over a few mesh spacings and denoted by CD and C'D'. The method of strained coordinates, as given in reference 1, would strain the x-coordinate such that the midpoints of the shock capture regions CD and C'D' coincide. The actual details of the shock capture region are not considered since they are in any event artificial phenomena.

It can be seen from figure 1 that in the leading edge region the rapid change in the pressure distribution can cause large pressure changes for a small perturbation if the location of the pressure rise shifts slightly in the x-direction. This large effect seriously limits the range of validity of the perturbation analysis since all pressure changes are assumed small. A method

of avoiding this difficulty is to strain the coordinates such that representative point on the AB and A'B' curves coincide. This then increases the range of validity in a similar way as the treatment of the shock waves in reference 1.

A further point concerns the treatment of the shock capture regions CD and C'D'. In the earlier applications (refs. 1 and 2) of the theory the same mesh and differential equations were used for computing the pressure distribution in all examples and hence the shock capture characteristics were essentially the same for all cases. For other problems, for example, those discussed later in Section 4, the shock capture characteristics may differ substantially and it is desirable to correct this behavior. Accordingly, the coordinates can be strained such that both the points C,C' and D,D' (the extremities of the shock capture) coincide. As before, the actual flow details in the region CD are considered irrelevant because of the artificial nature of the shock capture.

A more general statement of the above technique is as follows.

1. If a true discontinuity is present, the coordinate straining is such that the location of the discontinuities coincide.

2. If there is a shock capturing type of phenomena, then the straining is such that the extremities of the capture region coincide.

3. If large gradients are present in the solution, then the coordinate straining is chosen so that a representative point in the region of the large gradient coincides.

These conditions constitute perhaps a large number of requirements for the choice of straining. However, a piecewise straining is perfectly feasible provided the end points of the straining (which do not move) lie in regions of the solution for which a small perturbation analysis is valid, for example, in the region BC of figure 1.

3. APPLICATION OF THE STRAINED COORDINATE SYSTEM TO THE NAVIER-STOKES EQUATIONS

3.1 Theory for the Navier-Stokes Equations

Consider the set of equations, eq. (9).

$$\frac{\partial \bar{E}(\xi,\eta)}{\partial \xi} + \frac{\partial \bar{F}(\xi,\eta)}{\partial \eta} = R_e^{-1} \frac{\partial \bar{S}(\xi,\eta)}{\partial \eta} \tag{15}$$

Let both the independent variables (ξ,η) be strained such that the location of one or more discontinuities or rapid gradients are held invariant. The new coordinates are denoted by (ξ',η') where

$$\begin{aligned} \xi &= \xi' + \varepsilon\delta\xi\xi_1(\xi',\eta') + \ldots \\ \eta &= \eta' + \varepsilon\delta\eta\eta_1(\varepsilon',\eta') + \ldots \end{aligned} \tag{16}$$

where ε is the perturbation parameter, $\delta\xi,\delta\eta$ are measures of the movement of the straining points and $\xi_1(\xi',\eta')$, $\eta_1(\xi',\eta')$ are (fairly arbitrary) straining functions.

Now let the dependent variables be expanded in a series in ε. Thus

$$\begin{aligned} \bar{E}(\xi,\eta) &= \bar{E}_o(\xi',\eta') + \varepsilon\bar{E}_1(\xi',\eta') + \ldots \\ \bar{F}(\xi,\eta) &= \bar{F}_o(\xi',\eta') + \varepsilon\bar{F}_1(\xi',\eta') + \ldots \\ \bar{S}(\xi,\eta) &= \bar{S}_o(\xi',\eta') + \varepsilon\bar{S}_o(\xi',\eta') + \ldots \end{aligned} \tag{17}$$

Using eqs. (16) and (17) the perturbation equation for eq. (15) (the coefficient of ε) is

$$\begin{aligned} &\frac{\partial \bar{E}_1}{\partial \xi'} - \delta\xi\left(\frac{\partial \bar{E}_o}{\partial \xi'}\,\xi_{1_{\xi'}} + \frac{\partial \bar{F}_o}{\partial \eta'}\,\xi_{1_{\eta'}}\right) + \frac{\partial \bar{F}_1}{\partial \eta'} - \delta\eta\left(\frac{\partial \bar{F}_o}{\partial \eta'}\,\eta_{1_{\eta'}} + \frac{\partial \bar{E}_o}{\partial \xi'}\,\xi_{1_{\eta'}}\right) \\ &\quad = R_e^{-1}\left(\frac{\partial \bar{S}_1}{\partial \eta'} - \delta\eta\,\frac{\partial \bar{S}_o}{\partial \eta'}\,\eta_{1_{\eta'}} - \delta\eta\,\frac{\partial \bar{S}_o}{\partial \xi'}\,\eta_{1_{\xi'}}\right) \end{aligned} \tag{18}$$

Now since ε is not contained in eq. (18) it follows that a solution to this equation can be applied to any value of ε. As in the previous work (ref. 2) the perturbation equation is not solved, instead the solution of the perturbation equation is assumed to be the difference between two complete solutions, differing only by a perturbation characterized by the parameter ε_o. Hence, for example, if

$$\bar{\xi} = \xi' + \varepsilon_o \delta\xi \; \xi_1(\xi',\eta')$$
$$\bar{\eta} = \eta' + \varepsilon_o \delta\eta \; \eta_1(\xi',\eta') \tag{19}$$

and, if for the velocity component, $u(\xi,\eta)$, the two solutions are denoted by $u_o(\xi,\eta)$ (base solution) and $u_1(\xi,\eta)$ (calibration solution, $\varepsilon = \varepsilon_o$). Then, following the previous work[4],

$$u(\xi,\eta) = u_o(\xi',\eta') + \frac{\varepsilon}{\varepsilon_o}\left[u_1(\bar{\xi},\bar{\eta}) - u_o(\xi',\eta')\right] \tag{20}$$

and

$$\xi = \xi' + \varepsilon \; \delta\xi \; \xi_1(\xi',\eta') = \xi' + \frac{\varepsilon}{\varepsilon_o}(\bar{\xi} - \xi')$$
$$\eta = \eta' + \varepsilon \; \delta\eta \; \eta_1(\xi',\eta') = \eta' + \frac{\varepsilon}{\varepsilon_o}(\bar{\eta} - \eta') \tag{21}$$

The coordinates $\bar{\xi},\bar{\eta}$ are found from eq. (19) by making the straining points, e.g., C,C' in figure 1, coincide. A similar relation to eq. (20) applies for all the dependent variables, the most useful of which is the pressure coefficient $C_p(\xi,\eta)$. Thus

$$C_p(\xi,\eta) = C_{p_o}(\xi',\eta') + \frac{\varepsilon}{\varepsilon_o}\left[C_{p_1}(\bar{\xi},\bar{\eta}) - C_{p_1}(\xi',\eta')\right] \tag{22}$$

In the present work only values on the airfoil surface ($\eta = 0$) are considered and only the ξ coordinate is strained. The coordinate straining function $\xi_1(\xi',0)$ is given by the following equation or

by a piecewise application of the following equation, depending on the number of straining points required.

$$\xi_1(\xi,0) = \delta\xi'_A \left[\frac{\xi'(1-\xi')(\xi'-\xi'_B)}{\xi'_A(1-\xi'_A)(\xi'_A-\xi'_B)}\right] + \delta\xi'_B \left[\frac{\xi'(1-\xi')(\xi'-\xi'_A)}{\xi'_B(1-\xi'_B)(\xi'_A-\xi'_B)}\right]$$

$$0 \le x' \le 1$$

$$\xi_1(\xi,0) = 0 \qquad 1 < x' < 0$$

This straining relation keeps invariant the leading and trailing edges and two straining points, A,B.

A further result can be obtained from eq. (22) for the lift and pitching moment coefficients C_L, C_m. Consider the lift coefficient C_L, where

$$C_L = \int_o^1 \Delta C_p(\xi,0)\,d\xi \tag{23}$$

where $C_p(\xi,0)$ denotes the pressure jump between upper and lower surfaces. Using eqs. (19), (21), and (22) the lift coefficient is then given by

$$C_L = \int_o^1 \left\{\Delta C_{p_o}(\xi',0') + \frac{\varepsilon}{\varepsilon_o}\left[\Delta C_{p_1}(\bar{\xi},\bar{0}) - \Delta C_{p_o}(\xi',0')\right]\right\} \times \left\{d\xi' + \frac{\varepsilon}{\varepsilon_o}\left[d\bar{\xi} - d\xi'\right]\right\} \tag{24}$$

Now the basis of the perturbation theory implies that

$$\left[C_{p_1}(\bar{\xi},\bar{\eta}) - C_{p_o}(\xi',\eta')\right] \sim \underline{0}\ (\varepsilon)$$

$$\left[d\bar{\xi} - d\xi'\right] \sim \underline{0}\ (\varepsilon)$$

and also that $d\bar{\xi} = d\xi' + \underline{0}(\varepsilon)$. Using these results in eq. (24) it can be shown that

$$C_L = \int_0^1 \left[\Delta C_{p_o}(\xi',0)d\xi' + \frac{\varepsilon}{\varepsilon_o} \Delta C_{p_1}(\bar{\xi},0)d\bar{\xi} - \frac{\varepsilon}{\varepsilon_o} \Delta C_{p_o}(\xi',0)d\xi' \right] \quad (25)$$

or

$$C_L = C_{L_o} + \frac{\varepsilon}{\varepsilon_o} [C_{L_1} - C_{L_o}], \quad (26)$$

where C_{L_o}, C_{L_1} are the lift coefficients for the base and calibration solutions, respectively. A similar result applies for the pitching moment C_m, namely

$$C_m = C_{m_o} + \frac{\varepsilon}{\varepsilon_o} [C_{m_1} - C_{m_o}]. \quad (27)$$

3.2 Discussion of Results

The variation of lift coefficient for a Korn airfoil at $M_\infty = 0.755$, for various angles of attack, is shown in figure 2. Two separate cases are considered, namely flows with shock waves and shock free flow. For shocked flow the base and calibration solutions were taken at $\alpha = 1.2°$ and $\alpha = 2.66°$, and for shock free flow at $\alpha = -0.5°$ and $\alpha = 0.4°$. In both cases the values predicted by the formula eq. (26) agree satisfactorily with directly computed results. In figure 3 the variation of C_L with M_∞ is shown, with base and calibration Mach numbers of 0.8 and 0.85, respectively. The airfoil is a NACA 64A410 section at -3.0° angle of attack. Again it can be seen that the simple formula agrees satisfactorily with the direct calculation, except for $M_\infty = 0.75$. The reason for this is that for all the other Mach numbers the flow separates after the shock wave, and this phenomena is implicitly included in the formula via the C_{L_1} and C_{L_o}. At $M_\infty = 0.75$ the flow is attached and hence the flow does not change

smoothly from the base and calibration flows. A smooth change is necessary for the application of the present theory.

The pressure distribution around the upper surface of two different airfoils calculated by the present method are shown in figures 4-7. The first of these airfoils is the NACA64A410 section at -3.0° angle of attack and the theory is applied for different free-stream Mach numbers. The base and calibration Mach numbers are 0.8 and 0.88, respectively. It can be seen from figures 4 and 5 that the present method agrees fairly well with direct calculations. At the higher Mach number, $M_\infty = 0.9$ the agreement at the shock is not quite satisfactory; this may be due to the direct solutions changing character, either physically or numerically, from the flow at the base and calibration Mach numbers. These flows presented in these figures have shock induced separation.

In figures 6 and 7 the pressure distributions around the upper surface of the Korn airfoil at $M_\infty = 0.755$ at different angles of attack are shown. The base and calibration angles of attack are $\alpha = 1.2°$ and $\alpha = 2.66°$, respectively. The agreement between the present results and the results of direct calculations is again satisfactory.

It should be pointed out that in the present investigation it is necessary to take the base and calibration solutions further apart than is the case for potential flows. This is because the Navier-Stokes solutions are either not converged to the same level of accuracy, or that there is some physical unsteadiness in the solution. Both these phenomena lead to "fluctuations" which can dominate the theoretically steady perturbation.

4. THE CORRECTION THEORY FOR NUMERICAL CALCULATIONS

The next two sections deal with the idea of correcting approximate solutions to give solutions typical of a more accurate theory. It is assumed that the more approximate solution can be

generated much more rapidly, and less expensively than an accurate solution. Also, it is assumed that the addition of a correction to the approximate theory does not significantly increase the computing time. In the next section the idea of correcting transonic small-disturbance solutions to give results typical of Navier-Stokes solutions is investigated. In section 6 the extension of the work of reference 3, that is the correction of coarse grid solutions to fine grids and of small-disturbance theory to full potential theory are examined. The basic idea behind the correction theory has appeared elsewhere[3] but is repeated here for convenience.

Approximate equations are frequently in some sense a logical approximation (rather than an empirical approximation) of an exact equation. This means that the approximate equation can be formally obtained from the exact equation by an expansion in some perturbation parameter; powers of this parameter greater than some specified power are negligible. Approximate equations can be derived by such an expansion are referred to below as consistent approximations. The difference between solutions of this approximate equation and solutions of the exact equation is the error. One example of such a consistent approximation is given by the central finite difference to ϕ_{xx}. Thus

$$\phi_{xx} = \frac{\phi_{i+1} - 2\phi_i + \phi_{i-1}}{2\Delta x^2} + \Delta x^2 R \,, \tag{28}$$

where R is the remainder of the truncated Taylor series leading to the difference formula. Finite-difference representations of a differential equation can be represented by an equivalent differential equation which smoothly approaches the exact differential equation as the mesh size is reduced to zero. For a finite mesh size the difference between the equivalent and exact differential equations can be represented by a perturbation equation with a perturbation parameter characterizing the truncation error.

In general, if an approximate equation is a consistent approximation of an exact equation then the difference between the equations can be represented to a specified accuracy by a linear perturbation equation with a perturbation parameter, ε, which is a measure of the error. If this perturbation equation is known, it can be solved using standard methods to give a correction to the solution of the approximate equation. The main difficulty is in actually determining the correct form of the perturbation equation.

It is obvious that if the exact equation can be solved then it is not necessary to know the form of the perturbation equation to obtain the correction since the difference between the exact solution and the approximate solution gives the perturbation solution with the addition of (formally) negligible terms. If the exact solution is known, of course, then there is little point in solving for the perturbation correction. However, the perturbation equation gives a formal measure of error ε between approximate and exact equations and is assumed to be small. If a second perturbation equation that differs from the proper perturbation equation by an error Δ then the formal error in using the second equation to compute the correction is $\underline{0}\ (\varepsilon\Delta)$. A problem which has an error described by this second perturbation equation is referred to as a "nearby" problem. Its essential characteristics differ from the real problem by a small amount characterized by the error Δ.

If

$$L(\phi) = 0 \text{ is the exact equation}$$
$$L_o(\phi_o) = 0 \text{ is the approximate equation}$$
$$L_1(\phi_1) = 0 \text{ is the perturbation equation}$$

then

$$\phi = \phi_o + \varepsilon\phi_1 + \underline{0}(\varepsilon^2). \tag{29}$$

If a superscript Δ denotes the nearby problem then, if

$$L^{\Delta}(\phi^{\Delta}) = 0$$
$$L_o^{\Delta}(\phi_o^{\Delta}) = 0$$
$$L_1^{\Delta}(\phi_1^{\Delta}) = 0$$

Then, as before,

$$\phi^{\Delta} = \phi_o^{\Delta} + \varepsilon^{\Delta}\phi_1^{\Delta} + \underline{O}(\varepsilon^2) \tag{30}$$

Subtraction of eqs. (31) and (30) then gives, to first order in ε,

$$\phi = \phi_o + (\varepsilon\phi_1 - \varepsilon^{\Delta}\phi_1^{\Delta}) + (\phi^{\Delta} - \phi_o^{\Delta}). \tag{31}$$

If the nearby, approximate, solution ϕ_1^{Δ} is such that

$$|\varepsilon\phi_1 - \varepsilon^{\Delta}\phi_1^{\Delta}| << |\varepsilon\phi_1|\ , \tag{32a}$$

Then a good approximation to the exact solution is given by

$$\phi = \phi_o + (\phi^{\Delta} - \phi_o^{\Delta}).$$

Since a basic premise of perturbation theory assumes that derivatives of a quantity are the same order of magnitude as the quantity, an alternative to eq. (32a) is

$$|\varepsilon\phi_{1_x} - \varepsilon^{\Delta}\phi_{1_x}^{\Delta}| << |\varepsilon\phi_{1_x}| \tag{32b}$$

The "nearby" solution is defined by a solution that satisfies eqs. (30,32). In particular applications it is assumed that the adequacy of a nearby solution can be determined by examination of its approximate solution in a part of the solution domain, for example, an airfoil surface rather than the entire flow field. This assumes that the characteristics of the complete solution can be determined by examining only a dominant part. A discussion on the existence of the nearby solution is given in Appendix B.

The theory just outlined does not formally take account of shock waves or adequately treat solutions with rapid gradients. If either shock waves or rapid gradients are present in the solution then the strained coordinate method outlined in section 2 should be used. In this case, each of the solutions discussed above should be written in the appropriate strained coordinates which constrain rapid gradients to the same location.

5. CORRECTION PROCEDURES OF THE TRANSONIC SMALL-DISTURBANCE THEORY

5.1 Theory

The transonic small-disturbance equation (TSD) can be written in terms of a perturbation velocity potential $\phi(x,y)$ as

$$(1 - M_\infty^2)\phi_{xx} + \phi_{yy} = (\gamma + 1)M_\infty^q \phi_x \phi_{xx} \tag{33}$$

where the perturbation velocity components in the x and y directions are u,v, respectively and are given by

$$u(x,y) = \frac{\partial \phi}{\partial x}(x,y); \quad v(x,y) = \frac{\partial \phi}{\partial y}(x,y) \tag{34}$$

The parameter "q" is a transonic parameter and within the confines of small-disturbance theory is arbitrary. If the slope of the airfoil is given by $y_s'(x,\pm 0)$ where "+" denotes the upper surface and "-" sign denotes the lower surface then the thin airfoil boundary conditions are

$$v(x,\pm 0) = y_s'(x,\pm 0) \tag{35}$$

Before proceeding with the correction analysis it is perhaps pertinent to mention a few properties of TSD theory. The TSD equation can be regarded as an approximation to the conservation of mass equation; it does not really represent any of the other

conservation laws such as energy, or momentum. The parameter q can be derived in a number of ways. If the actual full potential equation (ref. 7) is truncated using the limiting idea of TSD theory then q = 2. If the actual continuity equation is truncated (ref. 8) then the term $(\gamma+1)M^2$ is replaced by $(3+\overline{\gamma-2}M_\infty^2)M_\infty^2$. A commonly-used value for q is 1.75, which is Krupp scaling, and is chosen to make TSD solutions agree with full potential theory solutions. All of these factors reduce to the same value, $(\gamma+1)$, in the transonic limit of $M_\infty \to 1$. The main point of the brief discussion of transonic small-disturbance theory is that the theory is flexible and can be altered within a certain range without altering the formal accuracy.

It is interesting to briefly examine the behavior of TSD solutions compared with Navier-Stokes or Euler equation solutions and with solutions of the full potential theory. The pressure distributions over the upper surface of a Korn airfoil at $M_\infty = 0.755$ and at an angle of attack of 1.2° is shown in figure 8. It can be seen that both the TSD and full potential equation results give a shock location much further aft than the Euler and Navier-Stokes equation results.

The difference in shock location between the full potential equation result and the Euler equation result is about 80% of the difference between the potential location and the Navier-Stokes location. Hence, it can be argued that the cause of disagreement in the shock location is not primarily a viscous phenomenon, but is due to the assumption of irrotationality used in the potential formulation. The reason for the error in shock location for the TSD theory may be readily obtained from an examination of the shock strengths for the TSD equation and the Euler equation for a given pre-shock pressure. The normal shock strength variation is plotted in figure 9 and it can be seen that, as the magnitude of the pre-shock pressure coefficient increases, the TSD strength increasingly becomes much larger than the corresponding Euler strength. This greater shock strength then requires the shock on an airfoil to

move further aft in order to accommodate it, in comparison to the weaker Euler equation shock. The Navier-Stokes shock strength is similar to the Euler strength. If a base criterion, that is, some Mach number and angle of attack are defined, and if these criteria are changed slightly, it is possible that the change in shock location for the TSD solution will be considerably larger than the change in an Euler equation solution. This implies that, while at the reference station the difference in shock location between Euler and TSD solutions may be small, the difference in the rate of change of shock location for both solutions is not small. This type of behavior can raise problems in a perturbation analysis, such as the present work, since perturbation theory usually requires that not only are certain quantities small, but that their rates of change are of comparable magnitude. Accordingly, this problem has been addressed in the present work.

The basic idea of the correction theory has been outlined earlier in section 4. In the present case the solution to be corrected is a TSD solution and correction is obtained from a Navier-Stokes solution. From the above discussion it is apparent that if the TSD solution to be corrected differs significantly in shock strength from the "near-by" solution used to compute the correction, then the new shock location will be considerably in error, even when the correction for viscous effects is used. As noted earlier, the TSD equation has a built-in flexibility in which the transonic parameter can be varied. It is possible to choose this parameter to alter the shock strength or any other flow variable to agree with some datum value. It is assumed here that the error in shock location between a TSD solution and a Navier-Stokes solution is solely due to the different shock strengths. Accordingly, the TSD parameter is chosen such that, for a given pre-shock pressure, the difference between the TSD shock strength and the Euler equation shock strength is the same as in the near-by case used to compute the correction. The means of accomplishing this device is as follows.

For the near-by problem let the subscript o denote a TSD solution for some value of the transonic parameter q, and the subscript 1 denote another TSD solution for a second value of the transonic parameter. The subscript 2 denote a Navier-Stokes solution of the near-by problem. Finally, a subscript 3 denotes the TSD solution to be corrected. If σ denotes the shock strength this application of the usual form of the correction theory will give a new shock strength σ_N where

$$\sigma_N = \sigma_3 + \lambda(\sigma_2 - \sigma_o) \tag{36}$$

where

$$\lambda = \left(\frac{M_o}{M_3}\right)\left(\frac{1 - M_3^2}{1 - M_o^2}\right) \tag{37}$$

This may not give the correct shock strength, and hence location, and so a modified equation for the shock strength, within the realm of small-disturbance theory, is used, namely

$$\sigma = \sigma_3 + \lambda(\sigma_2 - \sigma_o) + \varepsilon\lambda(\sigma_1 - \sigma_o) \tag{38}$$

The parameter ε is found by ensuring that

$$\sigma - \sigma_3 - \varepsilon\lambda(\sigma_1 - \sigma_o) = \sigma_2 - \sigma_o \tag{39}$$

Since $\sigma_1 - \sigma_o$ is small and since the "near-by" solution is by definition close to the solution to be corrected this device is equivalent to tuning the small-disturbance theory to get approximately the correct shock jump. In eq. (39) the shock strength σ is determined at $C_{p_3}^+$, the TSD pre-shock pressure coefficient, by the relation

$$\sigma = \frac{2\gamma}{\gamma+1}\left(\frac{2}{\gamma M_\infty^2} + C_{p_3}^+\right)(M^+)^2 - 1 \tag{40}$$

where M_B is the free-stream Mach number and M^+ is the pre-shock Mach number given by

$$(M^+)^2 = \frac{1}{\gamma-1} \frac{2 + (\gamma-1)M^2}{\left(\frac{\gamma+1}{2} M_\infty^2 C_{p_3}^+ + 1\right)^{\frac{\gamma+1}{\gamma-1}}} - 2 \tag{41}$$

A similar relation holds for σ_1. The TSD strength is given by

$$\sigma_o = -2(C_{p_o}^+ - C_{p_o}^*) \tag{42}$$

where

$$C_{p_o}^* = \frac{-2}{\gamma+1} \frac{(1 - M_\infty^2)}{M_o^2}$$

A similar relation holds for σ_1, σ_3.

Having obtained ε, the final value for the pressure coefficient on the airfoil surface is given by

$$C_p(x) = C_{p_3}(x_3) + \lambda[C_{p_2}(x_2) - C_{p_o}(x')] + \varepsilon\lambda[C_{p_1}(x_1) - C_{p_o}(x')] \tag{43}$$

where

$$x = x_3 + x_2 - x' + \varepsilon(x_1 - x') \tag{44}$$

and

$$\begin{aligned} x_1 &= x' + \delta x_{s_1} x_1(x') \\ x_2 &= x' + \delta x_{s_2} x_1(x') \\ x_3 &= x' + \delta x_{s_3} x_1(x') \end{aligned} \tag{45}$$

where δx_{s_1}, δx_{s_2}, δx_{s_3} are the amounts by which the shock wave moves for each of the solutions, relative to the base solution

$$(M^+)^2 = \frac{1}{\gamma-1} \frac{2 + (\gamma-1)M^2}{\left(\frac{\gamma+1}{2} M_\infty^2 C_{p_3}^+ + 1\right)^{\frac{\gamma+1}{\gamma-1}}} - 2 \tag{41}$$

A similar relation holds for σ_1. The TSD strength is given by

$$\sigma_o = -2(C_{p_o}^+ - C_{p_o}^*) \tag{42}$$

where

$$C_{p_o}^* = \frac{-2}{\gamma+1} \frac{(1 - M_\infty^2)}{M_o^2}$$

A similar relation holds for σ_1, σ_3.

Having obtained ε, the final value for the pressure coefficient on the airfoil surface is given by

$$C_p(x) = C_{p_3}(x_3) + \lambda[C_{p_2}(x_2) - C_{p_o}(x')]$$

$$+ \varepsilon\lambda[C_{p_1}(x_1) - C_{p_o}(x')] \tag{43}$$

where

$$x = x_3 + x_2 - x' + \varepsilon(x_1 - x') \tag{44}$$

and

$$\begin{aligned} x_1 &= x' + \delta x_{s_1} x_1(x') \\ x_2 &= x' + \delta x_{s_2} x_1(x') \\ x_3 &= x' + \delta x_{s_3} x_1(x') \end{aligned} \tag{45}$$

where δx_{s_1}, δx_{s_2}, δx_{s_3} are the amounts by which the shock wave moves for each of the solutions, relative to the base solution

$C_{p_O}(x')$. (Note: The above idea of a "self tuning" transonic theory is of use in its own right. A short paper on this subject is attached as Appendix C.)

5.2 Discussion of Results

Several examples of the correction technique have been computed using both Euler equations and the transonic small disturbance equation as a base. With the exception of the result shown in figure 10, when the Navier-Stokes solver of Steger (ref. 6) is used, the Navier-Stokes and Euler equation solver used is that of Deiwert (refs. 9 and 10). An earlier example for a NACA64A410 airfoil at $\alpha = 0$ and $M_\infty = 0.8$ is shown again in figure 10. The basic calculation is an Euler equation solution and is corrected for viscous effects from a near-by solution at the same angle of attack and $M_\infty = 0.82$. A similar correction for a Korn airfoil at $M_\infty = 0.755$ and $\alpha = 2.66°$ is shown in figure 11, where the near-by solution is at the same Mach number and $\alpha = 1.2°$. Both these examples have attached flow in the near-by solution but the second example has mildly separated flow in the test case. It can be inferred from these examples that the correction technique does work when Euler equation solutions are corrected. It is also apparent that the error between the Euler equation solution and the Navier-Stokes equation solution is not great and that these examples are perhaps not a good test of the method. Furthermore, the computation time of the Euler solver is about half that of the Navier-Stokes solver and the prospective overall savings in computation cost is not as dramatic as would be the case of correcting TSD equation solutions. Accordingly, most of the effort was put into investigating the correction procedure for the TSD equations.

In figure 12 the pressure distribution around a Korn airfoil at $M_\infty = 0.755$ and $\alpha = 1.2°$ is shown. The base result is a TSD calculation using Spreiter scaling and the correction is computed for the same airfoil, at the same Mach number, with $\alpha = 1.7°$. In figure 13 the pressure distribution around the Korn airfoil at

$M_\infty = 0.755$ at $\alpha = 2.66°$ is shown. The near-by solution is the same as in the previous example. It may be seen that for both these examples that the corrected result is fairly satisfactory although the shock location is not quite right. However, the results are a considerable improvement on the uncorrected TSD solution using Spreiter scaling and a greater improvement over those computed with Krupp scaling. It should be noted here that the present method effectively chooses its own transonic scaling through the use of eq. (35). It is interesting to investigate what effect the use of eq. (35) has on the solution. Hence, the preceding case was computed without the use of the shock strength scaling correction and the result shown in figure 14. It can be seen that the shock strength correction is indeed an essential part of the theory.

The previous example is one primarily of attached flow. An attempt is made here to try to compute a separated flow example. Although separation is really an unsteady process, the results used here are computed using a steady version of Deiwert's Navier-Stokes solver. The flow around an 18% thick biconvex airfoil at $\alpha = 0°$ and $M_\infty = 0.775$ is shown in figure 15. The near-by solution is the same airfoil at the same angle of attack but at $M_\infty = 0.79$. The agreement between the corrected result and the direct result is fairly good although the pressure in the separation region is too high. However, the corrected result is again a considerably improvement over the TSD solution. It is worthwhile noting that the turbulence model had to be the same both for the near-by case and for the direct comparison computation; different turbulence models can produce considerably different results.

It is one of the implications of the present method that the near-by solution need not be for the same airfoil on the test case only that its basic characteristics, i.e., rapid gradients should be similar. Accordingly, an example for a NACA0012 airfoil at $\alpha = 0°$ and $M_\infty = 0.8$ was computed using the correction obtained for the upper surface of the Korn airfoil at $M_\infty = 0.755$ and $\alpha = 1.2°$.

The resulting pressure distribution, shown in figure 16 agrees surprisingly well with the direct result. The NACA0012 result is mildly unsteady and the range of unsteadiness is indicated by the symbols on the figure. An attempt was made to use the correction obtained for a NACA64A410 airfoil at $M_\infty = 0.8$ and $\alpha = -3.0°$ for the biconvex airfoil discussed above. This result is shown in figure 17 and it can be seen that although the use of the correction procedure upgrades the TSD solution, the overall improvement is not really satisfactory. The main reason for the error in the pressure in the separation region seems to be that the inviscid TSD solution for the NACA64A410 airfoil does not have as large a pressure gradient at the trailing edge region as the biconvex airfoil solution. Incidently, it should be noted that the examples shown in figures 12 and 13 are formally beyond the bounds of small disturbance theory.

In general then it appears that the correction theory works for correcting Euler equation solutions and for TSD equation solutions for attached flow. The shock locations can be in error and this may be due to the extreme nature of some of the examples. It also appears that the use of a different airfoil for the correction computation can work although in extreme cases like that shown in figure 17 the improvement may be minimal. Also, from the one example computed, it seems as if massively separated flows can be computed although more work is required to determine the range of applicable "near-by" solutions.

Most of the examples discussed above are fairly extreme in their degree of flow complexity. One of the difficulties, in abortive attempts to compute the flow over the NACA64A410 airfoil at $\alpha = -3.0°$ and the Mach numbers used in figures 4 and 5, is that the TSD solution gives a shock location at the trailing edge even for quite high values of the transonic parameter, thus destroying any chance of using the shock location correction of eq. (35). The overall conclusion reached from the small range of examples

computed is that the correction theory does appear to work, but that a much greater range of examples both less extreme than the present ones and with massive separation need to be investigated. A major difficulty in implementing the suggestion economically is to predict in advance what kind of flow a Navier-Stokes solution will exhibit. A further point that should be investigated is some means (probably semi-empirical) of identifying when a separated or attached flow correction should be used.

6. THE CORRECTION THEORY IN THREE-DIMENSIONS

6.1 General Comments

The extension of the mathematical perturbation theory to three dimensions is a straightforward development of the theory described in section 4. The correction for a given problem is obtained by computing one exact and one approximate solution and taking the difference. The strained coordinate method is used to treat shock waves and any rapid gradients in the flow. The only fundamental difference between two and three dimensional applications of the theory is that in three dimensions provision has to be made for a spanwise straining to treat possible shock intersection points.

The examples considered in the present investigation all concerned the ONERA M6 wing. It is obviously desirable to treat the theory over a wide range of wings, but the relative unavailability of wing input data and shortage of time inhibited the use of wings other than the M6 wing as test cases. However, the pressure distribution around this wing at typical transonic speeds is fairly complex and usually contains two shock waves intersecting inboard of the wing tip, together with a large pressure gradient in the vicinity of the leading edge. In the test cases various combinations of angle of attack and wing twist were used to try to produce a relatively wide range of perturbations.

An important decision in the use of the theory is to determine the number and location of the straining points. A typical section pressure distribution for the M6 wing is shown in figure 18. It can be seen that the leading edge shock wave is weak and is considerably smeared by the finite-difference schemes; this can cause difficulties in identification. Consequently it was decided to simply treat the leading edge region as a region of high gradients and to pick some identifier (not necessarily the shock) to hold invariant. The ultimate choice is the location of the bottom of the first compression gradient (point A in figure 18). The other points held invariant in the straining functions are the beginning and end of the capture region of the strong aft shock, points B, C, respectively in figure 18. The leading and trailing edges are also held invariant. In addition to this section data a shock intersection point on the span is also held invariant. It should be noted that the solution accuracy is unchanged if a previously specified rapid gradient does not exist at some straining point, since the straining does not degrade a normally valid or accurate perturbation. One problem that arises in a diverse straining, such as the one necessary in the present problem, is that the usual cubic straining function used in section 3 can give strained coordinates that tie off the wing. In order to remove this tendency a piecewise version of the linear straining given in reference 2 is used. For a chord length of unity, the three straining points A, B, C, the straining function is

$$\xi_1(\xi,0) = \xi' + \xi'\delta\xi_A H(\xi'_A-\xi') + [\delta\xi_B(\xi'-\xi'_A) - \delta\xi'_A(\xi'-\xi'_B)]/(\xi'_B-\xi'_A)$$

$$\times H(\xi'-\xi'_A)H(\xi'_B-\xi') + [\delta\xi'_C(\xi'-\xi'_B) - \delta\xi'_B(\xi'-\xi'_C)]/(\xi'_C-\xi'_B)$$

$$\times H(\xi'-\xi'_B)H(\xi'_C-\xi') + \delta\xi'_C(1-\xi')/(1-\xi'_C)H(\xi'-\xi'_C) \qquad (46)$$

where $H(\xi)$ is the step function, and $\delta\xi'_A$, $\delta\xi'_B$, and $\delta\xi'_C$ are the perturbations in the points ξ'_A, ξ'_B, ξ'_C.

This straining function is used in the computation of all the test cases.

6.2 Discussion of Results

The correction for all the examples is taken from various computations of the ONERA M6 wing at $M_\infty = 0.84$ and $\alpha = 3.06°$ and zero twist angle. Both full potential calculations, using Jameson's finite volume method (ref. 11), and modified small-disturbance calculations, using a variant of the Bailey-Ballhaus (ref. 12) code are performed. Calculations are carried out relatively coarse and fine grids. The type and magnitudes of errors involved in the various approximations are indicated in figure 19. The span stations η are such that $\eta = 0$ denotes the wing root and $\eta = 1$ denotes the wing tip. As pointed out in section 4, the main criteria for both correction results and the approximate or coarse grid results is that they must contain all of the essential features of the flow. For example, in problems of the type sketched in figure 18, a coarse grid solution must capture the leading edge compression in an adequate fashion otherwise the location of the forward straining point cannot be found. Another interesting variation of the criteria for validity is that the convergence level for all solutions on the same grid must be the same. If the convergence level (and hence the truncation error) is different for different cases, then the equivalent perturbation equation for the correction is not the same, and the present correction technique is invalid. It is possible however to envisage a correction which would treat different convergence levels.

The first two examples, shown in figures 20 and 21, indicate the application of the correction technique for grid size. The

approximate solutions are obtained using the finite-volume method (ref. 11) and are on a grid of dimensions 80×8×16; the fine grid has dimensions of 160×16×32. The results for $M_\infty = 0.84$ and $\alpha = 3.06$ are shown in figure 20 for various span stations η and it can be seen that the agreement of the present method with direct calculations is fairly good. In figure 21 the pressure distribution around the upper surface of the M6 wing at $M_\infty = 0.84$, $\alpha = 3.06$ and with 3.0° of wing twist. Again it can be seen that the agreement between the corrected solutions and the directly calculated solutions is adequate.

In figure 22 and figure 23 the corrections for the use of the TSD equation is shown. The TSD solution uses the grid embedding technique of Boppe. In figure 22 the pressure distribution for $M_\infty = 0.84$ and $\alpha = 3.06$ is shown, and in figure 23 the pressure distribution for $M_\infty = 0.84$, $\alpha = 4.0°$ and 1.5° of twist is shown. In both cases the agreement with direct calculations is adequate.

Finally, in figure 24 and figure 25, the correction for grid size and the use of the TSD equation is investigated. The TSD solutions are computed on a grid with 31 streamwise points and the full potential equation on the grid of 160 16 32 as before. In figure 24 the pressure distribution for $M_\infty = 0.84$, $\alpha = 3.06$ is shown and it can be seen that the agreement with the direct calculation is not really adequate away from the wing root. This is almost certainly due to the inability of the coarse grid TSD solution to adequately represent a main feature of the final solution, in this case the "bulge" in the pressure distribution in the region of the leading edge recompression. It should be noted, however, that the present technique still upgrades the solution, especially the shock location. In figure 25 the pressure distribution for $\alpha = 4.0°$ and 1.5° of twist is shown. It can be seen that these corrected results compare fairly well with the results of direct calculations.

In summary then, the correction technique derived for two-dimensional flows in earlier reports does appear to work in

three-dimensions although care must be exercised in the choice of the grid size. A major criterion of the work is that only one wing, the ONERA M6 wing, is used in the tests. The reason is given elsewhere, but the method should be more comprehensively tested for other wings. A second point is that the computer code used in the present research is not entirely automatic. A future code should have an automatic identification method for the straining points.

7. CONCLUDING REMARKS

The main object of the present work is to extend some recent development in perturbation theories of transonic flow. One topic is the extension of the physical perturbation theory to treat solutions of the Navier-Stokes equation. A second topic is the investigation into the possibility of correcting lower grade inviscid solutions for viscous effects using the mathematical perturbation theory. Thirdly, the extension of the mathematical perturbation theory for potential flows to three dimensions is considered. The extension of the physical perturbation theory to solutions of the Navier-Stokes equations is straightforward, the only additional fact to appear is that the necessary base and calibration solutions should not be too close together, otherwise the perturbation quantities can be seriously degraded by the numerical error in the solution.

Application of the correction technique to upgrade potential equation solutions to include viscous effects introduced some interesting problems. The main difficulty proved to be due to the fact that, for relatively strong shock waves, the potential theories give shock locations that are much further aft than those predicted by the Euler or Navier-Stokes equations. This raised problems in the application of the concept of near-by solutions, since the sensitivity of some of the examples to small geometry changes could allow a flow change from one with a relatively weak shock to one with a strong shock. This led to the necessity for

a correction for the purely inviscid errors due to the use of the potential equation rather than the Euler equations. Examples computed with the subsequent correction theory compare adequately with direct calculations.

The extension of the mathematical correction theory to three-dimensions is a straightforward development of the two-dimensional theory. Within certain limits the perturbation method appears satisfactory. However, in all of the topics discussed above, it is desirable that a more comprehensive testing procedure be performed over a wider range of airfoils and wings in order to assess the range of applicability of the theories.

REFERENCES

1. Nixon, D.: Perturbation of a Discontinuous Transonic Flow. AIAA Journal, Vol. 16, No. 1, 1978.

2. Nixon, D.: Perturbations in Two and Three Dimensional Transonic Flow. AIAA Journal, Vol. 16, No. 7, 1978.

3. Nixon, D.: Techniques for Correcting Approximate Finite Difference Solutions. AIAA Paper 79-0277, 1979.

4. Nixon, D.: Design of Transonic Airfoils Using a Similarity Theory. AIAA Paper 79-0076, 1979.

5. Baldwin, B.S. and Lomax, H.: Thin Layer Approximation and Algebraic Model for Separated Turbulent Flows. AIAA Paper 78-257, 1978.

6. Steger, J. L.: Implicit Finite Difference Simulation of Flow about Arbitrary Geometries with Application to Airfoils. AIAA Paper 77-665, 1977.

7. Guderly, K.: Transonic Flow. Pergamon Press, England, 1962.

8. Van der Vooren, J., Sloof, J. W., Huizing, G. H., and van Essen, A.: Remarks on the Suitability of Various Transonic Small Perturbation Equations to Describe Three-Dimensional Transonic Flow; Examples of Computations Using a Fully Conservative Rotated Difference Scheme. Proceedings of Symposium Transsonicum, Springer Verlag, 1976.

9. Deiwert, G. S.: Numerical Simulation of High Reynolds Number Transonic Flows. AIAA Journal, Vol. 13, No. 10, 1975.

10. Deiwert, G. S.: Private communication, July 1979.

11. Jameson, A. and Caughey, D.: A Finite Volume Method for Transonic Potential Flow Calculations. Proc. AIAA 3rd Comp. Fluid Dynamics Conference, 1977.

12. Ballhaus, W. F., Bailey, F. R., and Frick, J.: Improved Computational Treatment of Transonic Flow about Swept Wings. Advances in Eng. Sci., Vol. 4, NASA CP2001, 1976, pp. 1311-1320.

TABLE 1.- VARIATION OF ε AND $\frac{\varepsilon}{\varepsilon_o}$ WITH MACH NUMBER

M_∞	$(\varepsilon)_{TSD}$	$(\varepsilon)_{NAVIER-STOKES}$	$\left(\frac{\varepsilon}{\varepsilon_o}\right)_{TSD}$	$\left(\frac{\varepsilon}{\varepsilon_o}\right)_{NAVIER-STOKES}$
0.82	0.622	-0.0753	0.618	0.678
0.85	1.9787	-0.178	1.965	1.609
0.87	3.3502	-0.242	3.327	2.176

(a) $(\varepsilon_o)_{TSD} = +1.007$; $(\varepsilon_o)_{NAVIER-STOKES} = -0.111$

$M_o = 0.8$, $M_1 = 0.83$

M_∞	$(\varepsilon)_{TSD}$	$(\varepsilon)_{NAVIER-STOKES}$	$\left(\frac{\varepsilon}{\varepsilon_o}\right)_{TSD}$	$\left(\frac{\varepsilon}{\varepsilon_o}\right)_{NAVIER-STOKES}$
0.82	0.622	-0.0753	0.314	0.422
0.84	1.454	-0.145	0.735	0.814
0.87	3.3502	-0.242	1.693	1.352

(b) $(\varepsilon_o)_{TSD} = 1.979$; $(\varepsilon_o)_{NAVIER-STOKES} = -0.178$

$M_o = 0.8$, $M_1 = 0.85$

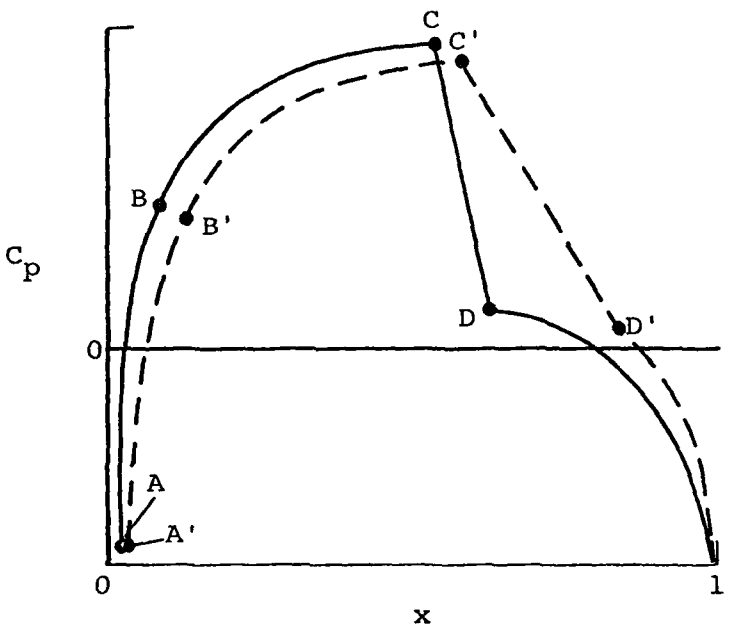

Figure 1.- Sketch of pressure distribution in transonic flow.

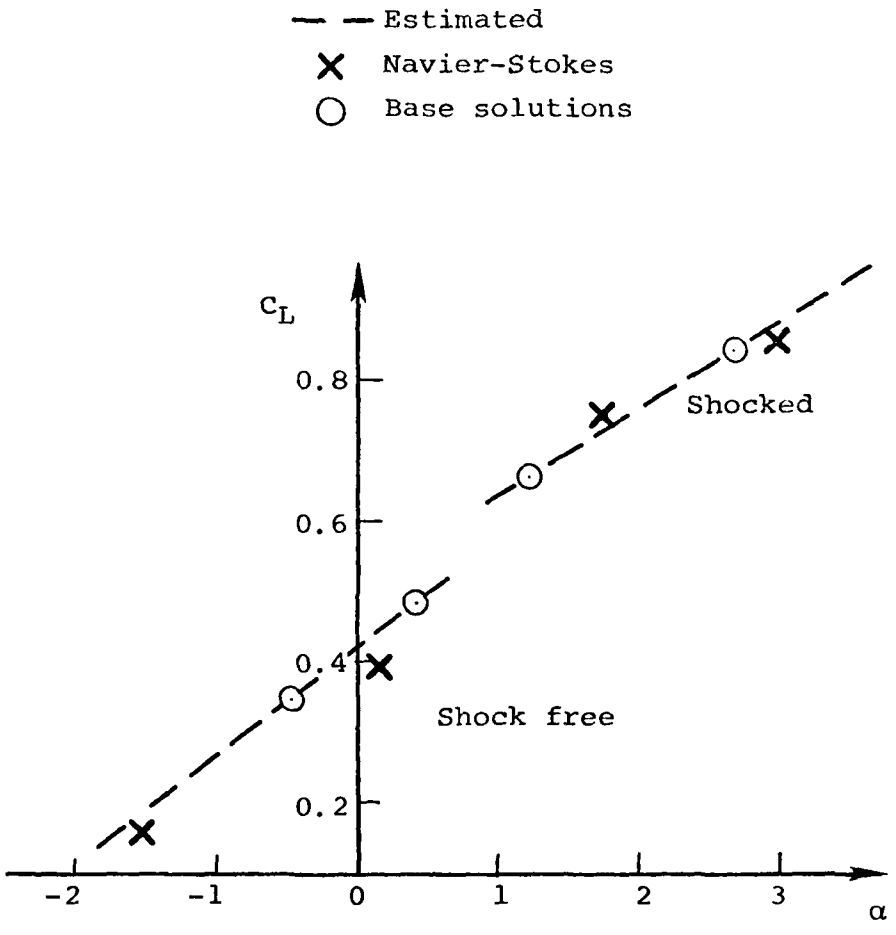

Figure 2.- Variation of C_L with α, Korn airfoil; $M_\infty = 0.755$.

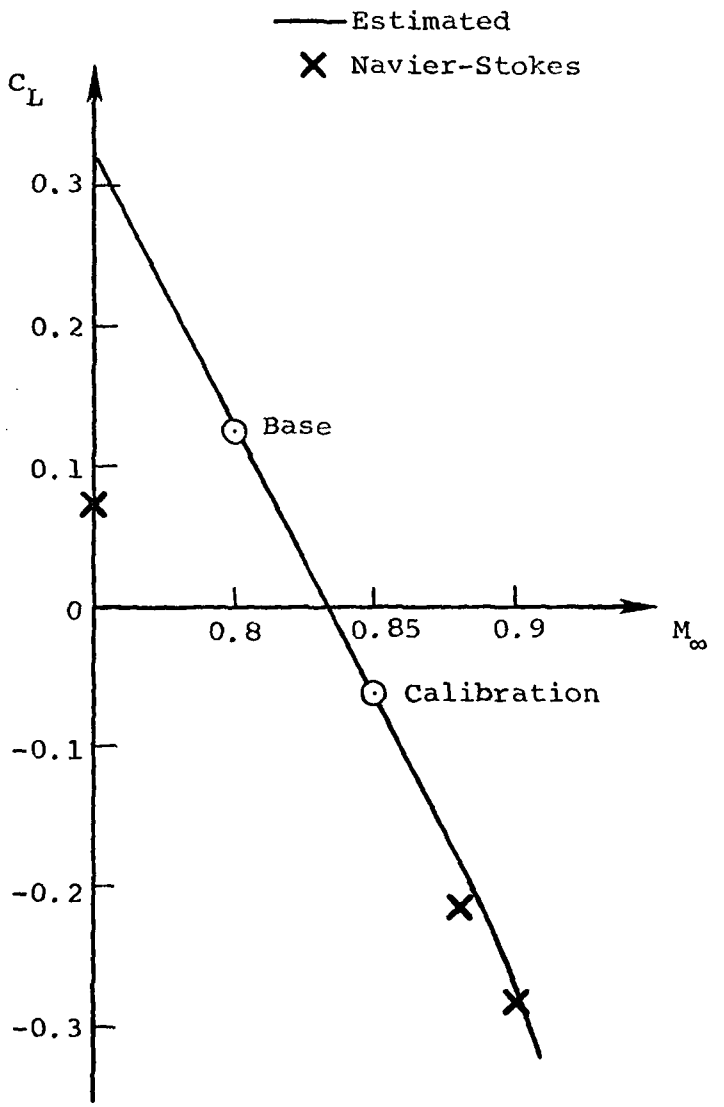

Figure 3.- Variation of C_L with M_∞; NACA64A410 airfoil, $\alpha = -3.0^\circ$.

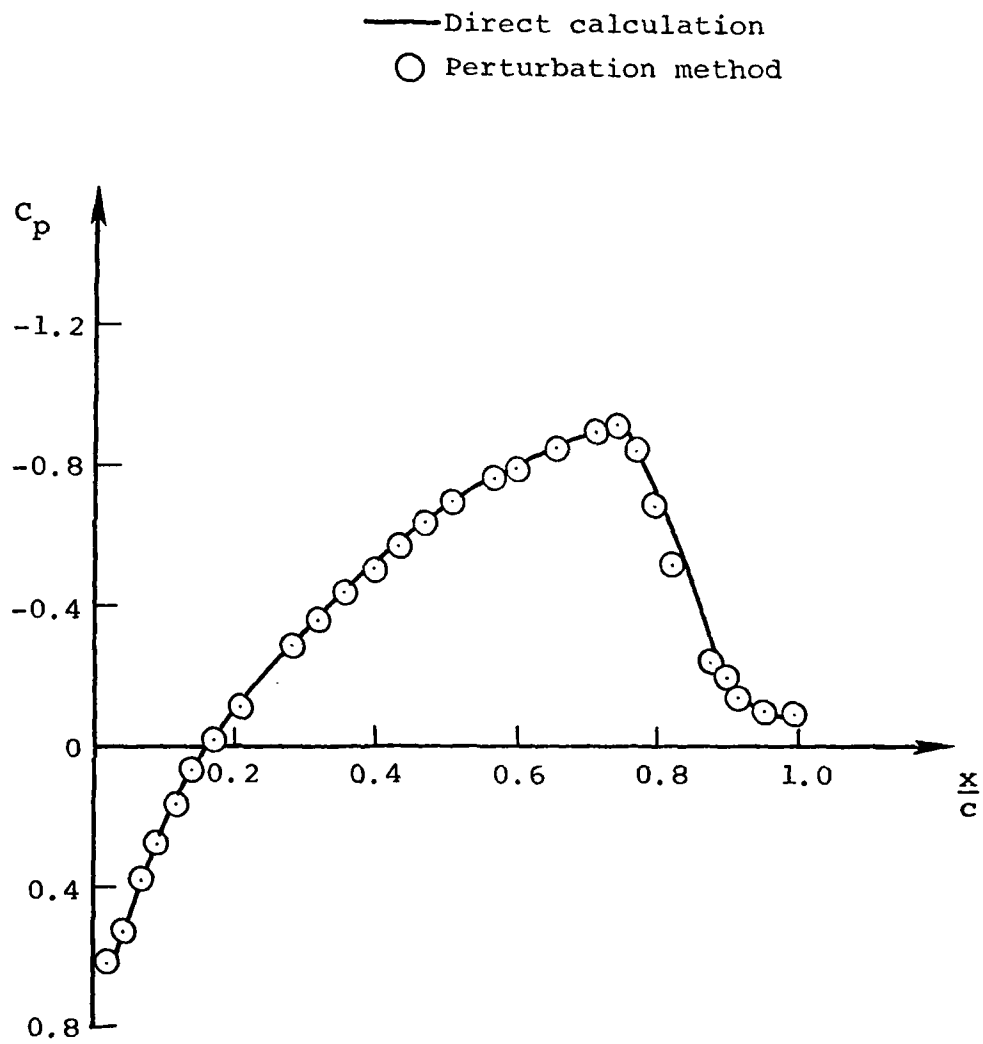

Figure 4.- Pressure distribution around the upper surface of a NACA64A410; $M_\infty = 0.85$, $\alpha = -3.0$.

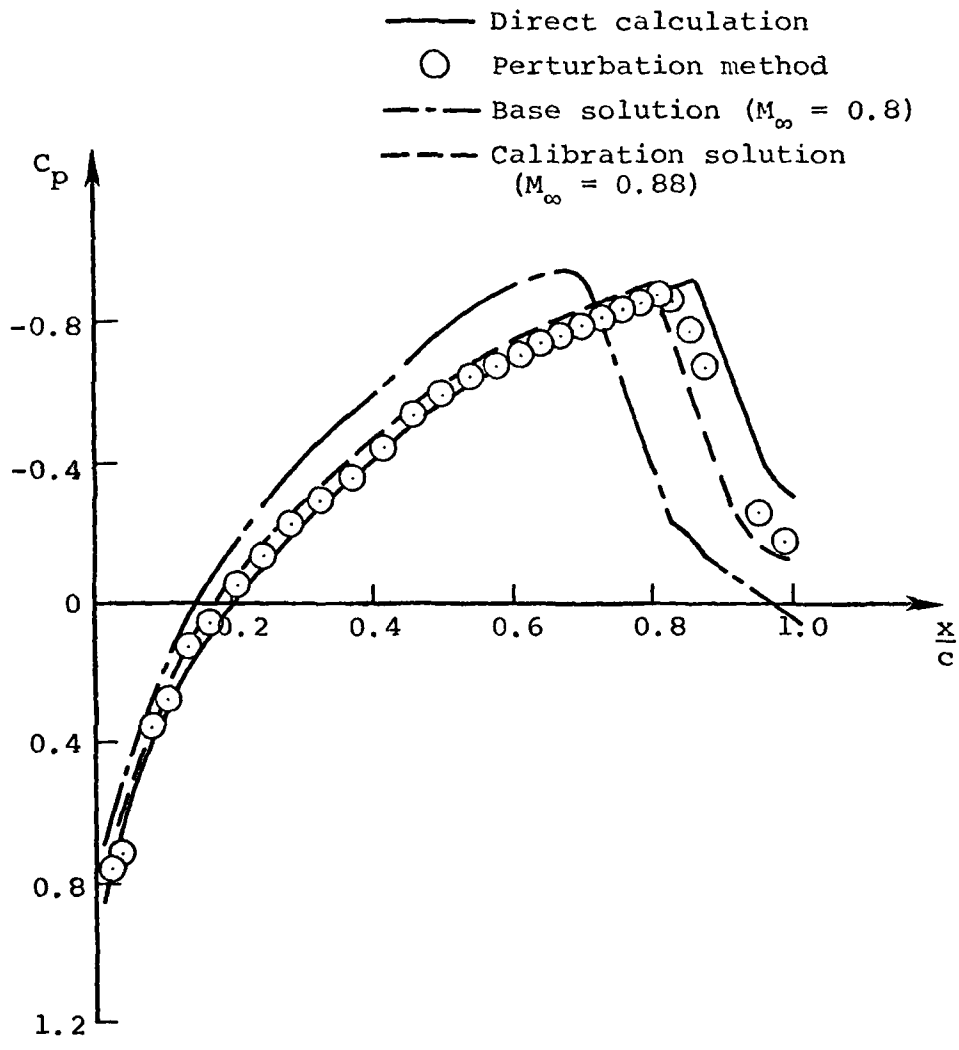

Figure 5.- Pressure distribution around the upper surface of NACA64A410 airfoil; $M_\infty = 0.9$, $\alpha = -3.0^\circ$.

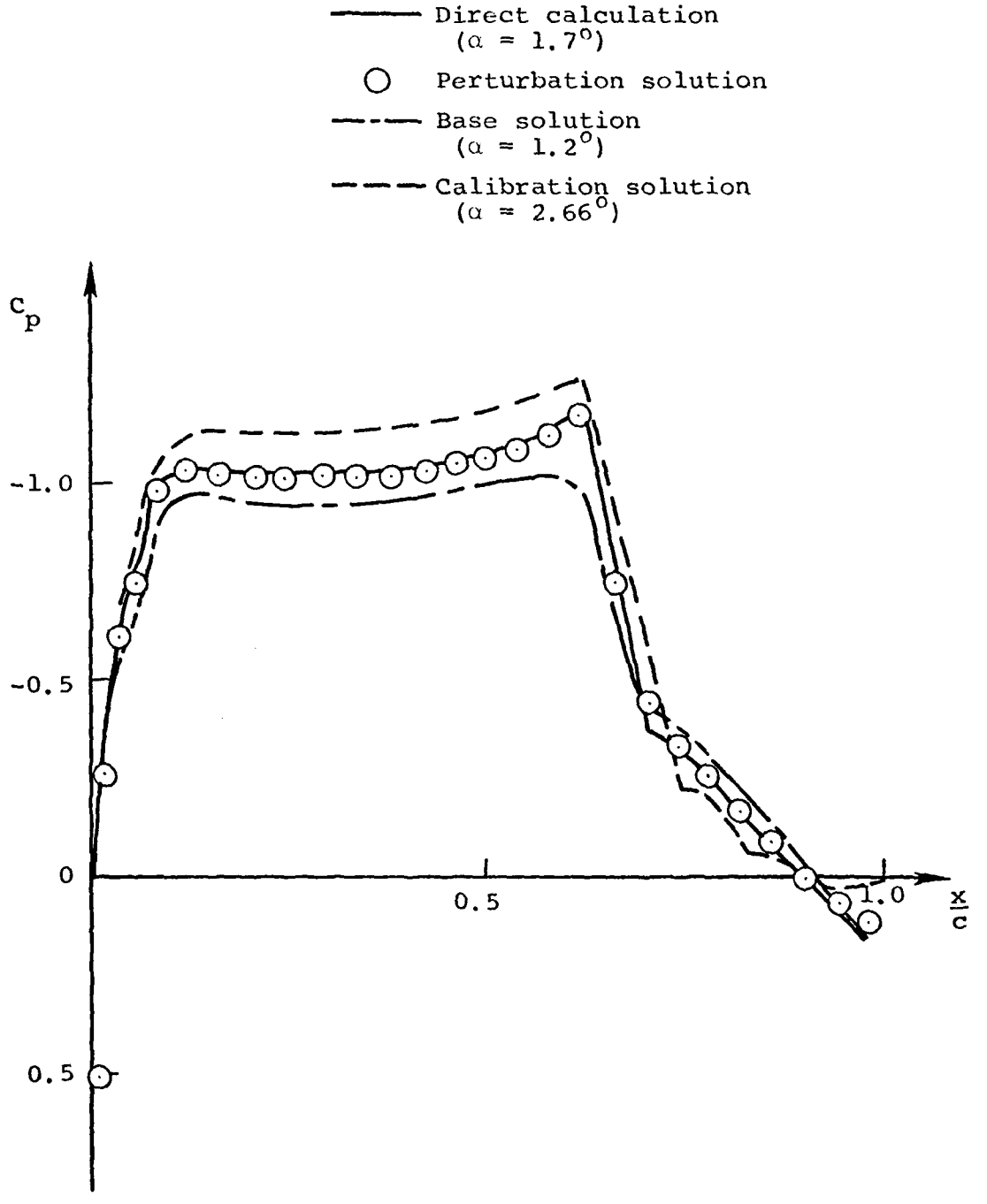

Figure 6.- Pressure distribution around the upper surface of Korn airfoil; $M_\infty = 0.755$, $\alpha = 1.7^\circ$.

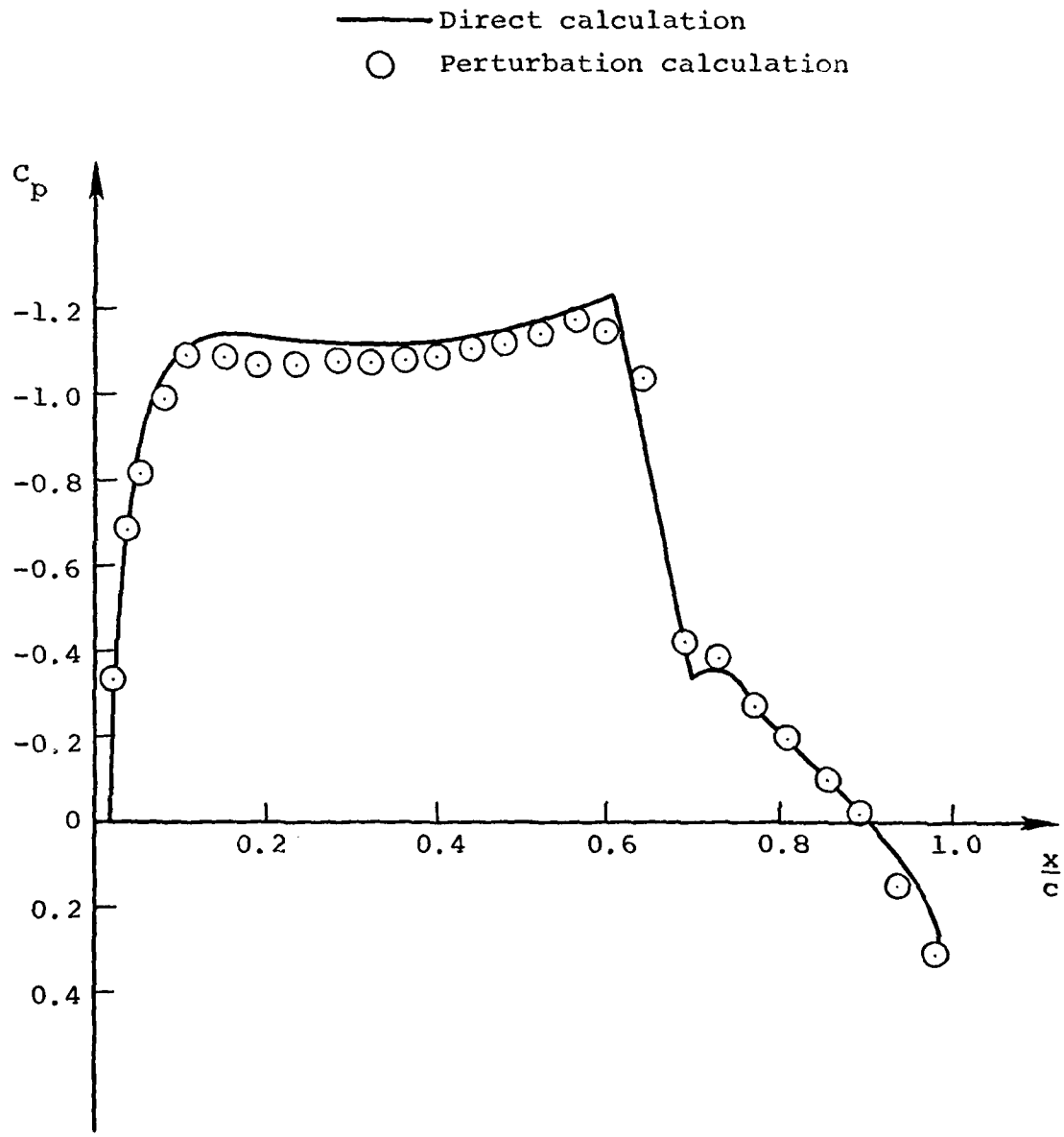

Figure 7.- Pressure distribution around the upper surface of a Korn airfoil; $M_\infty = 0.75$, $\alpha = 2^\circ$.

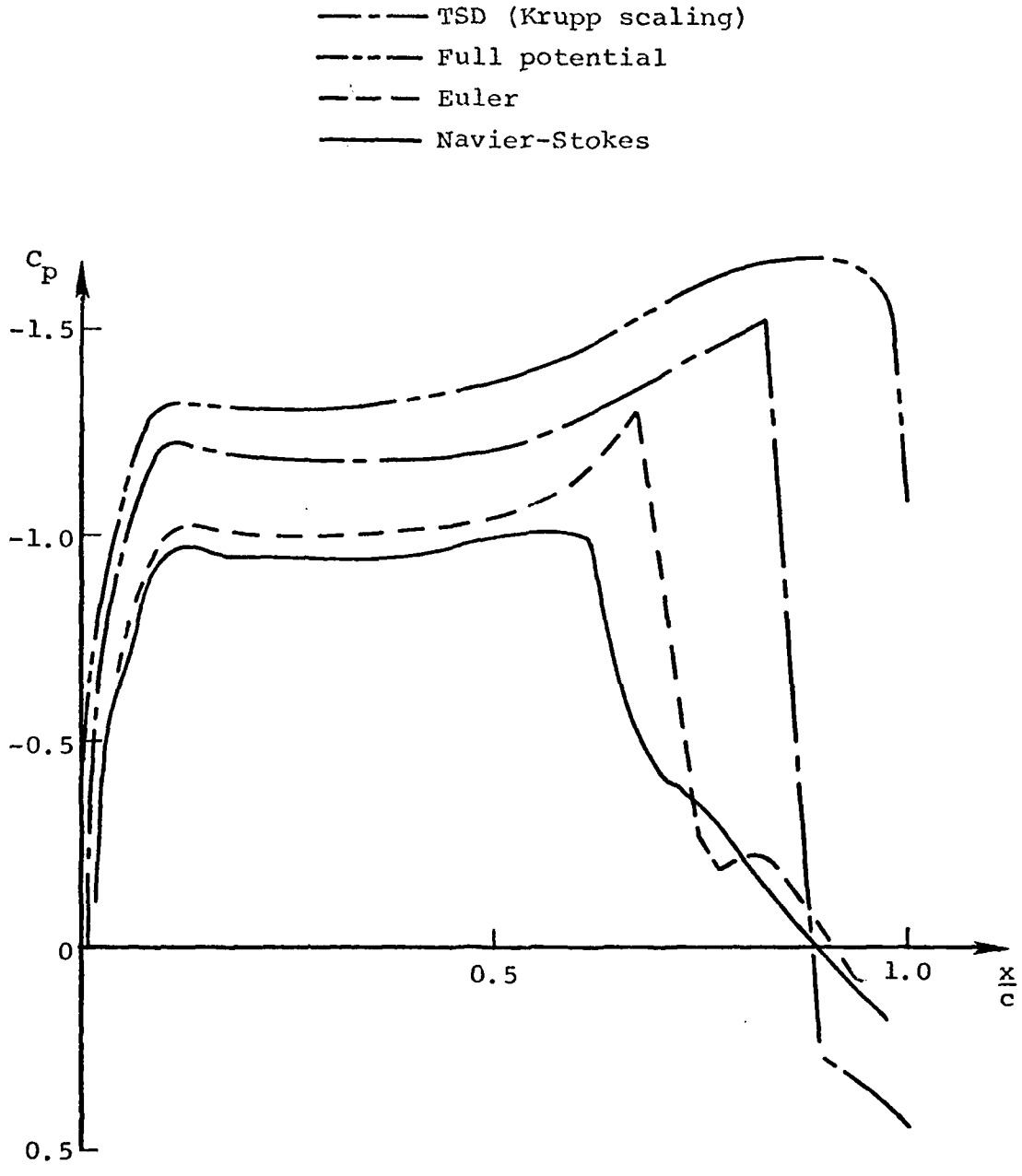

Figure 8.- Pressure distribution over the upper surface of a Korn airfoil; $M_\infty = 0.75$, $\alpha = 1.2^o$.

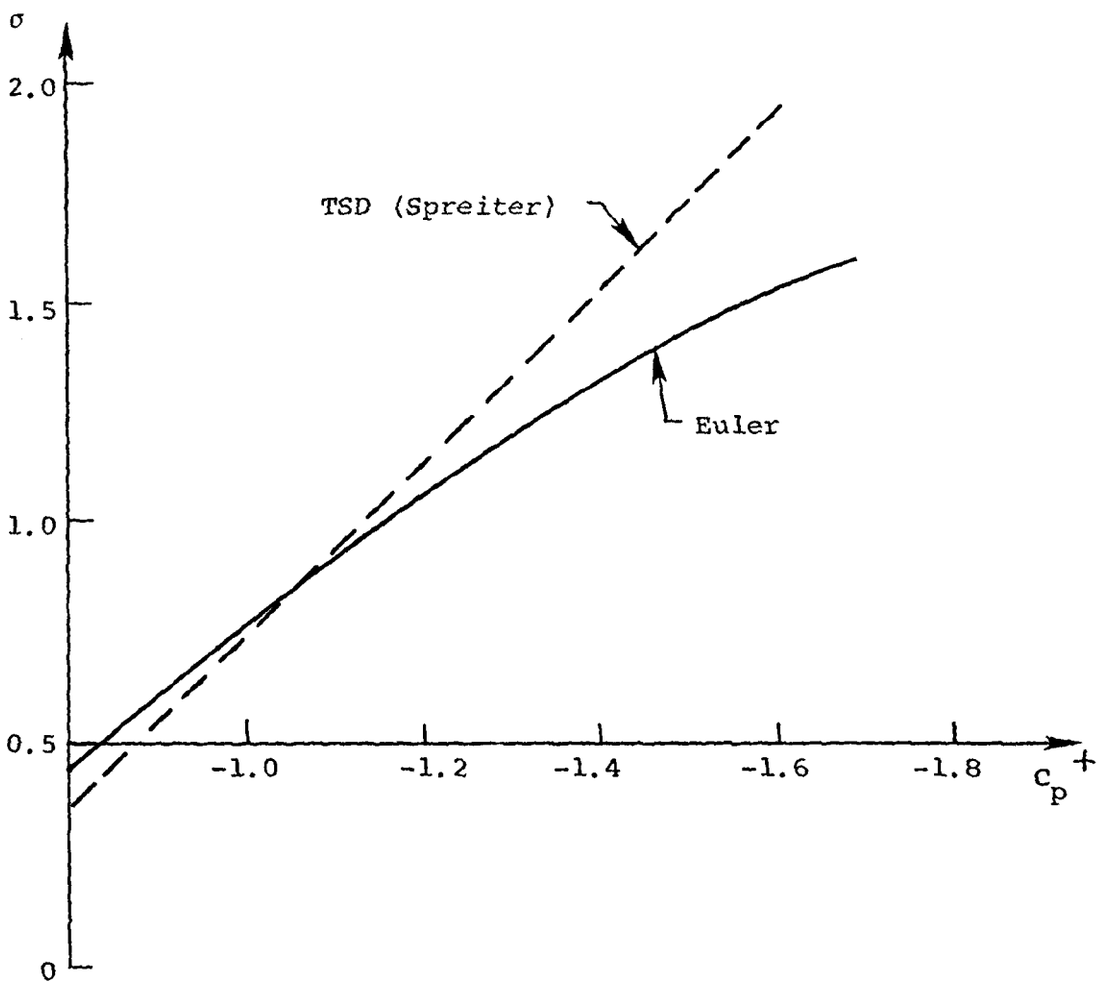

Figure 9.- Variation of shock strength with pre-shock pressure. (M_∞ = 0.755)

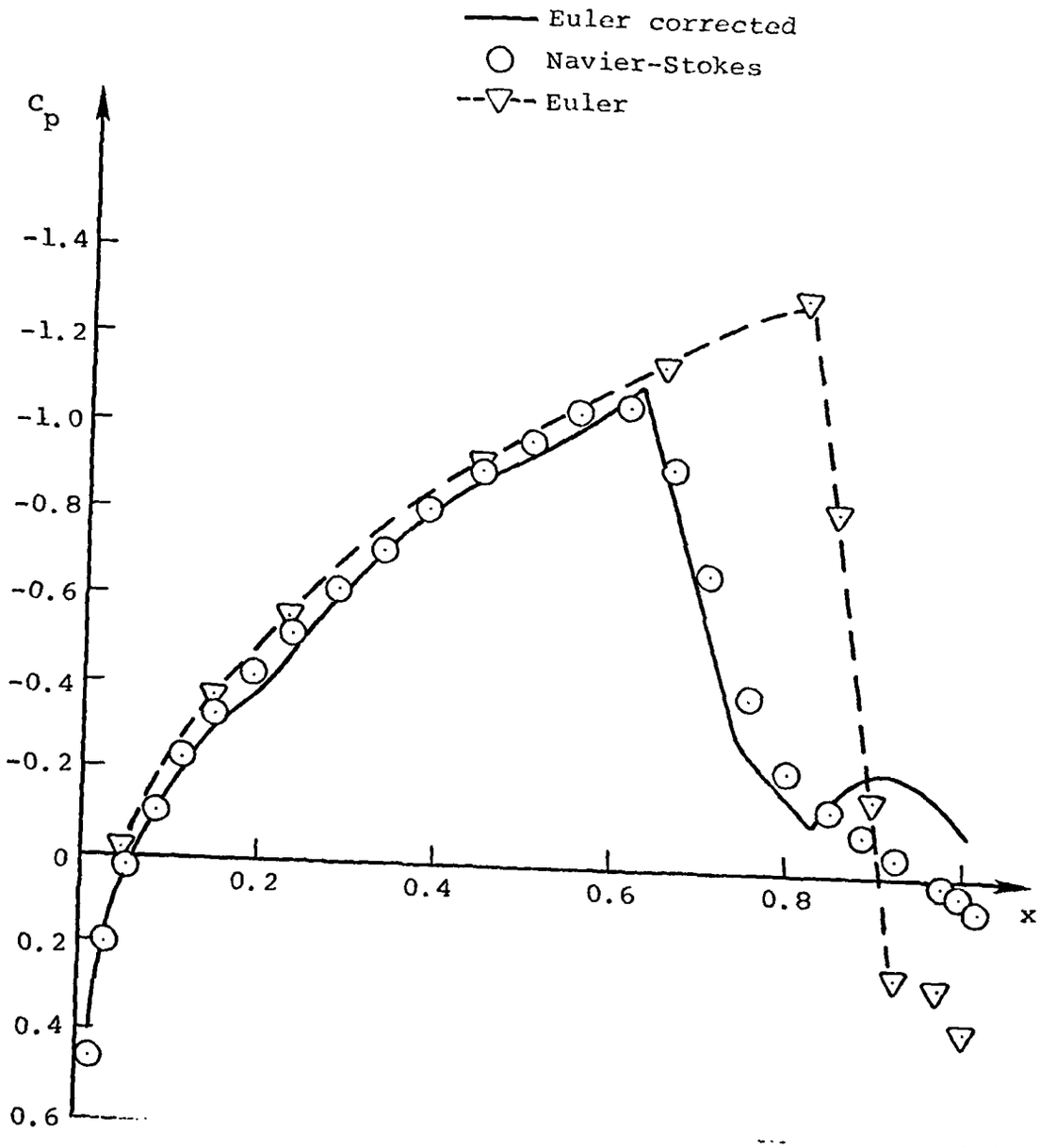

Figure 10.- Pressure distribution around NACA64A410 airfoil; $M_\infty = 0.8$, $\alpha = 0^o$.

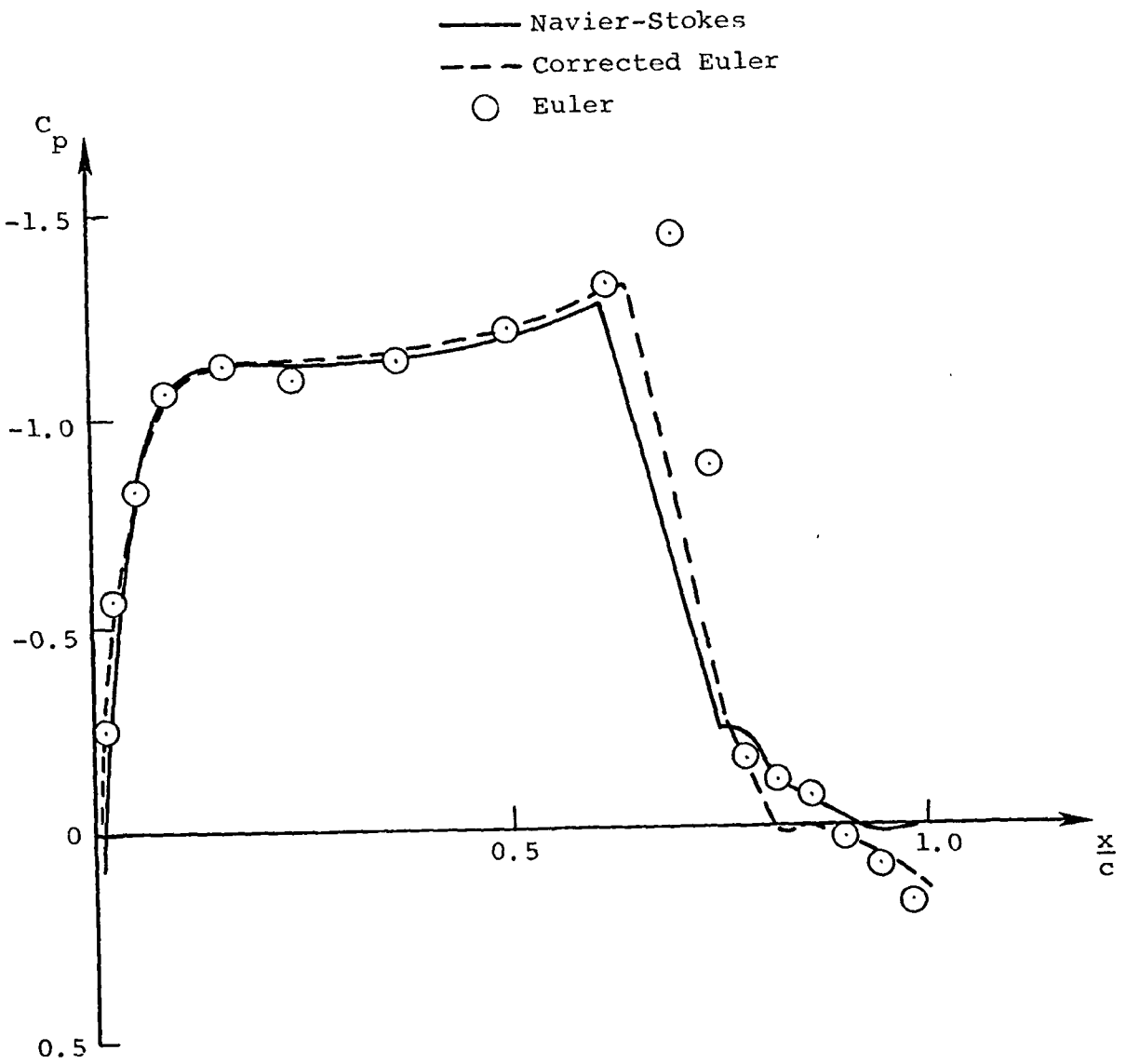

Figure 11.- Pressure distribution around the upper surface of a Korn airfoil; $M_\infty = 0.755$, $\alpha = 2.66$.

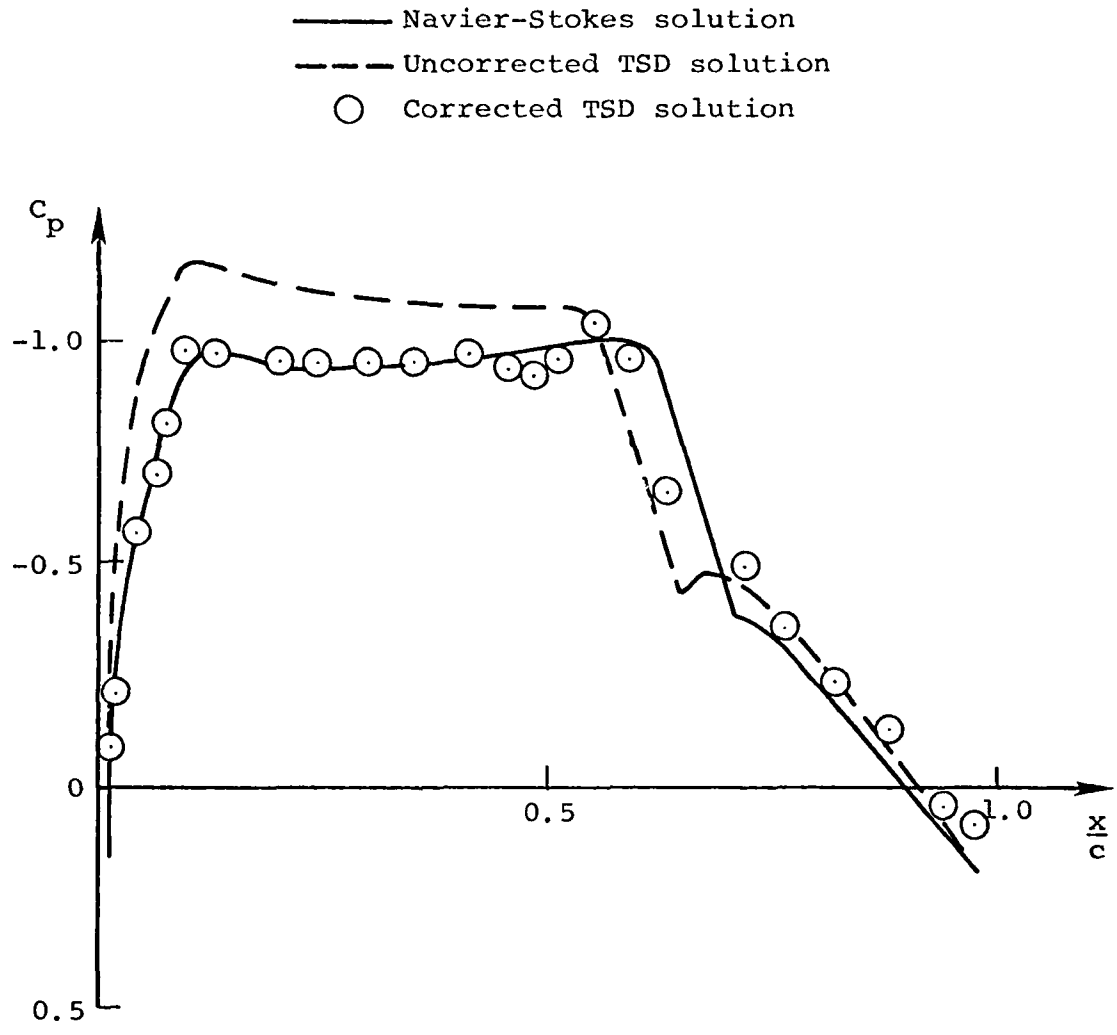

Figure 12.- Pressure distribution around the upper surface of a Korn airfoil; $M_\infty = 0.755$, $\alpha = 1.2^\circ$.

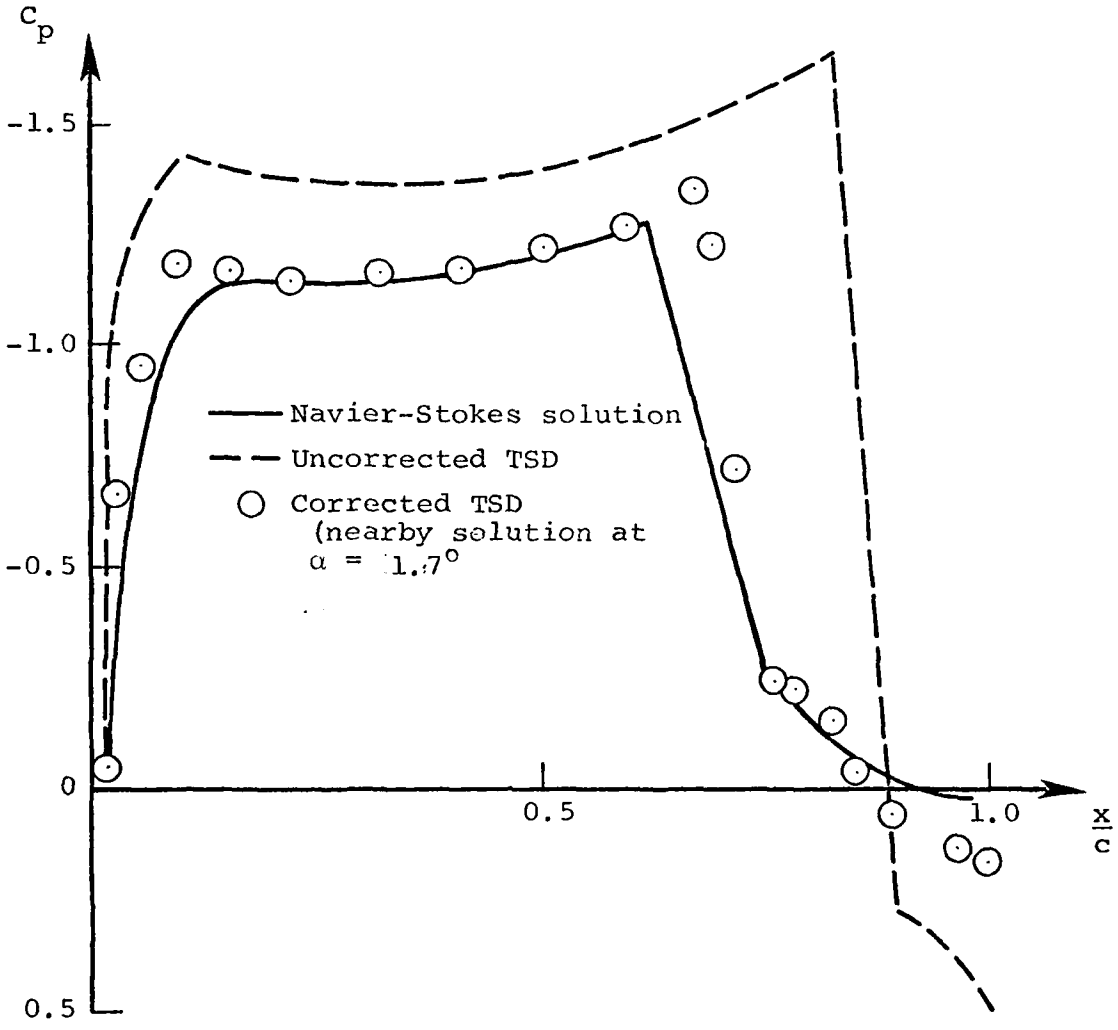

Figure 13.- Pressure distribution around the upper surface of a Korn airfoil; $M_\infty = 0.755$, $\alpha = 2.66^\circ$.

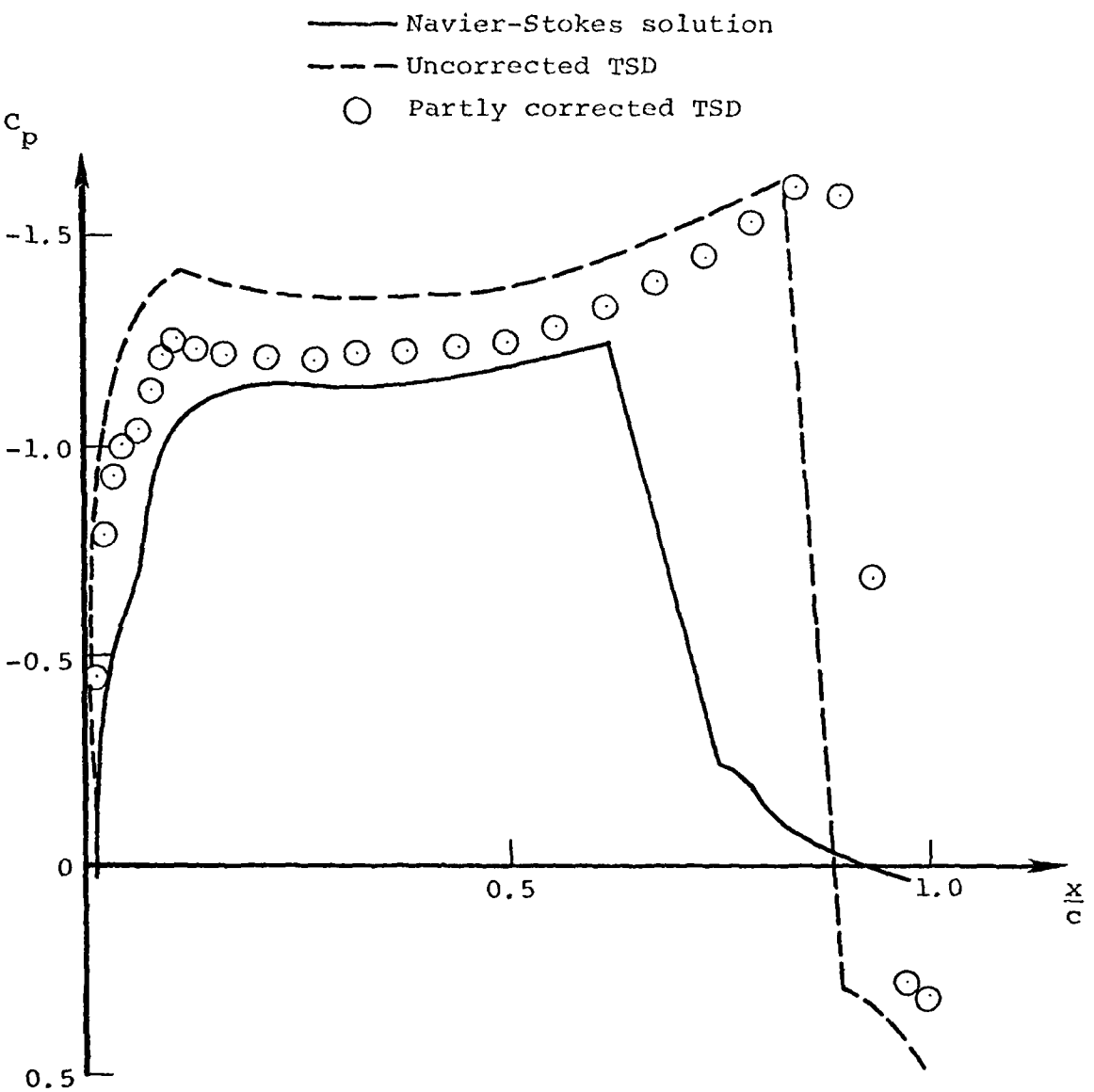

Figure 14.- Pressure distribution around the upper surface of a Korn airfoil; $M_\infty = 0.755$, $\alpha = 2.66^\circ$.

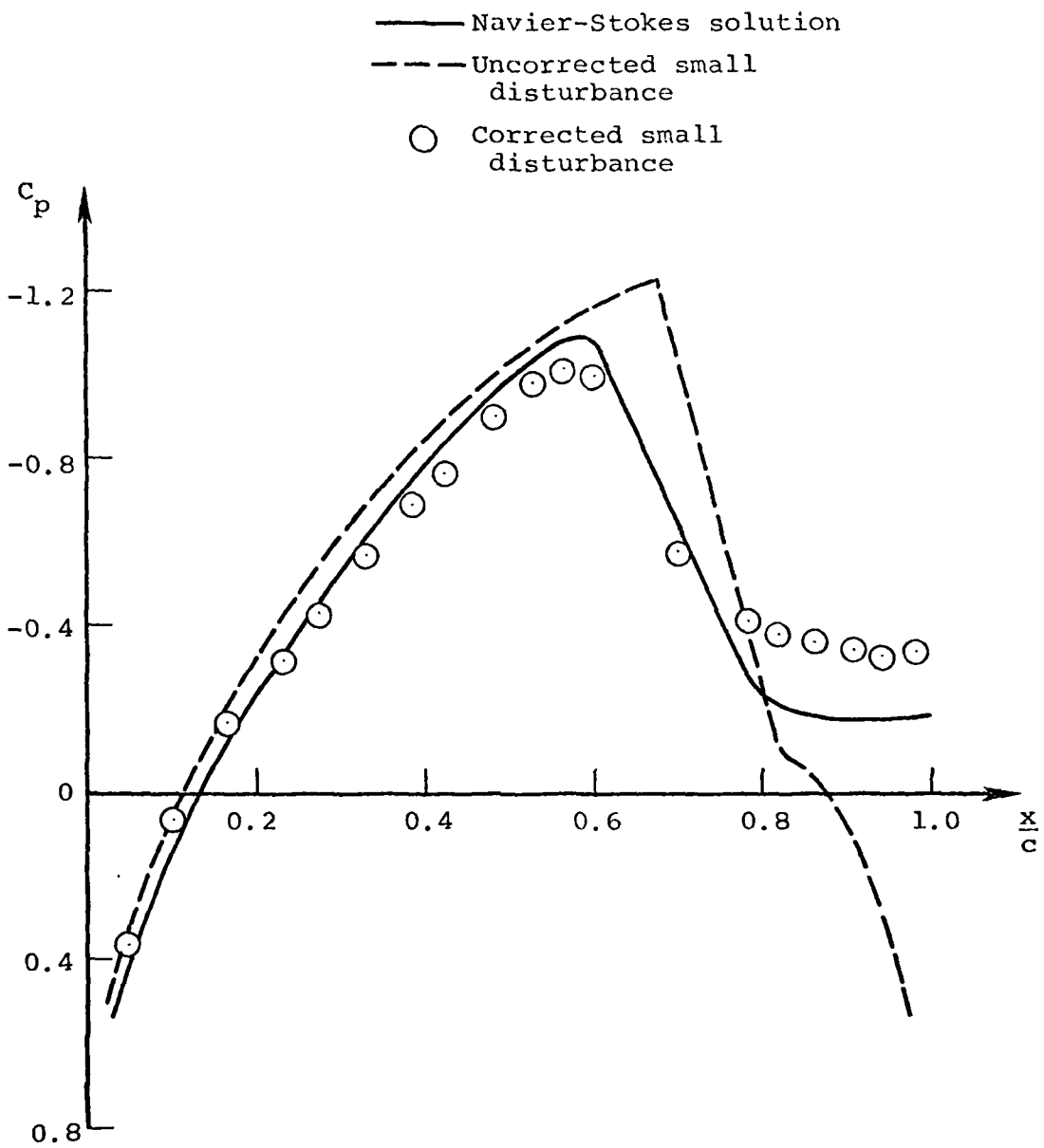

Figure 15.- Pressure distribution around a 18-percent Biconvex airfoil; $M_\infty = 0.775$, $\alpha = 0^o$.

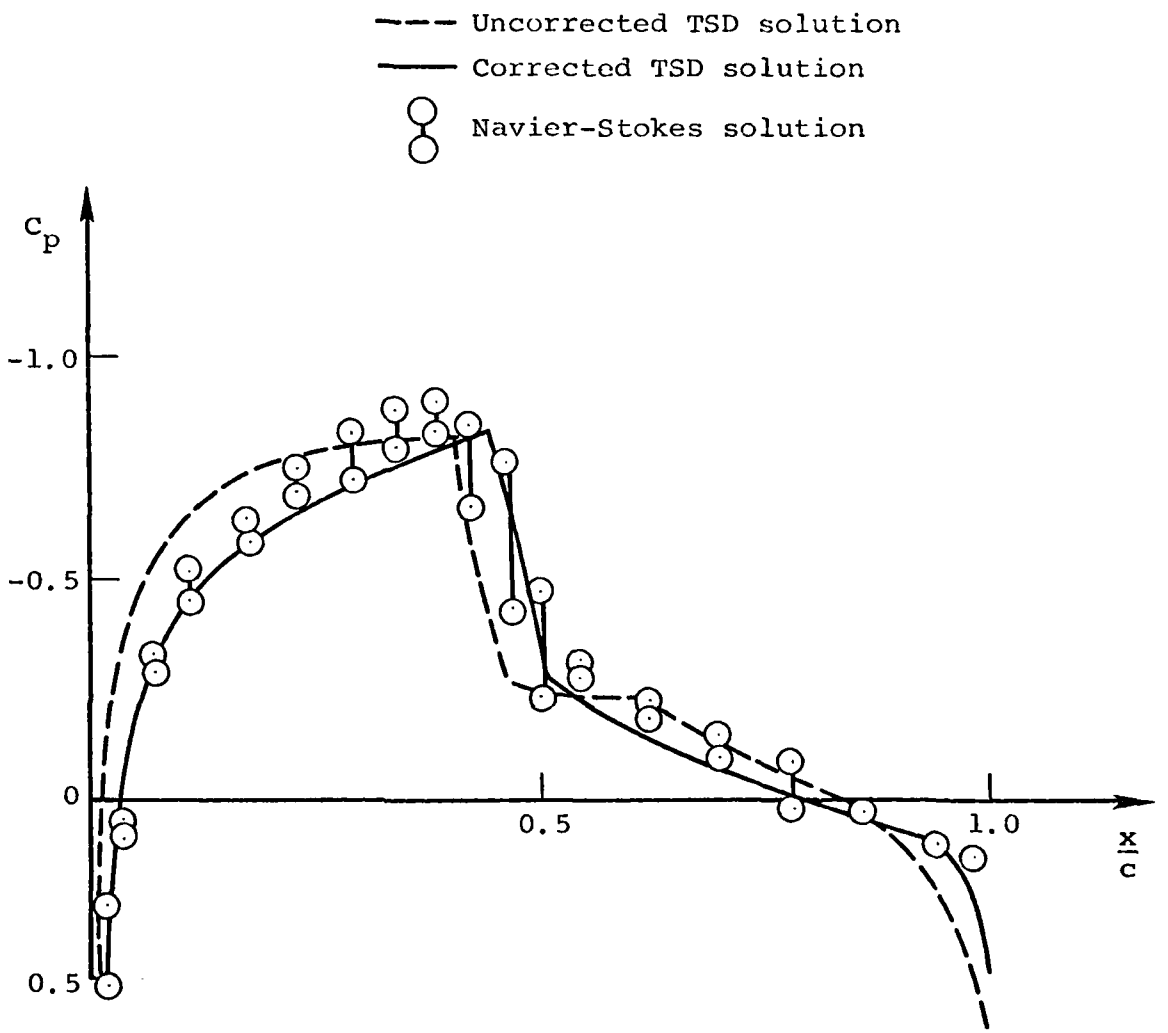

Figure 16.- Pressure distribution around a NACA0012 airfoil; $M_\infty = 0.8$, $\alpha = 0^o$.

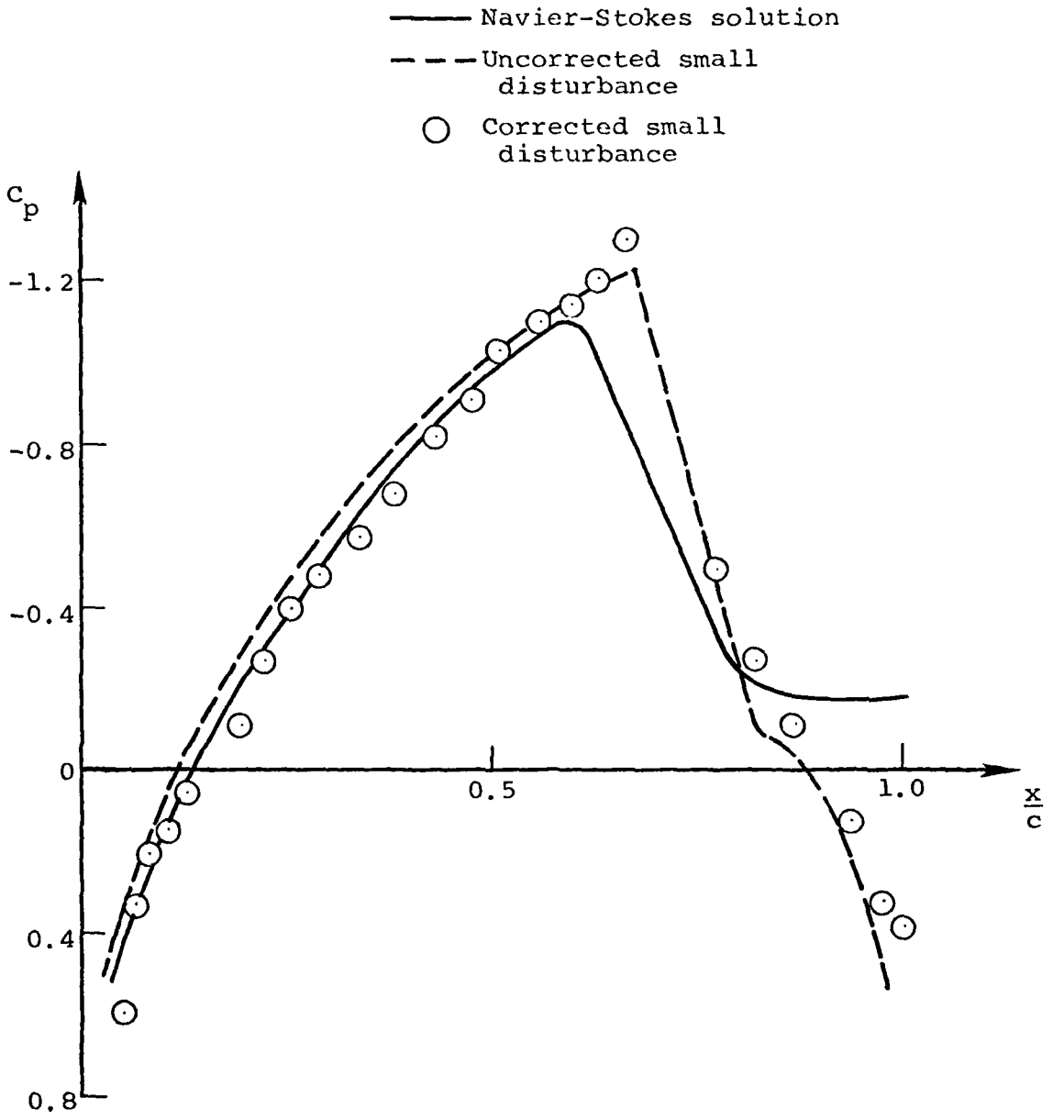

Figure 17.- Pressure distribution around a 18-percent biconvex airfoil; $M_\infty = 0.775$, $\alpha = 0^\circ$.

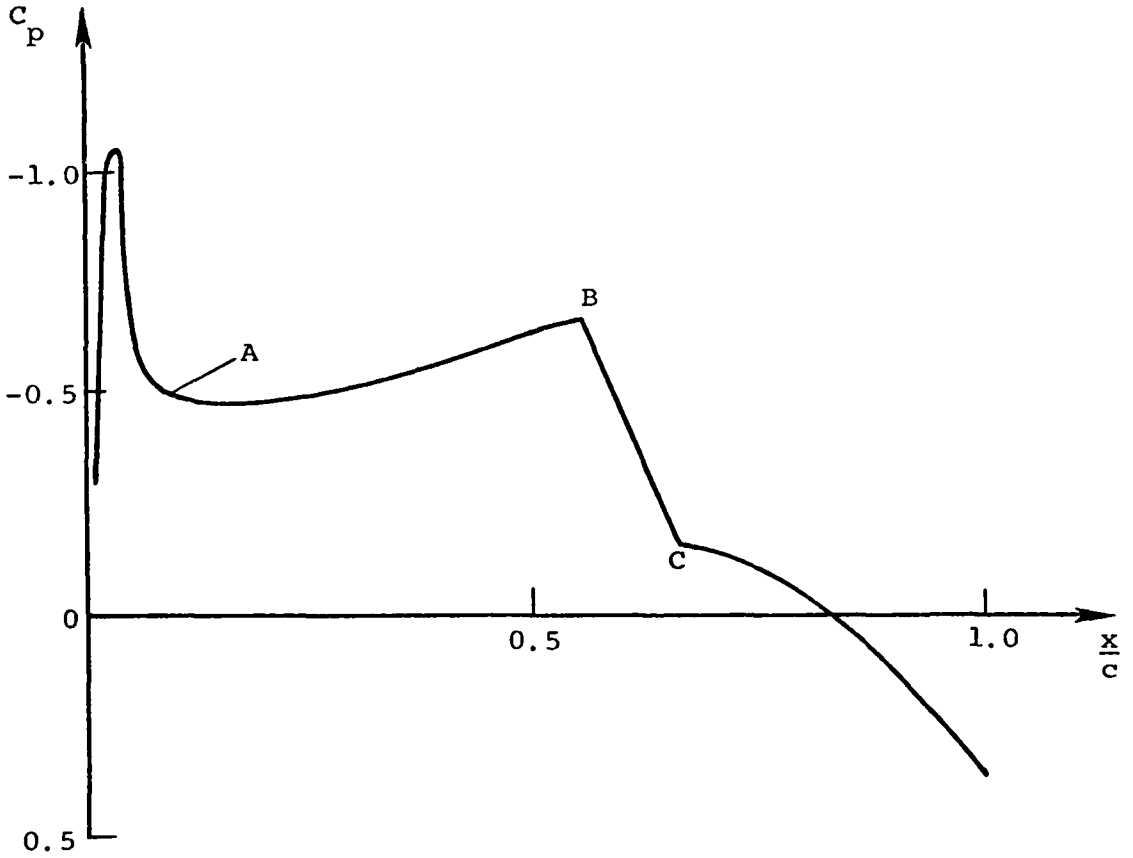

Figure 18.- Sketch of typical pressure distribution over the upper surface of the ONERA M6 wing.

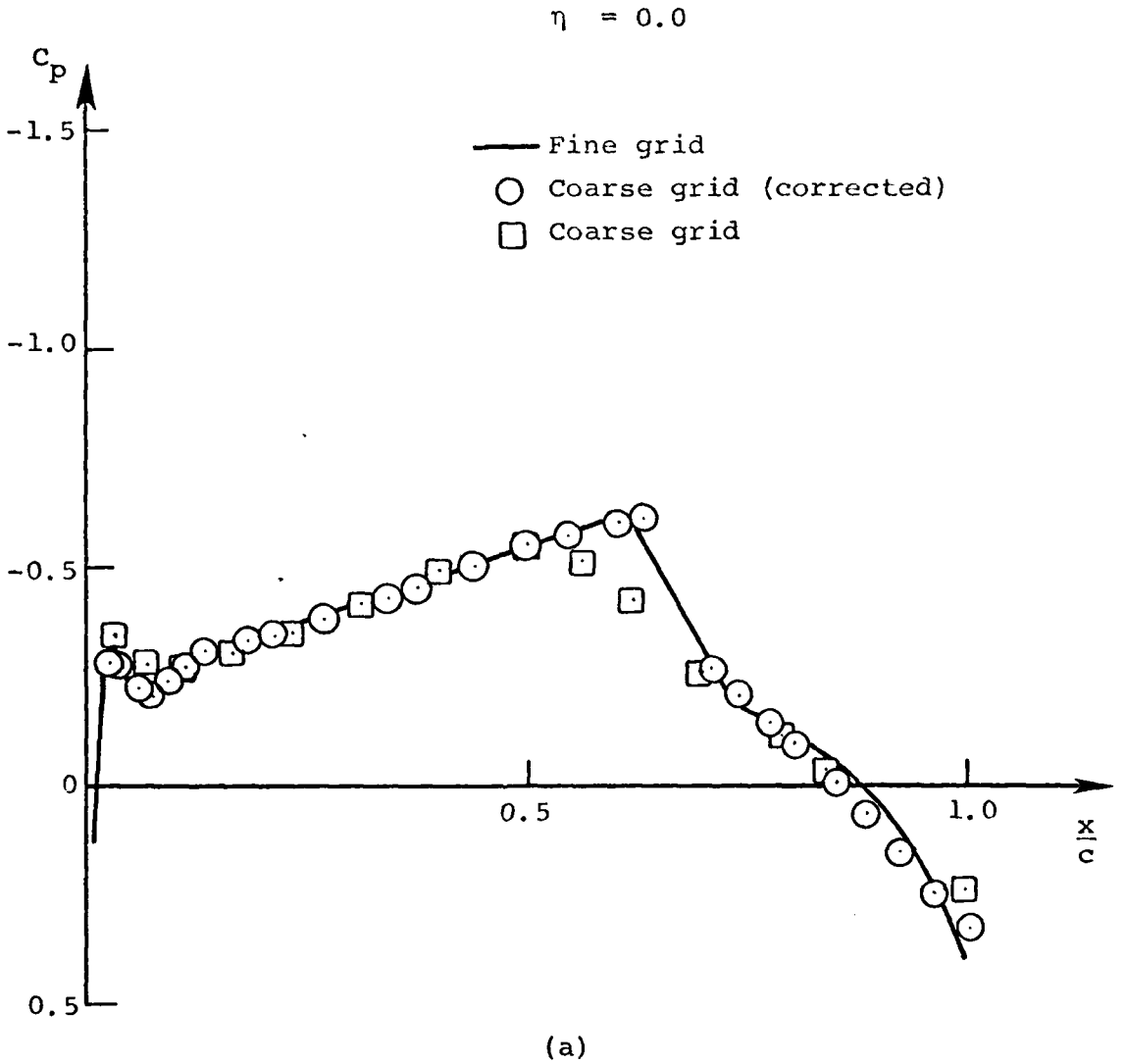

(a)

Figure 20.- Pressure distribution over the upper surface of the ONERA M6 wing; $M_\infty = 0.84$, $\alpha = 3.06$ (grid correction, full potential equation).

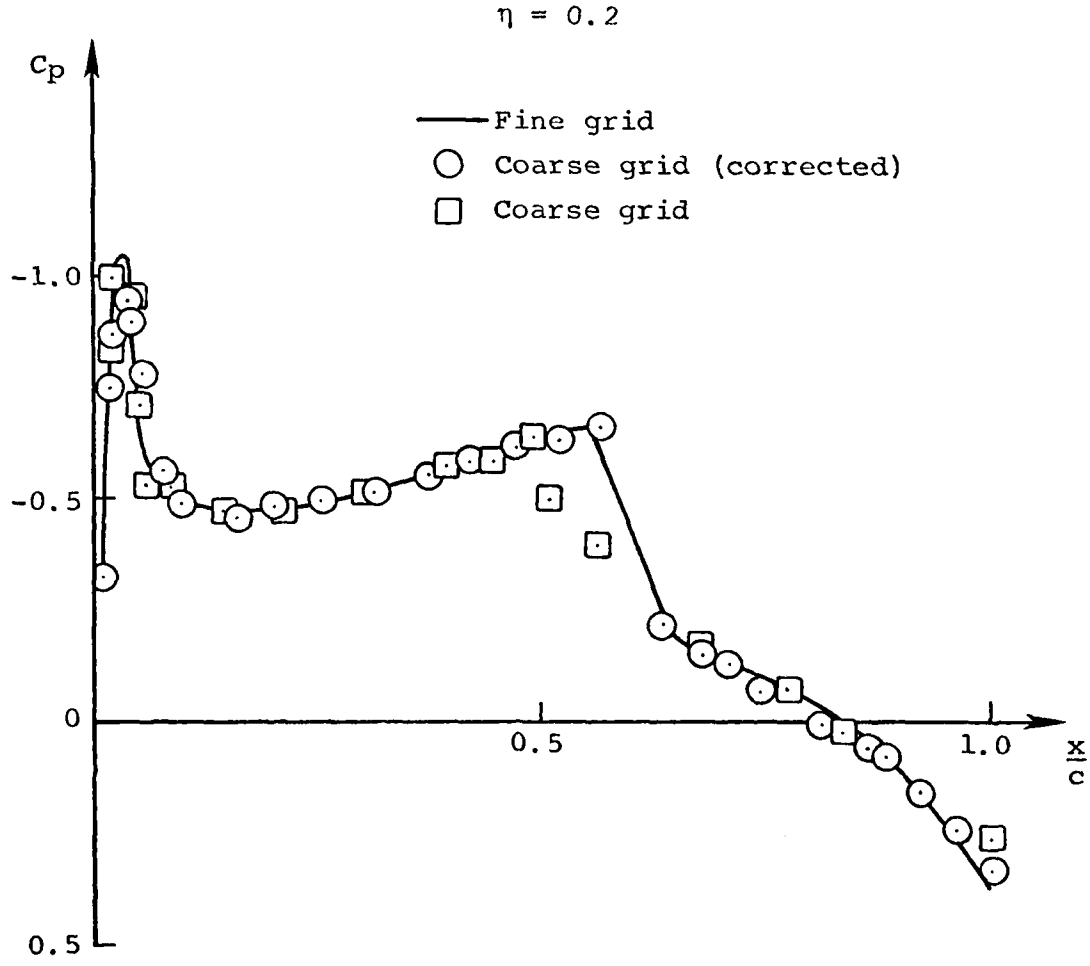

(b)

Figure 20.- Continued.

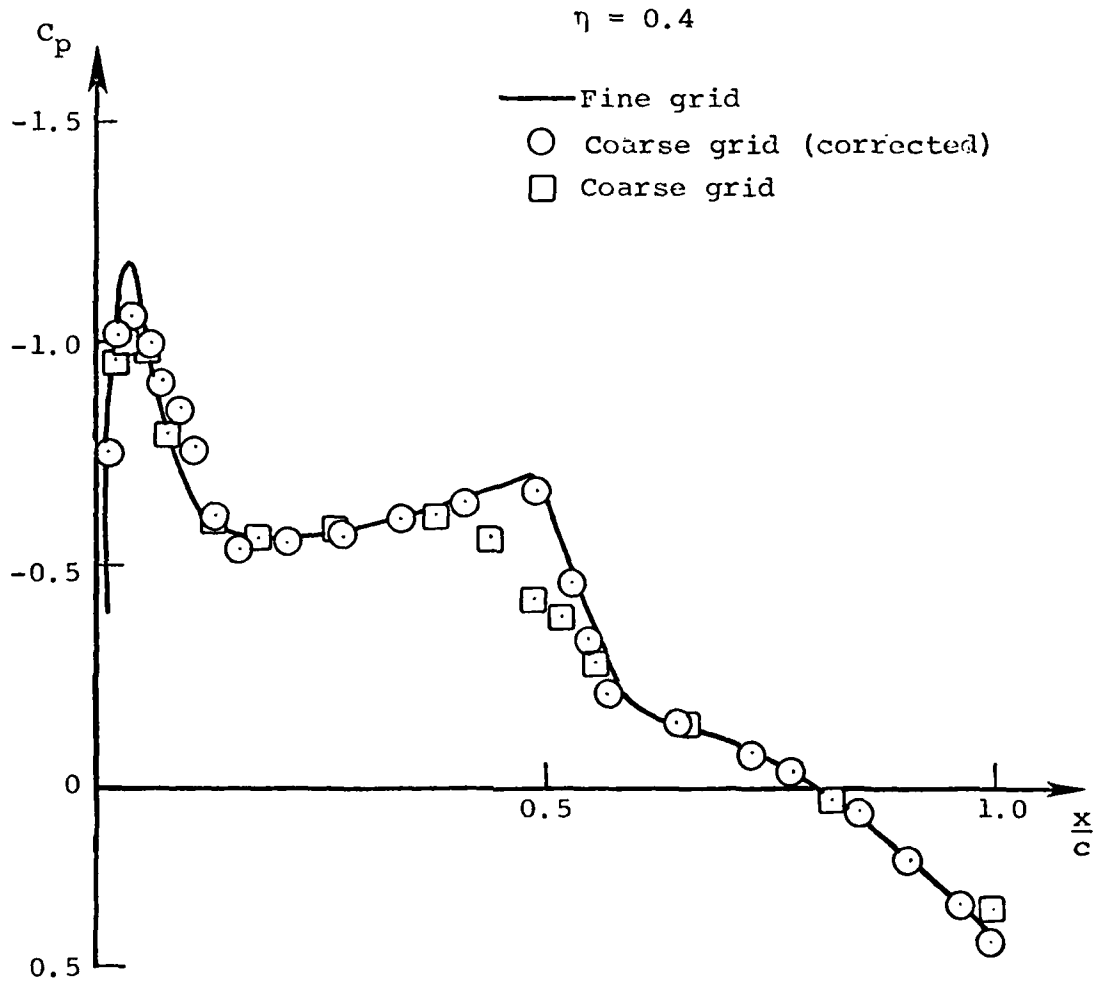

(c)

Figure 20.- Continued.

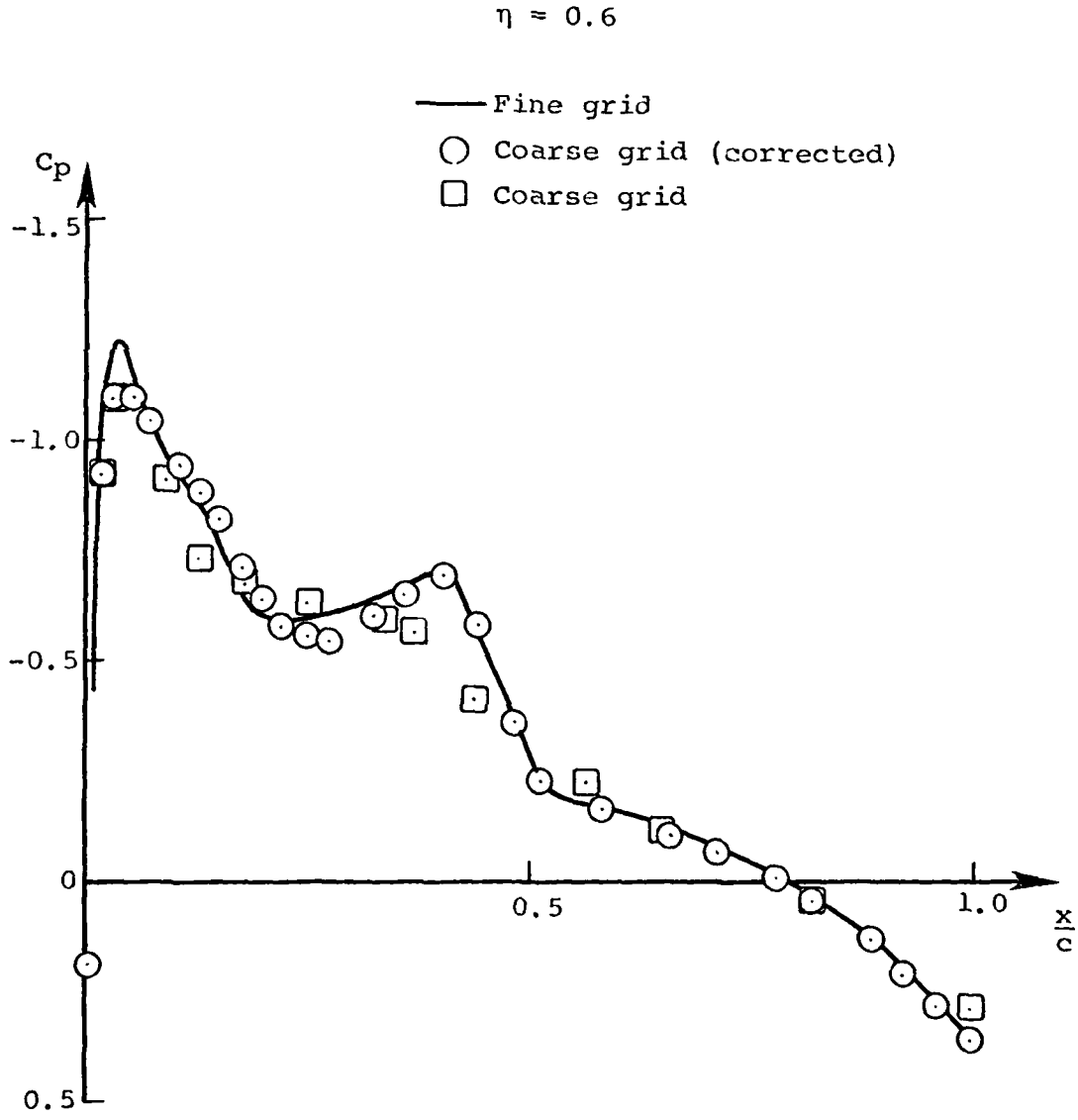

(d)

Figure 20.- Concluded.

$\eta = 0.0$

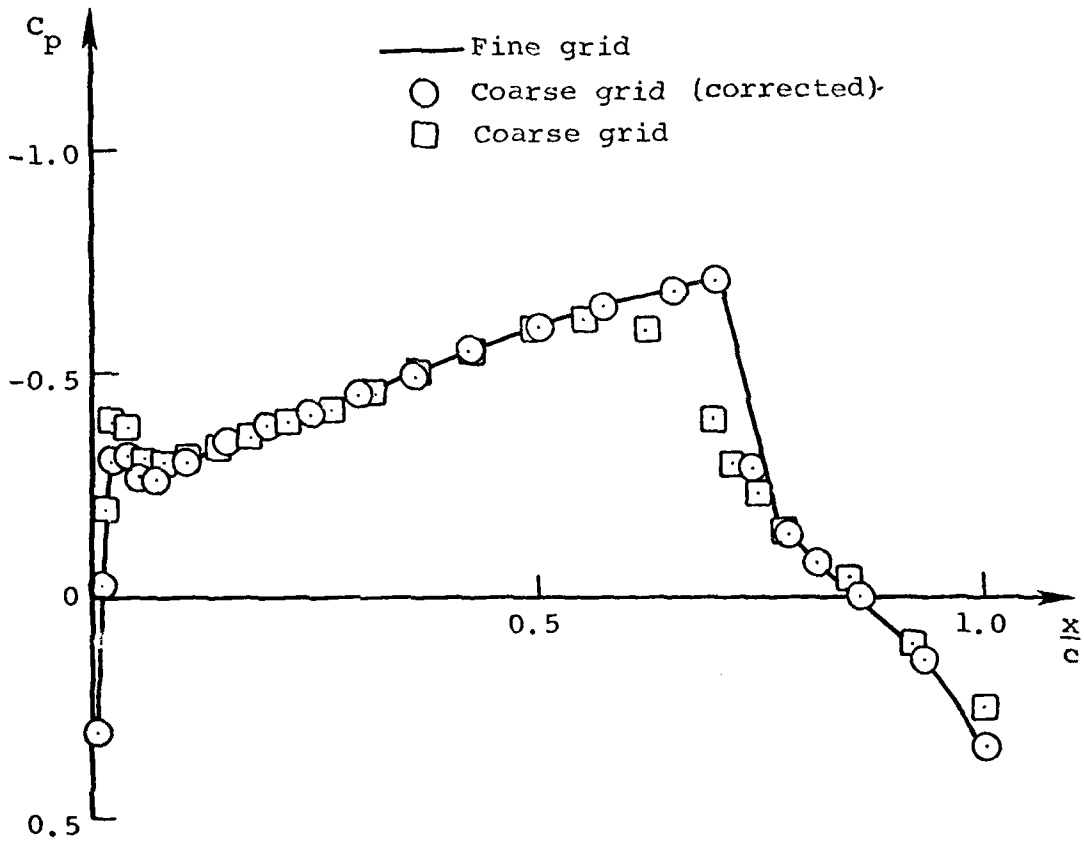

(a)

Figure 21.- Pressure distribution over the upper surface of the ONERA 176 wing; $M_\infty = 0.84$, $\alpha = 3.06$, $\theta_{twist} = 3^\circ$. (grid correction, full potential equation).

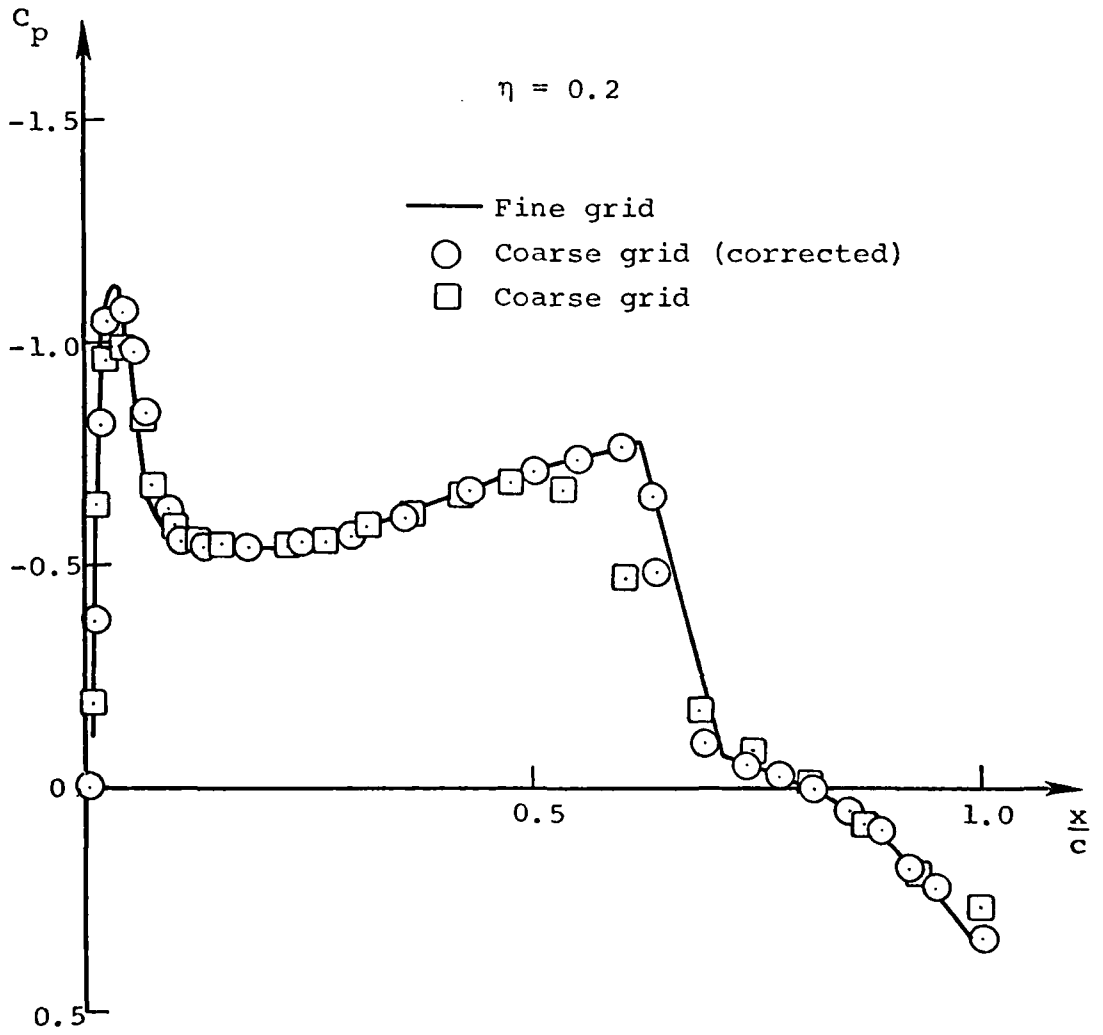

(b)

Figure 21.- Continued.

η = 0.4

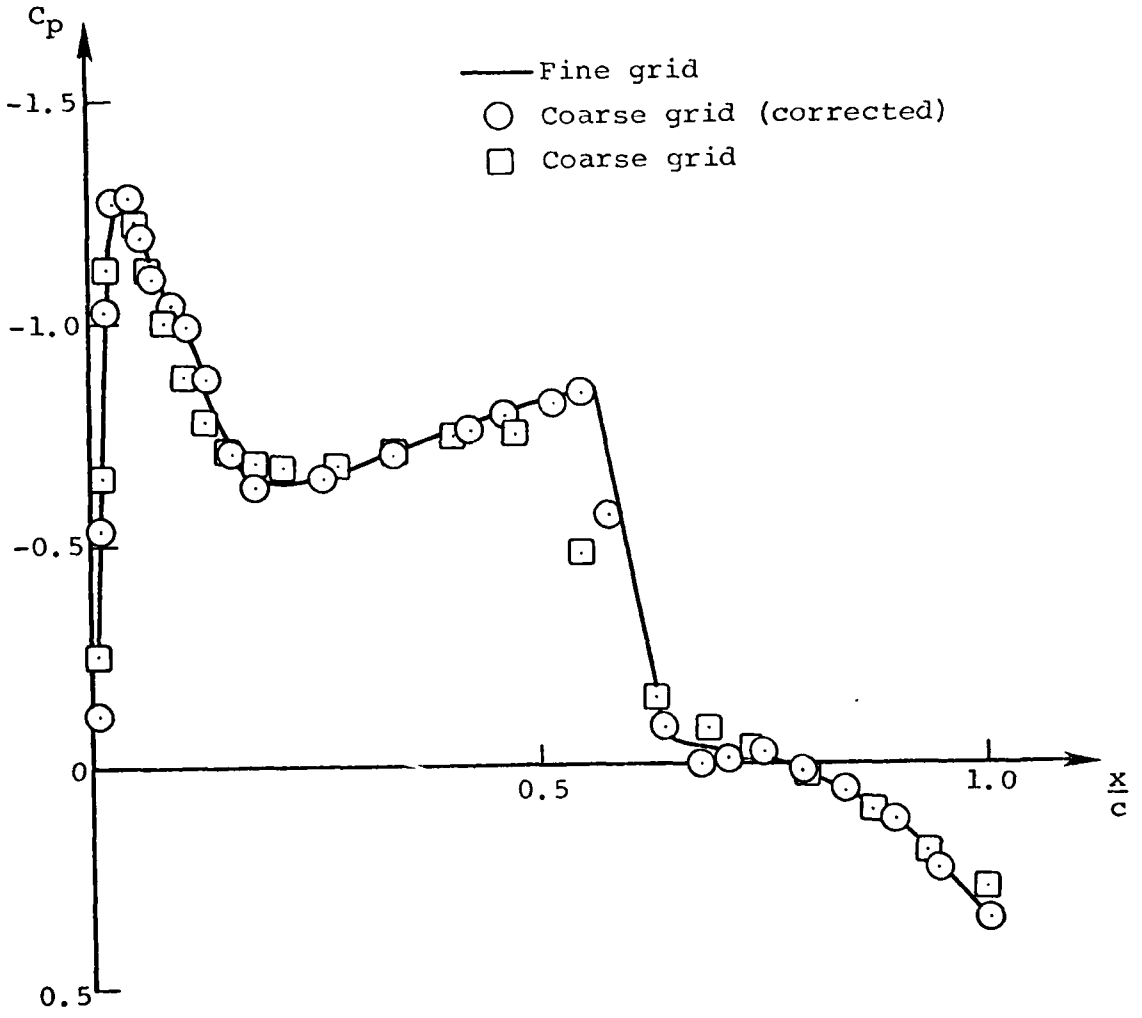

(c)

Figure 21.- Continued.

η = 0.6

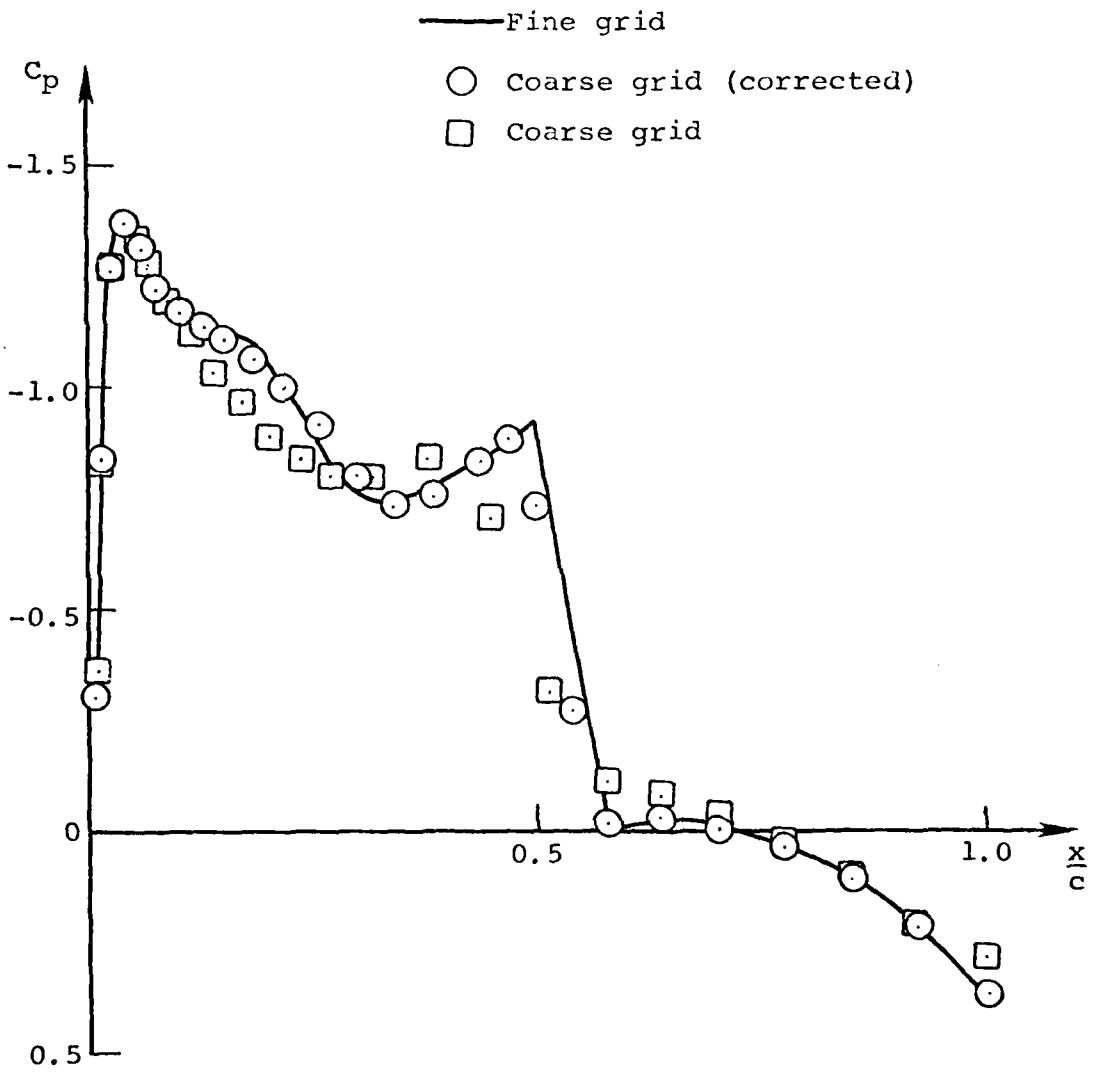

(d)

Figure 21.- Concluded.

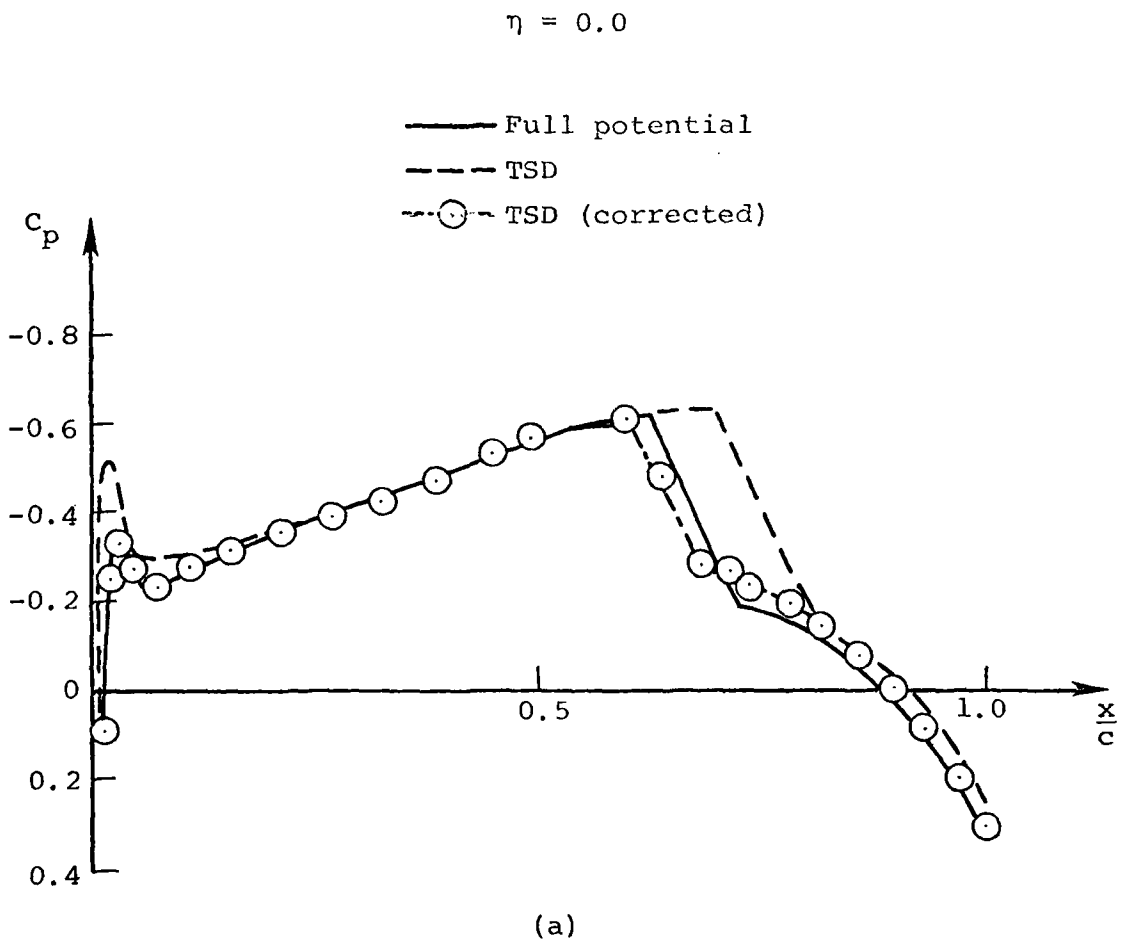

(a)

Figure 22.- Pressure distribution around the upper surface of ONERA M6 wing; $M_\infty = 0.84$, $\alpha = 3.06^\circ$ (TSD/full potential equation correction).

$\eta = 0.35$

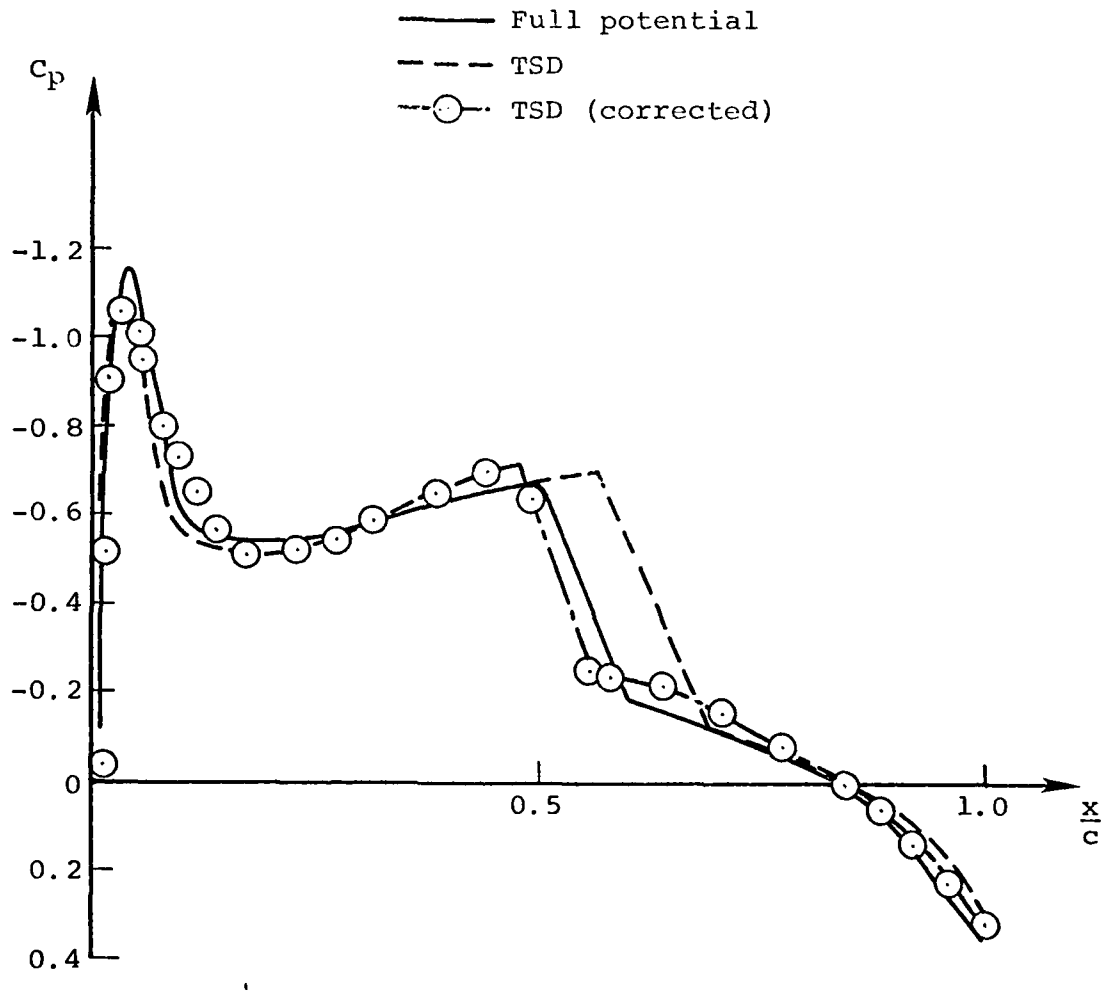

(b)

Figure 22.- Continued.

$\eta = 0.65$

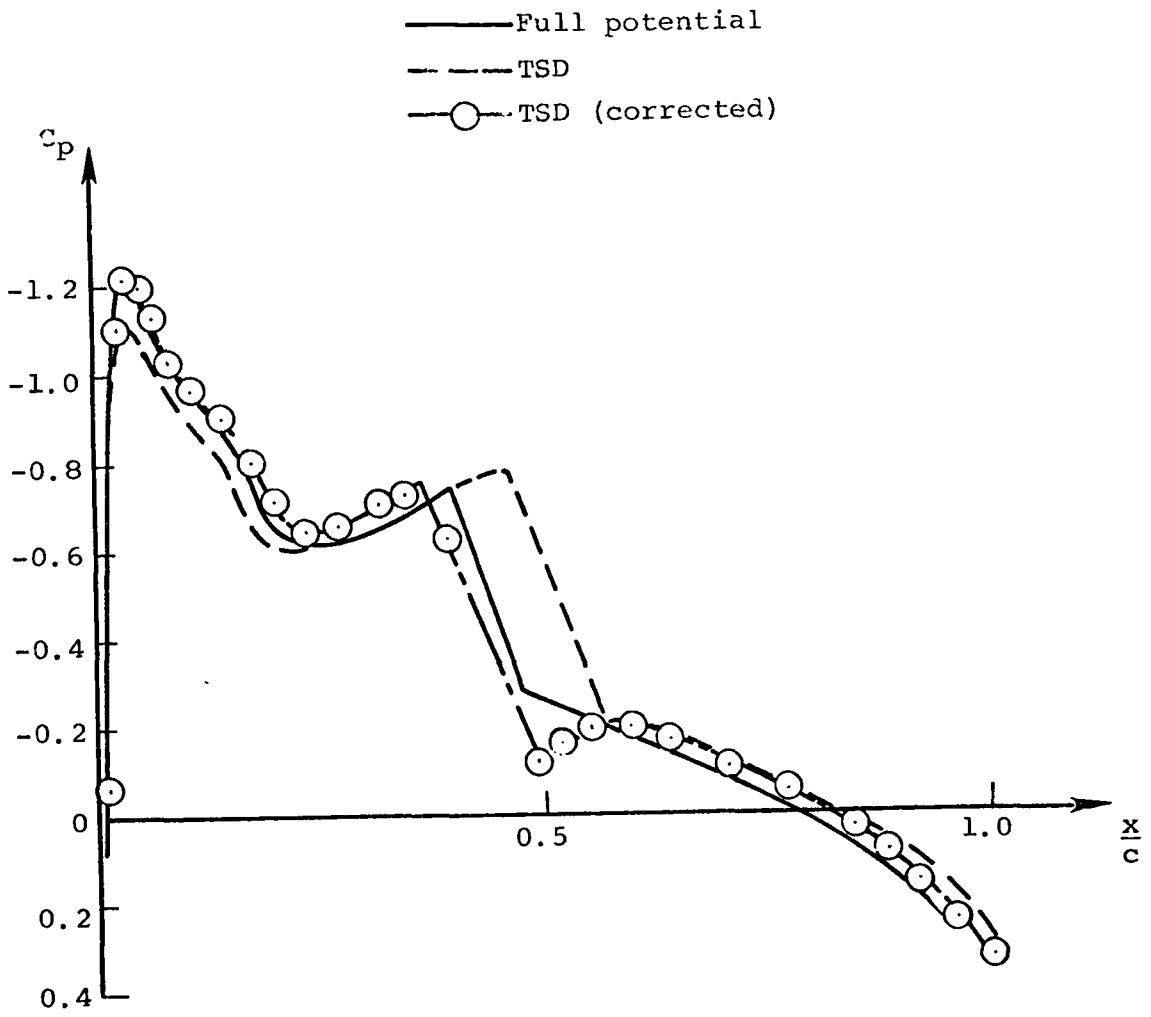

(c)

Figure 22.- Concluded.

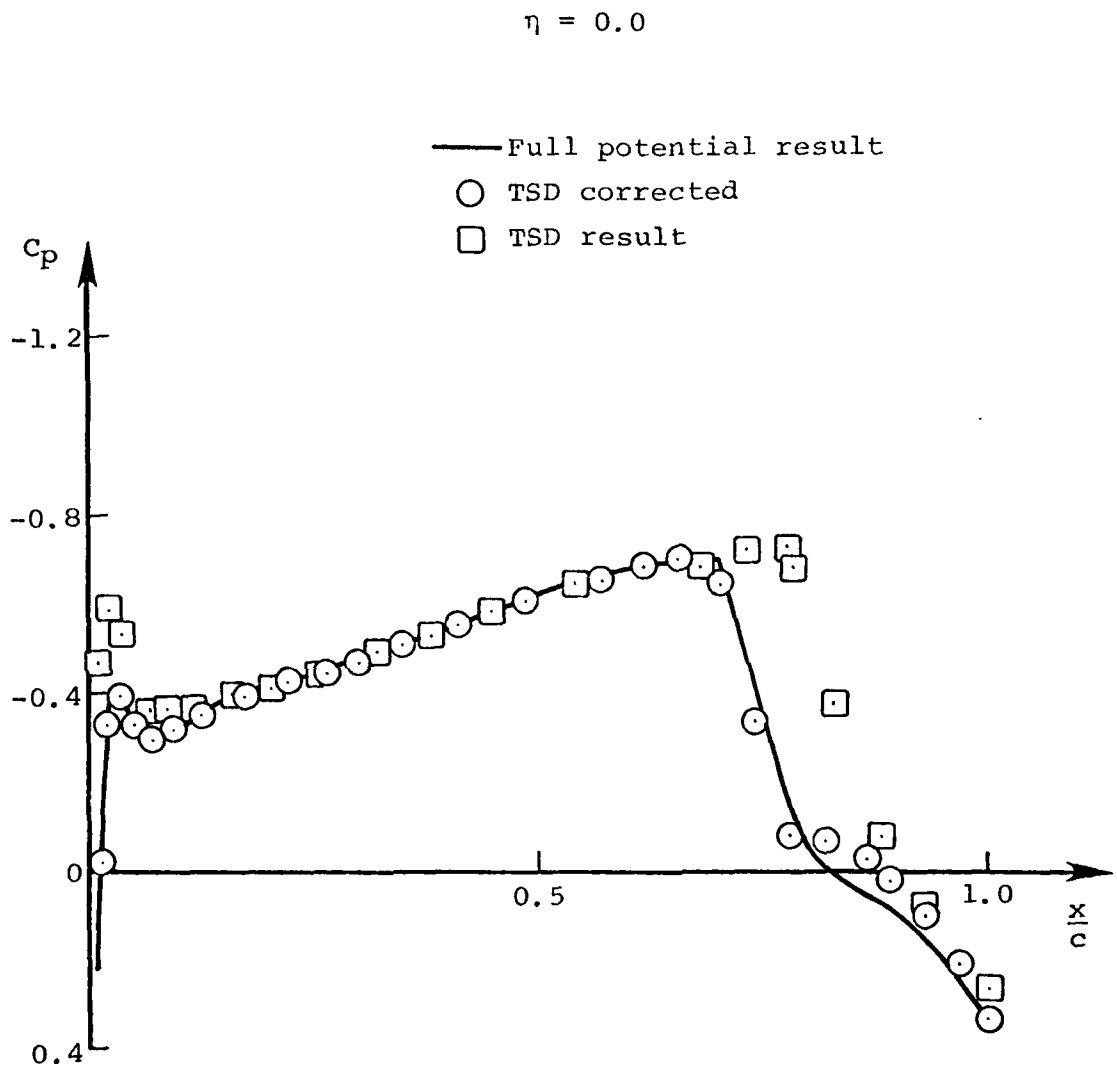

(a)

Figure 23.- Pressure distribution over the upper surface of the ONERA M6 wing; $\alpha = 4^{\circ}$, $\theta_{twist} = 1.5^{\circ}$ (TSD/full potential equation correction)

$\eta = 0.35$

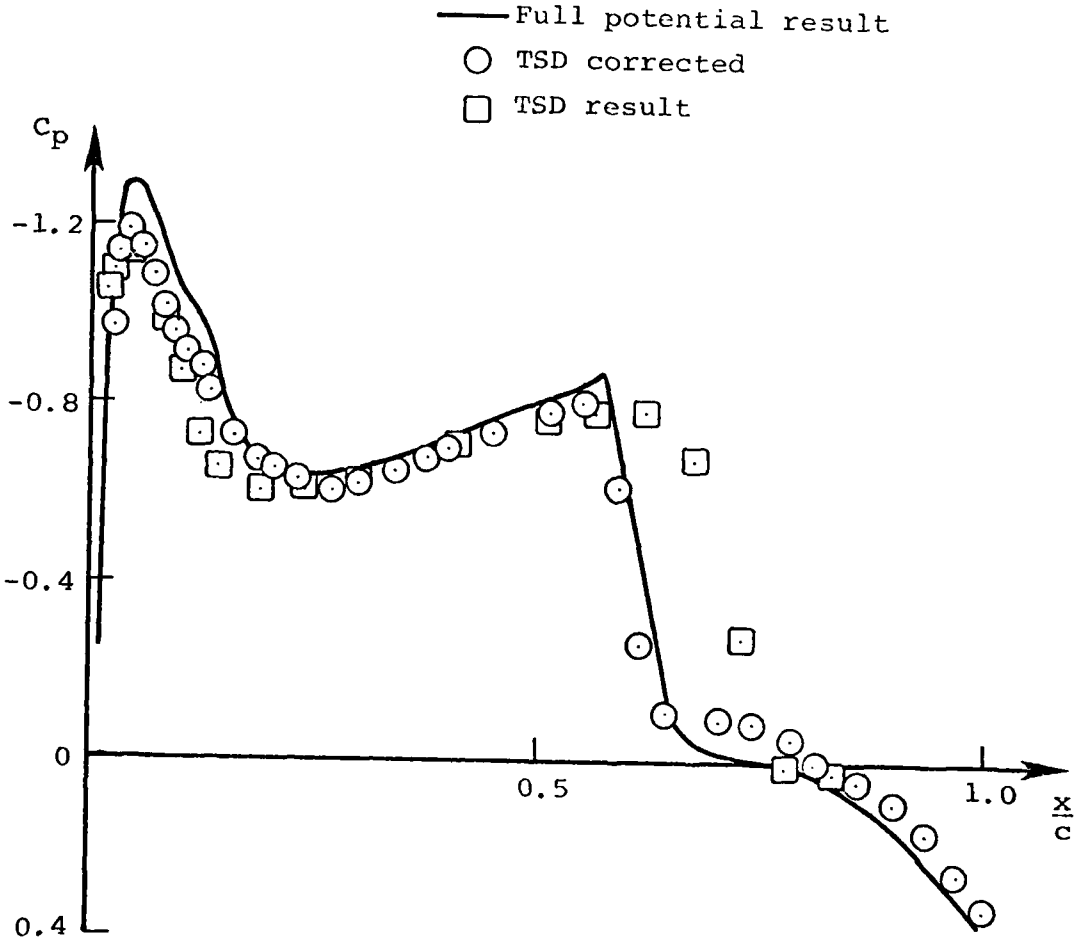

(b)

Figure 23.- Continued.

η = 0.65

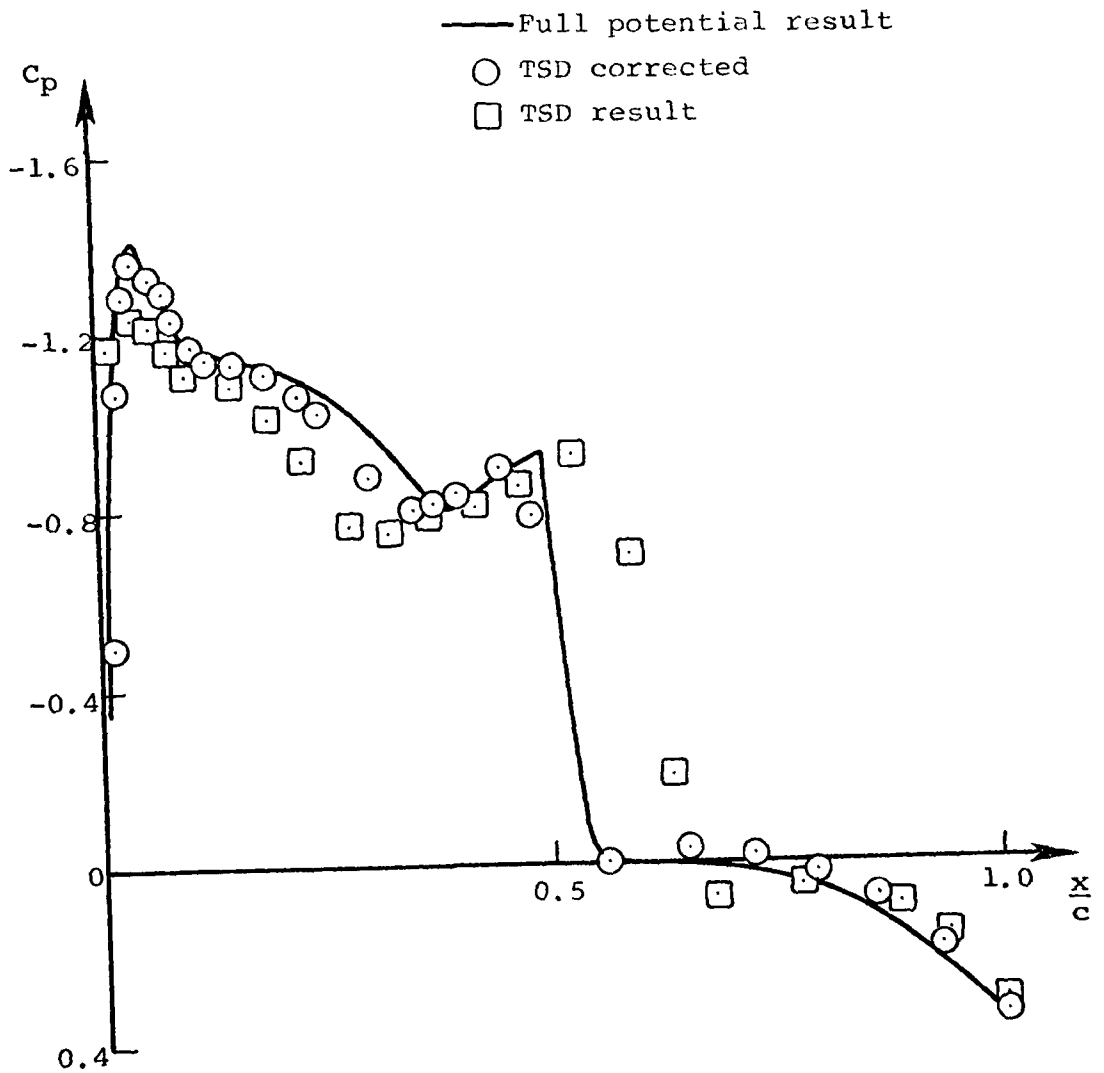

(c)

Figure 23.- Concluded.

$\eta = 0.0$

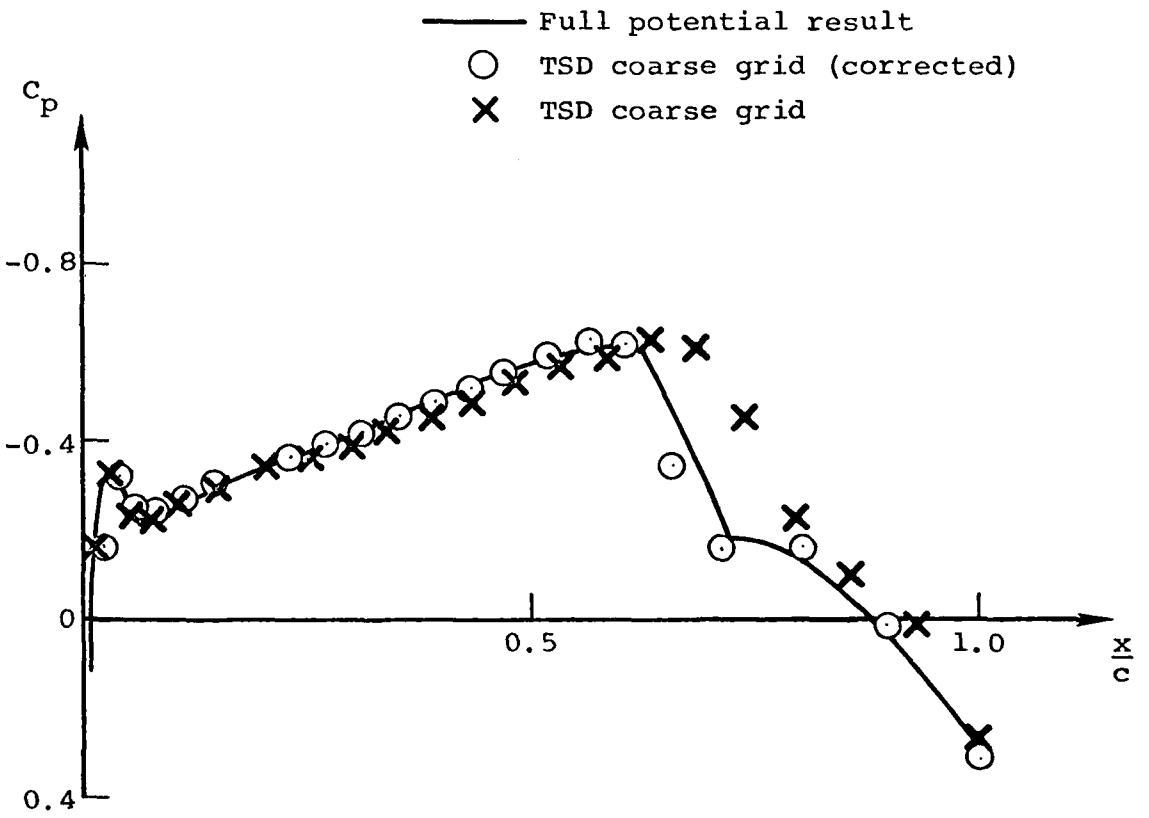

(a)

Figure 24.- Pressure distribution over the upper surface of the ONERA M6 wing; $M_\infty = 0.84$, $\alpha = 3.06$ (TSD coarse grid/full potential equation correction).

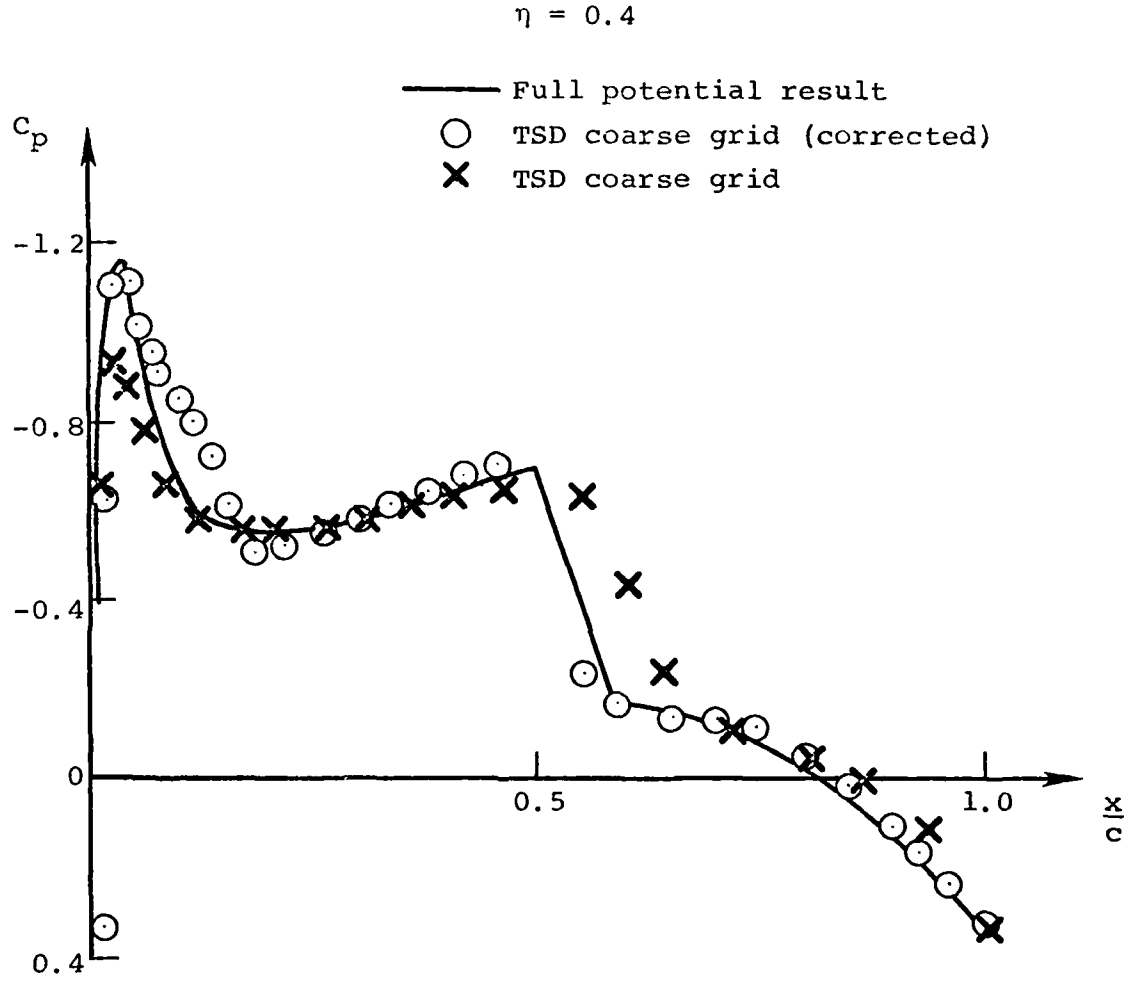

(b)

Figure 24.- Continued.

$\eta = 0.6$

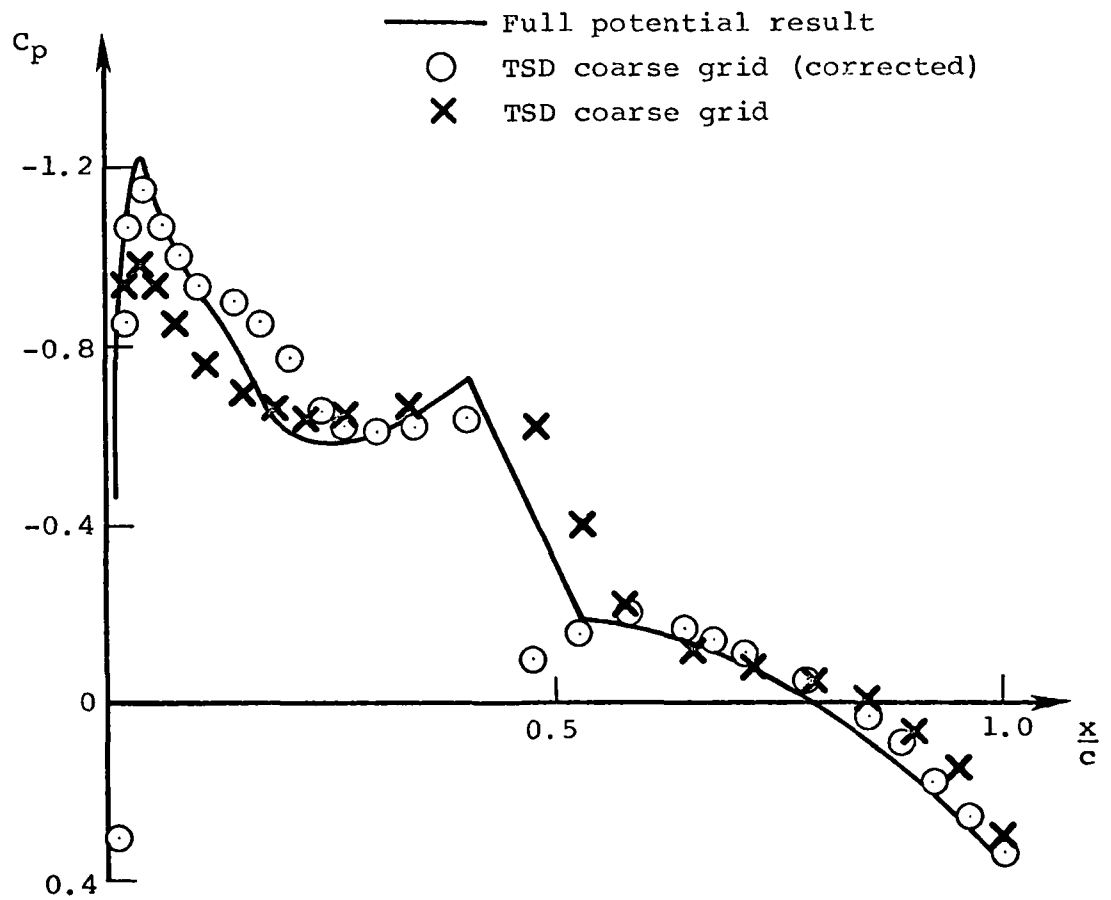

(c)

Figure 24.- Concluded.

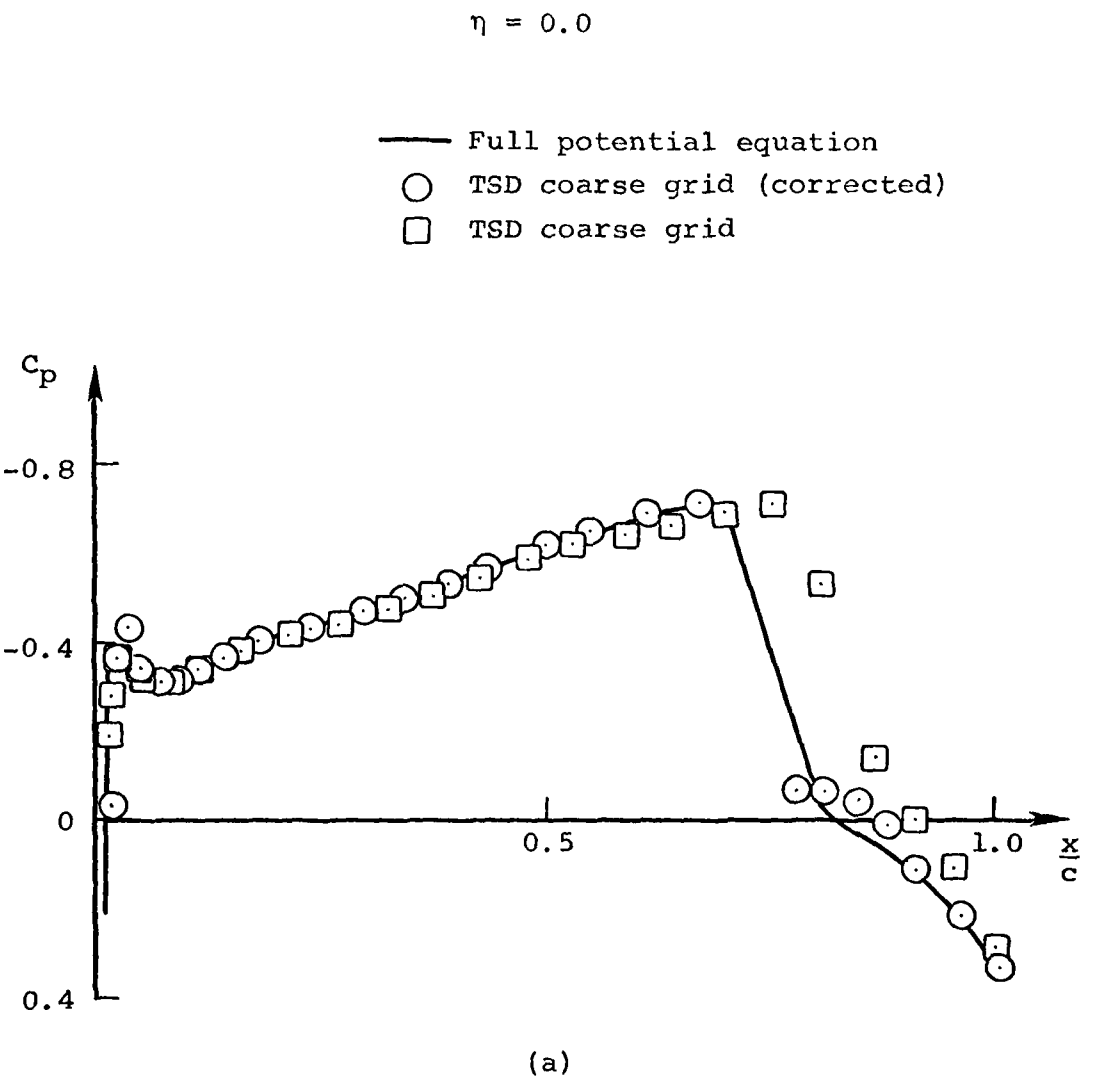

(a)

Figure 25.- Pressure distribution over the upper surface of the ONERA M6 wing; $M_\infty = 0.84$, $\alpha = 4^o$, $\theta_{twist} = 1.5^o$ (TSD coarse grid/full potential equation correction).

$\eta = 0.35$

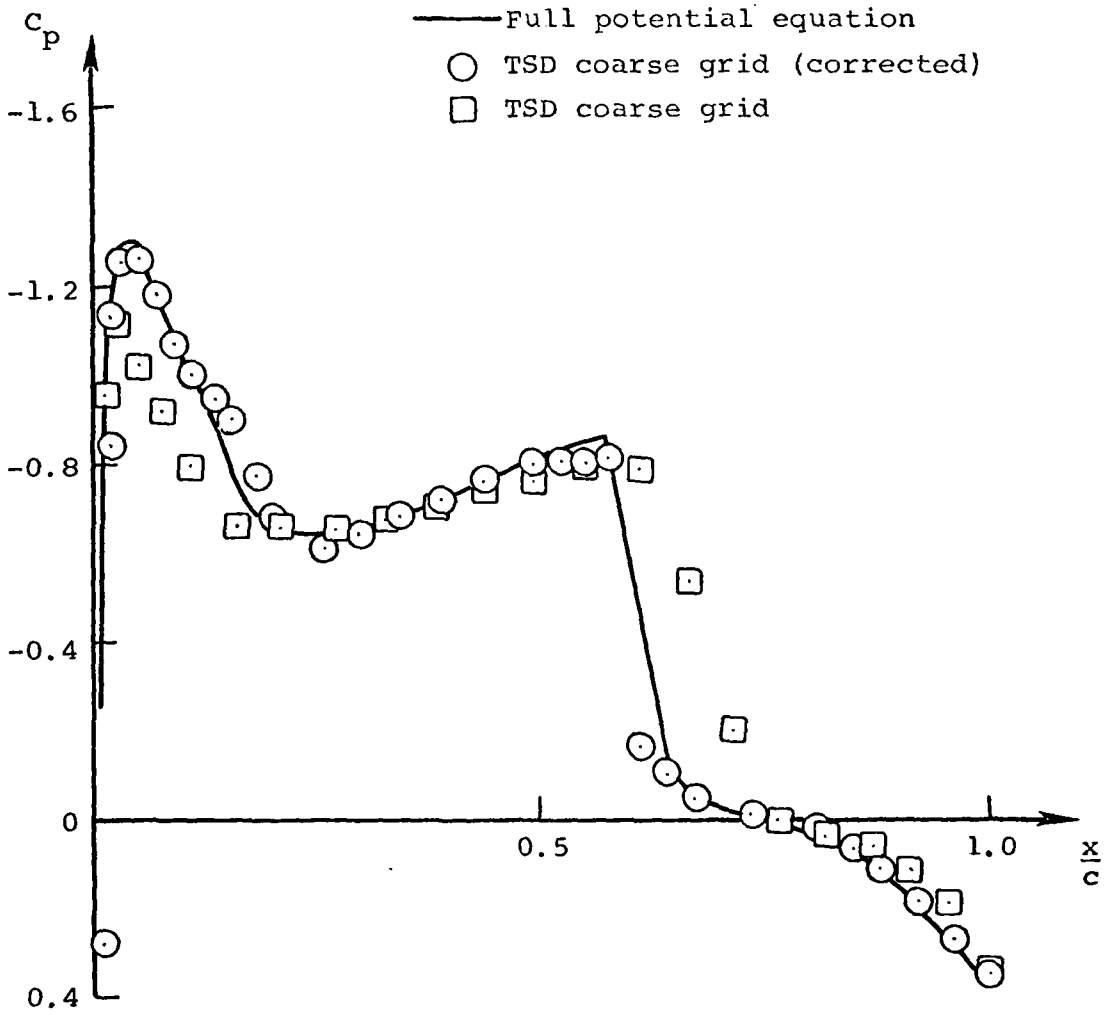

(b)

Figure 25.- Continued.

$\eta = 0.65$

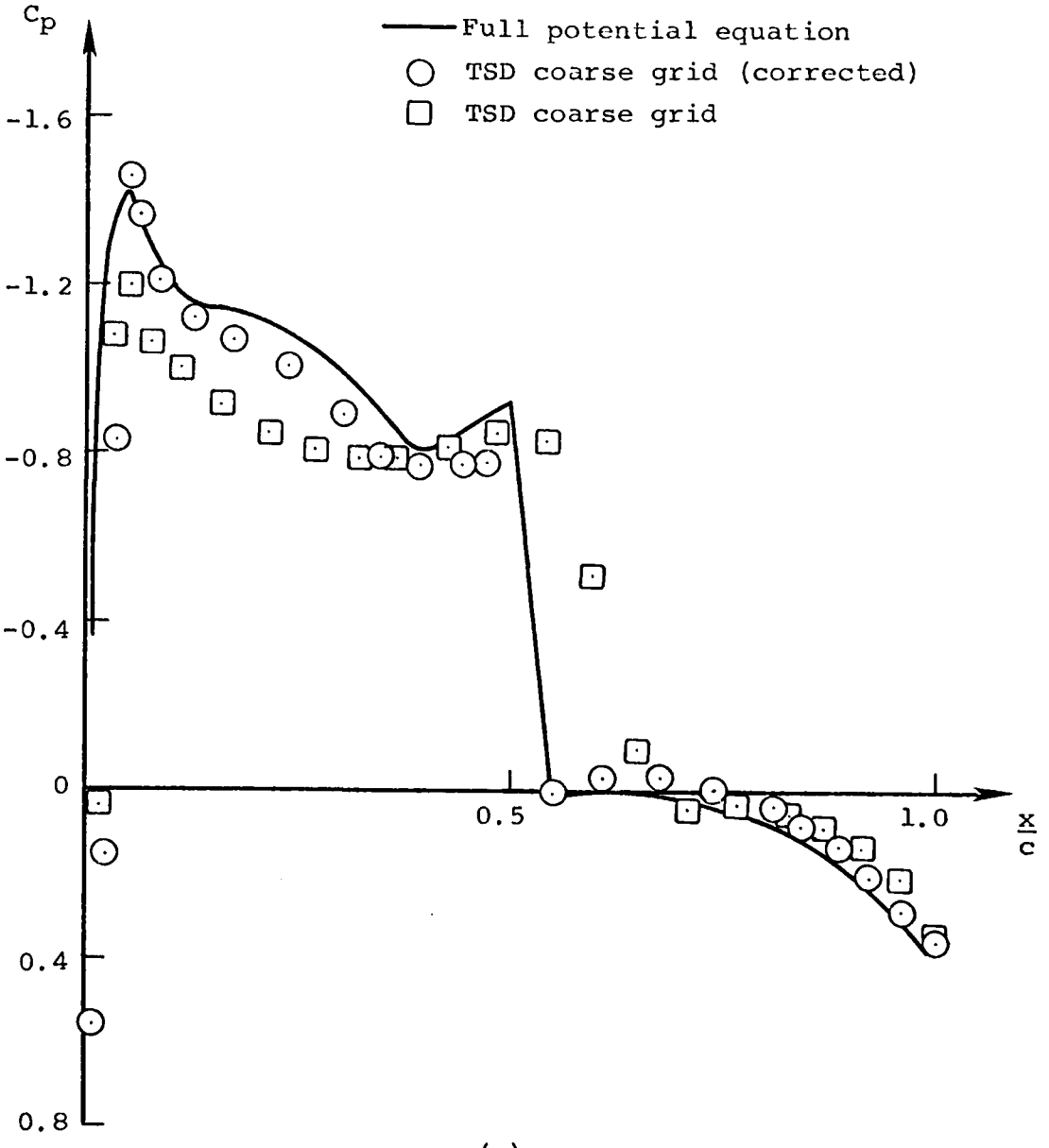

(c)

Figure 25.- Concluded.

APPENDIX A
OBSERVATIONS ON THE STRAINED COORDINATE METHOD FOR TRANSONIC FLOWS

By David Nixon*
Nielsen Engineering & Research, Inc.
Mountain View, California

Introduction

Recently papers[1,2] concerning a strained coordinate method for discontinuous transonic flow problems have appeared in the literature. In particular, the application of this technique for a linear interpolation or extrapolation between two known results has raised some questions regarding the relationship of the strained coordinate technique to normal interpolation procedures. Some confusion also seems to have occurred regarding the treatment of the Oswatitsch-Zierep[3] "shock foot singularity." It is the purpose of this note to examine these questions and (hopefully) finally resolve them.

Analysis

In figure 1 a typical velocity distribution, for transonic flow, u(x), is sketched. This is the curve ABCD. A shock wave is present, denoted by the line BC, with the shock foot singularity at the point C. At C the derivative $\frac{\partial u}{\partial x}$ is logarithmically singular. A second transonic flow related by some small parameter change to the first, is represented by the curve ABCD. The purpose of a linear interpolation procedure is to obtain a third

Index Categories: Transonic Flow; Analytical and Numerical Methods.
*Research Scientist, Associate Fellow AIAA

solution, A B" C" D from the first two (known) solutions.

Let the difference between the ABCD and AB'C'D solution be characterized by the small parameter ε_o and the difference between AB"C"D and ABCD characterized by ε. The shock locations C, C', C" are denoted by x_s', $\bar{x}_s$, x_s. In both the strained coordinate method and linear interpolation the new shock location is

$$x_s = x_s' + \frac{\varepsilon}{\varepsilon_o} (\bar{x}_s - x_s') \tag{1}$$

Consider now the velocity distribution u(x) in the region AB where no discontinuities or singularities appear. The strained coordinate method gives[2]

$$u(x) = u_o(x') + \frac{\varepsilon}{\varepsilon_o} [u_1(\bar{x}) - u_o(x')] \tag{2}$$

where $u_o(x')$ refers to ABCD, $u_1(\bar{x})$ refers to AB'C'D. The physical coordinate is x' and

$$\bar{x} = x' + \delta x_s x_1(x') \tag{3}$$

$$x = x' + \frac{\varepsilon}{\varepsilon_o} \delta x_s x_1(x') \tag{4}$$

where

$$\left.\begin{aligned} x_1(x') &= \frac{x'(1 - x')}{x_s'(1 - x_s')} \\ \text{and} \qquad \delta x_s &= \bar{x}_s - x_s' \end{aligned}\right\} \tag{5}$$

A normal linear interpolation procedure gives

$$u(x) = u_o(x) + \frac{\varepsilon}{\varepsilon_o} [u_1(x) - u_o(x)] \tag{6}$$

Now from equations (3) and (4)

$$x = x' + \frac{\varepsilon}{\varepsilon_o} \delta x_s x_1(x')$$

$$x = \bar{x} + \left(\frac{\varepsilon}{\varepsilon_o} - 1\right) \delta x_s x_1(x')$$

and thus, by a Taylor series expansion,

$$\begin{aligned} u_o(x) &= u_o(x') + \frac{\varepsilon}{\varepsilon_o} \delta x_s x_1(x') \frac{\partial u}{\partial x'} + \ldots \\ u_1(x) &= u_1(\bar{x}) + \left(\frac{\varepsilon}{\varepsilon_o} - 1\right) \delta x_s x_1(x') \frac{\partial u}{\partial \bar{x}} + \ldots \end{aligned} \tag{7}$$

Substitution of equation (7) into equation (6) and retaining only linear terms in δx_s and ε gives

$$\begin{aligned} u(x) = u_o(x') &+ \frac{\varepsilon}{\varepsilon_o} \left(\frac{\varepsilon}{\varepsilon_o} - 1\right) \delta x_s x_1(x) \left[\frac{\partial u}{\partial \bar{x}} - \frac{\partial u_o}{\partial x'}\right] \\ &+ \frac{\varepsilon}{\varepsilon_o} [u_1(\bar{x}) - u_o(x')] \end{aligned} \tag{8}$$

If, as will be the case in region AB,

$$\left[\frac{\partial u_1}{\partial \bar{x}} - \frac{\partial u_o}{\partial x'}\right] \sim \underline{0}\ (\varepsilon) \tag{9}$$

then the second term on the right of equation (8) can be neglected and it may be seen that the strained coordinate method and linear interpolation are equivalent. A similar equivalence occurs in the

region C'D provided the point in question is not too close to the singularity at C'. This would make $\frac{\partial u_1}{\partial \bar{x}}$ large compared with $\frac{\partial u_o}{\partial x'}$ and would invalidate the assumption of equation (9).

Consider now interpolation or extrapolation in the region BB'. An extrapolation for $u_o(x')$ can be made using a Taylor series expansion about some point x'_p close to B. Thus

$$u_o(x) = u_o(x'_p) + (x - x'_p)\left[\frac{\partial u_o}{\partial x'}\right]_{x_p} + \ldots \qquad (10)$$

A similar analysis to that previously given leads to the result

$$u(x) = u_o(x'_p) + \frac{\varepsilon}{\varepsilon_o}\left[u_1(\bar{x}) - u_o(x'_p)\right] + \frac{\varepsilon}{\varepsilon_o}\left\{\left[\frac{\varepsilon}{\varepsilon_o} - 1\right]\delta x_s x_1(x')\frac{\partial u_1}{\partial \bar{x}} - \Delta x_p\left[\frac{\varepsilon}{\varepsilon_o} - 1\right]\left[\frac{\partial u_o}{\partial x'}\right]_{x_p}\right\} \qquad (11)$$

If $\frac{\partial u_1}{\partial \bar{x}}$ and $\left[\frac{\partial u_o}{\partial x'}\right]_{x_p}$ are sufficiently close and if $\Delta x_p \sim \underline{0}\ [\delta x_s x_1(x')]$ then the third term in equation (11) is negligible and again the linear interpolation/extrapolation is equivalent to the strained coordinate method. A similar analysis can be applied to the region C"C' in which case if x'_p is close to C' $\left[\frac{\partial u_1}{\partial \bar{x}}\right]_{x_p}$ is very large and interpolation/extrapolation is not equivalent to the strained coordinate method since $\left[\frac{\partial u_1}{\partial \bar{x}}\right]_{x_p}$ would not be sufficiently close to the more regular $\frac{\partial u_o}{\partial x'}$ in C"C'. Indeed, it is difficult to see how C"C' can be obtained by linear interpolation/extrapolation would involve an expansion through the singularity at C'.

It is probably possible however to obtain a solution in CC' if the shock jump relations are used at B" to get values at C" and a higher order interpolation used in C'C".

Consider now the behavior of the strained coordinate method at the shock foot. The behavior of the velocity at C, C' is given by the form

$$u_1(\bar{x}) = u_1(\bar{x}_{s_-}) + \alpha_1(\bar{x} - \bar{x}_s)\ln(\bar{x} - \bar{x}_s)\varepsilon$$

$$u_o(x') = u_o(x'_s) + \alpha_o(x' - x'_s)\ln(x' - x'_s) \tag{12}$$

where $u_1(\bar{x}_{s_-})$, $u_o(x'_{s_-})$ are values at B' and B respectively and α_1, α_o are constants depending on the shock strength and the airfoil curvature. Using the strained coordinate method, equation (2), gives for values just downstream of C"

$$u(x) = u_o(x'_{s_-}) + \alpha_o(x' - x'_s)\ln(x - x'_s)$$

$$+ \frac{\varepsilon}{\varepsilon_o}\left\{u_1(\bar{x}_{s_-}) - u_o(x'_{s_-}) + \alpha_1(\bar{x} - \bar{x}_s)\ln(\bar{x} - \bar{x}_s)\right. \tag{13}$$

$$\left. - \alpha_o(x' - x'_s)\ln(x' - x'_s)\right\}$$

From equations (3) and (5) it can be seen that

$$(\bar{x} - \bar{x}_s) = x' - x'_s + \delta x_s(x_1(x') - 1)$$

If $(x' - x'_s) = \delta$ then, using equation (5),

$$(\bar{x} - \bar{x}_s) = \delta[1 + a(x')] \tag{14}$$

where

$$a(x') = \frac{\delta x_s(1 - x' - x'_s)}{x_s(1 - x_s)} \tag{15}$$

Substitution of equation (14) into equation (13) gives

$$u(x) = u_o(x_{s\_}) + \alpha_o \delta \ell n \delta + \frac{\varepsilon}{\varepsilon_o} \left\{ u_1(\bar{x}_{s\_}) - u_o(x'_{s\_}) \right.$$

$$\left. + \alpha_1 \delta [1 + a(x')] \ell n \delta [1 + a(x')] - \alpha_o \delta \ell n \delta \right\} \qquad (16)$$

Since δx_s is assumed small

$$\ell n \delta [1 + a(x')] \sim \ell n \delta$$

Then

$$u(x) = \left\{ u_o(x'_s) + \frac{\varepsilon}{\varepsilon_o} [u_1(\bar{x}_{s\_}) - u_o(x_{s\_})] \right\}$$

$$+ \left[\alpha_o + \frac{\varepsilon}{\varepsilon_o} \{\alpha_1 [1 + a(x')] - \alpha_o\} \delta \ell n \delta \right] \qquad (17)$$

The form of the singular part of u(x) at C" can be found by the above analysis to be

$$\alpha_2 \delta \left[1 + \frac{\varepsilon}{\varepsilon_o} a(x')\right] \ell n \delta \left[1 + \frac{\varepsilon}{\varepsilon_o} a(x')\right]$$

where α_2 is some constant.

Since a(x') is small this can be reduced to

$$\alpha_2 \left[\delta \ell n \delta + (\delta \ell n \delta) \frac{\varepsilon}{\varepsilon_o} a(x')\right]$$

Thus

$$\delta \ell n \delta \approx \delta \left[1 + \frac{\varepsilon}{\varepsilon_o} a(x')\right] \ell n \left\{ \delta \left[1 + \frac{\varepsilon}{\varepsilon_o} a(x')\right] \right\} \left[1 - \frac{\varepsilon}{\varepsilon_o} a(x')\right]$$

Substitution in equation (13) gives

$$u(x) = \left\{u_o(x'_s) + \frac{\varepsilon}{\varepsilon_o}\left[u_1(x_{s\_}) - u_o(x'_{s\_})\right]\right\}$$
$$+ \left[\alpha_o + \frac{\varepsilon}{\varepsilon_o}(\alpha_1 - \alpha_o) + \frac{\varepsilon}{\varepsilon_o}\left(1 - \frac{\varepsilon}{\varepsilon_o}\right)a(x')(\alpha_1 - \alpha_o)\right]$$
$$\times \delta\left[1 + \frac{\varepsilon}{\varepsilon_o}a(x')\right] \ell n\left\{\delta\left[1 + \frac{\varepsilon}{\varepsilon_o}a(x')\right]\right\} \qquad (18)$$

Since we are dealing in small perturbations it is obvious that $(\alpha_1 - \alpha_o)$ is small and hence the term $\frac{\varepsilon}{\varepsilon_o}(1 - \frac{\varepsilon}{\varepsilon_o})a(x')(\alpha_1 - \alpha_o)$ can be neglected in equation(18). It can then be seen that the strained coordinate system not only transfers the shock to its correct location, from equation (1), but also introduces the correct shock foot singularity with a strength $[\alpha_o + \frac{\varepsilon}{\varepsilon_o}(\alpha_1 - \alpha_o)]$, obtained by linear interpolation of the strengths at C, C'. Thus in the strained coordinate method the treatment of the shock foot singularity is consistent with the treatment of the smoother parts of the solution.

Conclusions

The strained coordinate interpolation method used for transonic flows has been compared with normal interpolation/extrapolation procedures. It is found that both methods are essentially equivalent in smooth regions of the solution. However, normal linear extrapolation does not appear to be applicable in the region just behind a shock wave where the acceleration is infinite. The strained coordinate method does move the shock, and its associated shock foot singularity to the correct location and scales the strength of the singularity according to linear interpolation.

Acknowledgement

This work was sponsored under AFOSR contract F49620-79-C-0053.

References

1. Nixon, D.: Perturbation of a Discontinuous Transonic Flow. AIAA J., Vol. 16, Jan. 1978, pp. 47-53.

2. Nixon, D.: Perturbations in Two- and Three-Dimensional Transonic Flow. AIAA J., Vol. 16, July 1978, pp. 699-710.

3. Oswatitsch, U. and Zierep, J.: Des Problem des Senkrechten Stassen an Eisen Geknumunten Wand. ZAMM, Vol. 40, Suppl., 1960, pp. 143-144.

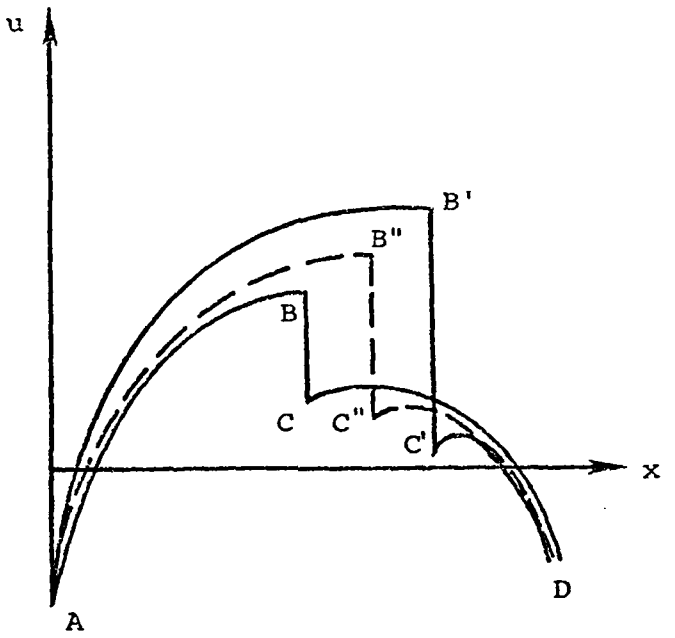

Figure 1.- Sketch of transonic velocity distribution on an airfoil.

APPENDIX B

COMMENTS ON THE EXISTENCE OF A "NEAR-BY" SOLUTION

In the preceding work the term "near-by solution" is used. The definition is very loose, being simply "a solution that has all the essential features of the basic solution." In this appendix an attempt is made to define a near-by solution on a quantitative basis.

Consider a differential operator, $L(\ )$ where

$$L(\phi) = 0 \tag{1}$$

Let an approximate representation of the system described by equation (1) be given by

$$L(\tilde{\phi}) + \varepsilon L_1(\tilde{\phi}) = 0 \tag{2}$$

where ε is a measure of the difference between approximate and exact solutions. $\tilde{\phi}$ is the solution to the approximate equation

$$L_2(\tilde{\phi}) = 0 \tag{3}$$

and $L_1(\ )$ is a differential operator. If

$$\phi = \tilde{\phi} + \varepsilon\phi' \tag{4}$$

where ε is a small parameter, then

$$L(\phi) = L(\tilde{\phi}) + \varepsilon\tilde{L}(\phi') + \ldots = 0 \tag{5}$$

where $\tilde{L}(\ )$ is a linear differential operator whose coefficients may be functions of $\tilde{\phi}$, and ϕ' is the correction to ϕ.

If equation (5) is subtracted from equation (2), then an expression for the correction ' is

$$\tilde{L}(\phi') = L_1(\tilde{\phi}) \tag{6}$$

Now let there be two solutions, a base solution, denoted by the subscript 1, and a near-by solution, denoted by the subscript 2. Thus, from equation (6)

$$\begin{aligned} \tilde{L}_1(\phi_1') &= L_1(\tilde{\phi}_1) \\ \tilde{L}_2(\phi_2') &= L_1(\tilde{\phi}_2) \end{aligned} \tag{7}$$

Subtraction of these equations give

$$\tilde{L}_1(\phi_1') - \tilde{L}_2(\phi_2') = L_1(\tilde{\phi}_1) - L_1(\tilde{\phi}_2) \tag{8}$$

Now generally in transonic flow problems $\tilde{L}(\ )$ is a mixture of first and second derivatives (no cross derivatives). Let $\tilde{L}(\ )$ be given by

$$\tilde{L}(\ ) \equiv \alpha(\tilde{\phi}) \frac{\partial^2}{\partial x^2} + \beta(\tilde{\phi}) \frac{\partial^2}{\partial y^2} + \gamma(\tilde{\phi}) \frac{\partial}{\partial x} + \delta(\tilde{\phi}) \frac{\partial}{\partial y} \tag{9}$$

The boundary condition for the perturbation equation, equation (6), is given by

$$\phi_y' = B \quad \text{on some boundary C} \tag{10}$$

The precise location of the boundary C may not be too critical; i.e., a mean surface boundary condition could be used.

Equations (8) and (9) can be combined to give

$$\alpha_1(\phi_1' - \phi_2')_{xx} + \beta_1(\phi_1' - \phi_2')_{yy} + \gamma_1(\phi_1' - \phi_2')_x + \delta_1(\phi_1' - \phi_2')_y$$

$$= (\alpha_2 - \alpha_1)\phi_{2xx}' + (\beta_2 - \beta_1)\phi_{2yy}' + (\gamma_2 - \gamma_1)\phi_{2x}'$$

$$+ (\delta_2 - \delta_1)\phi_{2y}' + L_1(\tilde{\phi}_1) - L_1(\tilde{\phi}_2) \tag{11}$$

with boundary conditions

$$(\phi_1' - \phi_2')_y \approx B_2 - B_1 \tag{12}$$

on some mean of C_1, C_2

If

$$\begin{aligned} &|\alpha_1 - \alpha_2| \ll |\alpha_1| \\ &|\beta_1 - \beta_2| \ll |\beta_1| \\ &|\gamma_1 - \gamma_2| \ll |\gamma_1| \\ &|\delta_1 - \delta_2| \ll |\delta_1| \\ &|B_1 - B_2| \ll |B_1| \\ &||L_1(\tilde{\phi}_1) - L_1(\tilde{\phi}_2)|| \ll ||L_1(\tilde{\phi}_1)|| \end{aligned} \tag{13}$$

where $||\ \ ||$ is some suitable norm for $L_1(\tilde{\phi})$, then equations (11) and (12) reduce to

$$\alpha_1\Phi_{xx}' + \beta_1\Phi_{xy}' + \gamma_1\Phi_x' + \delta_1\Phi_y' \approx 0 \tag{14}$$

$$\Phi_y' \approx 0 \tag{15}$$

where

$$\Phi' = \phi_1' - \phi_2'$$

The solution to equations (14) and (15) is

$$\phi' = 0$$

or

$$\phi_1' - \phi_2' = 0$$

Formally this implies

$$|\phi_1' - \phi_2'| << |\phi_1'|$$

which in turn implies that the correction ϕ_1' can be used for the problem denoted by subscript 2 provided in equation (13) is satisfied.

Example:

Consider the problem of truncation error in solutions of the TSD equation

$$B^2\phi_{xx} + \phi_{yy} = \phi_x\phi_{xx} \tag{16}$$

In this case

$$\begin{aligned} \alpha &= B^2 - \phi_x \\ \beta &= 1 \\ \gamma &= \tilde{\phi}_x \\ \delta &= 0 \end{aligned} \tag{17}$$

$$L_1(\tilde{\phi}) = \Delta x^2(B^2 - \tilde{\phi}_x)\frac{\partial^4\tilde{\phi}}{\partial x^4} + \Delta y^2\frac{\partial^4\tilde{\phi}}{\partial y^4}$$

Hence, the correction procedure is valid if

$$|B_1^2 - \tilde{\phi}_{1x} - B_2^2 + \tilde{\phi}_{2x}| << |B_1^2 - \tilde{\phi}_{1x}|$$

$$|\tilde{\phi}_{1x} - \tilde{\phi}_{2x}| << |\tilde{\phi}_{1x}|$$

$$\left|(B_1^2 - \tilde{\phi}_{1x}) \frac{\partial^4 \tilde{\phi}_1}{\partial x^4} - (B_2^2 - \tilde{\phi}_{2x}) \frac{\partial^4 \tilde{\phi}_2}{\partial x^4}\right| << \left|(B_1^2 - \tilde{\phi}_{1x}) \frac{\partial^4 \tilde{\phi}_1}{\partial x^4}\right|$$

$$\left|\frac{\partial^4 \tilde{\phi}_1}{\partial y^4} - \frac{\partial^4 \tilde{\phi}_2}{\partial y^4}\right| << \left|\frac{\partial^4 \tilde{\phi}_1}{\partial y^4}\right| \qquad (18)$$

The above formula are dependent on large gradients either vanishing or being constrained to the same location. The strained coordinate method takes account of the latter problem.

In practical applications it is assumed that the error bounds, equation (13), can be deduced from values on the airfoil surface. This does not seem unreasonable.

APPENDIX C

TRANSONIC SMALL DISTURBANCE THEORY WITH STRONG SHOCK WAVES

David Nixon*
Nielsen Engineering & Research, Inc.

Introduction

The most common methods of predicting aerodynamic characteristics at transonic speeds are either the Transonic Small Disturbance (TSD) theory[1] or the Full Potential Equation theory[2] (FPE). The more accurate Euler equation solutions[3] are expensive to obtain although for flows with strong shock waves such solutions are essential. The FPE theory requires that the flow is irrotational and treats the wing boundary conditions exactly (numerically). The TSD theory is an approximation to the FPE theory. One advantage of the TSD theory is the flexibility in deriving the approximate equation. This flexibility is generally utilized by a choice of a transonic scale parameter. The basic assumption of irrotationality in both these theories is only valid when the flow is shock free or contains only weak shocks. Both TSD and FPE solutions are in satisfactory agreement with realistic Euler equation solutions provided that the basic restriction to weak shock waves is not violated. The thin wing boundary conditions can also introduce errors into the TSD

Index Categories: Transonic Flow; Analytical and Numerical Methods.
*Research Scientist, Associate Fellow AIAA.

solutions. If the flow has strong shock waves, however, then there is considerable disagreement among all three theories. Generally the predicted shock locations for the potential theories are much further aft than for the Euler equations. The problem addressed in this paper is to examine the error in the shock location in the TSD theory in two-dimensional flow and to derive a correction procedure within the confines of small disturbance theory. The basic hypothesis of the present theory is that the error in shock location is primarily due to the stronger shock strength predicted by TSD theory compared to that of the Euler equations. The technique uses two TSD solutions with different scaling parameters and an interpolation scheme derived for discountinuous transonic flows to give a corrected shock strength.

Analysis

The TSD equation for the perturbation velocity potential, $\phi(x,y)$, at a free-stream Mach number M_∞, is

$$(1 - M_\infty^2)\phi_{xx} + \phi_{yy} = (\gamma + 1)M_\infty^q \phi_x \phi_{xx} \qquad (1)$$

where γ is the ratio of specific heats and q is the transonic scaling parameter. The two most commonly used[4] values of q are 2 (Spreiter scaling) and 1.75 (Krupp scaling). The pressure coefficient $c_p(x,y)$ is

$$c_p(x,y) = -2\ \phi_x(x,y) \qquad (2)$$

Associated with Eq. (1) are the usual tangency and far field boundary conditions. The weak shock jump conditions for Eq. (1) are

$$[\![\left(1 - M_\infty^2 - (\gamma + 1)M_\infty^q \phi_x\right)\phi_x]\!] + \tan \phi_s \; [\![\phi_y]\!] \tag{3}$$

where $[\![\;]\!]$ denotes a jump through a shock wave and ϕ_s is the angle between the shock normal and the x-axis. For a shock normal to the free stream the shock strength, σ_T, is defined as

$$\sigma_T = C_p^- - C_p^+ = -2(C_p^+ - C_p^*) \tag{4}$$

where C_p^+, C_p^- are the pressure coefficients just ahead of and behind the shock and

$$C_p^* = \frac{-2(1 - M_\infty^2)}{(\gamma + 1)M_\infty^q} \tag{5}$$

Consider now the Euler equation normal shock jump, σ_E, in terms of M_∞ and C_p^+ which is given[5] by

$$\sigma_E = \frac{2\gamma}{\gamma + 1}(M_e^2 - 1)\left(\frac{2}{\gamma M_\infty^2} + C_p^+\right) \tag{6}$$

AD-A081 531 NIELSEN ENGINEERING AND RESEARCH INC MOUNTAIN VIEW CALIF F/G 20/4
DEVELOPMENT OF PERTURBATION PROCEDURES FOR NONLINEAR INVISCID A--ETC(U)
JAN 80 D NIXON F49620-79-C-0054
UNCLASSIFIED NEAR-TR-214 AFOSR-TR-80-0129 NL

2 OF 2
AD A081531

END
DATE FILMED
3-80
DDC

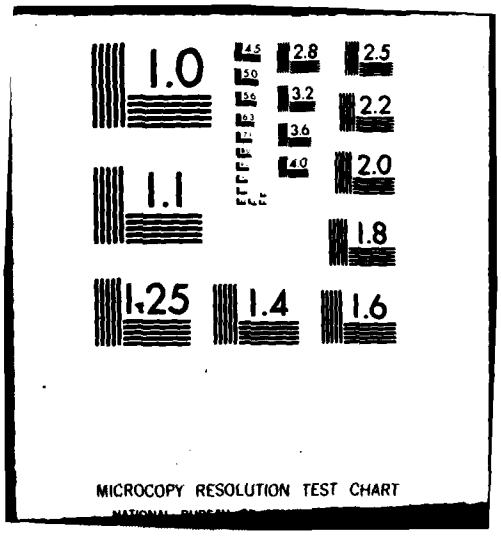
1.0
1.1
1.25
1.4
1.6
1.8
2.0
2.2
2.5
2.8
3.2
3.6
4.0
4.5
5.0
5.6
6.3
7.1
8.0
9.0
MICROCOPY RESOLUTION TEST CHART

where the upstream shock Mach number M_e is given by

$$M_e^2 = \frac{1}{(\gamma - 1)} \left\{ [2 + (\gamma - 1)M_\infty^2] / \left[\frac{(\gamma - 1)}{2} M_\infty^2 C_p^+ + 1 \right]^{\frac{\gamma}{\gamma - 1}} - 2 \right\} \tag{7}$$

Eqs. (4) and (6) are shown for $M_\infty = 0.755$ in figure 1 and it can be seen that as $|C_p^+|$ increases the discrepancy between σ_T and σ_E increases. Note that different transonic scalings not only give a different value of C_p^* but generally a different value of C_p^+. Thus, for different scalings the shock strength may vary considerably.

The error in the shock location in the TSD solutions seems to be primarily due to the error in the shock strength as exhibited in figure 1. If the TSD equation is altered, still within it's formal accuracy bounds, such that the shock jump approximates the Euler equation shock jump then the resulting equation is a better compromise in representing the actual flow. The reason for this statement is that by matching the shock jump the new equation implicitly introduces an additional mechanism, formally negligible, that cancels the rotationality errors in a potential formulation.

If the correct shock strength is known and if two TSD solutions with different scalings are also known then a TSD solution with correct shock strength may be estimated using a

linear combination of the known solutions. Thus, if σ_{T_1} and σ_{T_2} are the shock strengths of the TSD solutions, then a parameter ε can be found such that

$$\sigma_E = \sigma_{T_1} + \varepsilon(\sigma_{T_2} - \sigma_{T_1}) \tag{8}$$

where σ_E is the estimated Euler equation shock strength. If ε is known then the pressure distribution can be found using the strained coordinate method[6]. Thus,

$$C_p(x,y) = C_{p_1}(x',y) + \varepsilon[C_{p_2}(\bar{x},y) - C_{p_1}(x',y)] \tag{9}$$

where $C_{p_1}(x,y)$, $C_{p_2}(x,y)$ are the pressure coefficients from the TSD solutions and

$$\begin{aligned} \bar{x} &= x' + \delta x_{s_o} x_1(x') \\ x &= x' + \varepsilon(\bar{x} - x') \end{aligned} \tag{10}$$

where δx_{s_o} is the change in shock location between first and second TSD solutions. The function $x_1(x')$ is usually taken[6] to be

$$x_1(x') = \frac{x'(1 - x')}{x_s(1 - x_s)}$$

where x_s is the shock location for the first TSD solution.

The main problem now is to estimate the shock strength σ_E. This is given by Eq. (6) if C_p^+ is known. In TSD solutions Spreiter scaling gives good agreement[4] for moderately strong shocks and Krupp scaling gives good agreement for weak shocks. Hence it seems reasonable to take C_p^+ to be the average of the Spreiter and Krupp values of the preshock pressure coefficients. However, the justification for this choice really lies in the accuracy of the final results. Hence, given σ_E from Eqs. (6) and (7) the surface pressures can be found from Eqs. (8), (9), and (10).

Results

The present method was first tested for a weak shock example, namely the flow over the NACA 64A006 airfoil at zero angle of attack and $M_\infty = 0.875$, to see if the present method would give the accurate Krupp scaling. This result is compared to an Euler equation result[7] in figure 2 and it can be seen that, apart from the shock capture characteristics, the present method does agree satisfactorily with both the Euler solution and the Krupp solutions. An example for a flow with a strong shock is shown in figure 3. In figure 3 the flow around a Korn airfoil at $M_\infty = 0.755$ and 1.7° angle of attack is compared to an Euler equation[8] solution and it can be seen that the agreement of the shock location predicted by the present method is satisfactory, although there is an error in the leading edge, which is almost certainly due to the use of thin airfoil boundary

conditions in the TSD theory. Incidently, if Spreiter scaling is used, the TSD result is almost coincidental with the present result.

Concluding Remarks

A method to effectively choose a transonic scaling to place shock waves computed by small disturbance theory at the location predicted by Euler equation solutions has been developed. The technique does effectively correct the shock location although discrepancies in the leading edge region still persist. This is probably due to the use of thin wing boundary conditions.

Acknowledgement

This work was sponsored by AFOSR Contract No. F49620-79-C-0054.

References

1. Murman, E. and Krupp, J. A.: Computation of Transonic Flows Past Lifting Airfoils and Slender Bodies. AIAA Journal, Vol. 10, No. 6, 1972, pp. 880-886.

2. Jameson, A.: Transonic Potential Flow Calculations Using Conservation Form. Proceedings AIAA 2nd Computational Dynamics Conference, 1975, pp. 148-161.

3. Magnus, R. and Yoshihara, H.: Calculations of Transonic Flow Over an Oscillating Airfoil. AIAA Journal, Vol. 13, No. 12, 1975, pp. 1622-1628.

4. Ballhaus, W. F.: Some Recent Progress in Transonic Flow Computations. VKI Lecture Series: Computational Fluid Dynamics, von Kármán Institute for Fluid Dynamics, 1976.

5. Liepmann, H. and Roshko, A.: Elements of Gas Dynamics. (Wiley), 1957.

6. Nixon, D.: Perturbation of a Discontinuous Transonic Flow. AIAA Journal, Vol. 16, No. 1, 1978, pp. 47-52.

7. Magnus, R. and Yoshihara, H.: The Transonic Oscillating Flap A comparison of Calculations with Experiment. AGARD Conf. Proceedings, No. 226. Unsteady Airloads in Separated and Transonic Flow, 1977.

8. Deiwert, G. S.: Private Communication, 1979.

LIST OF FIGURES

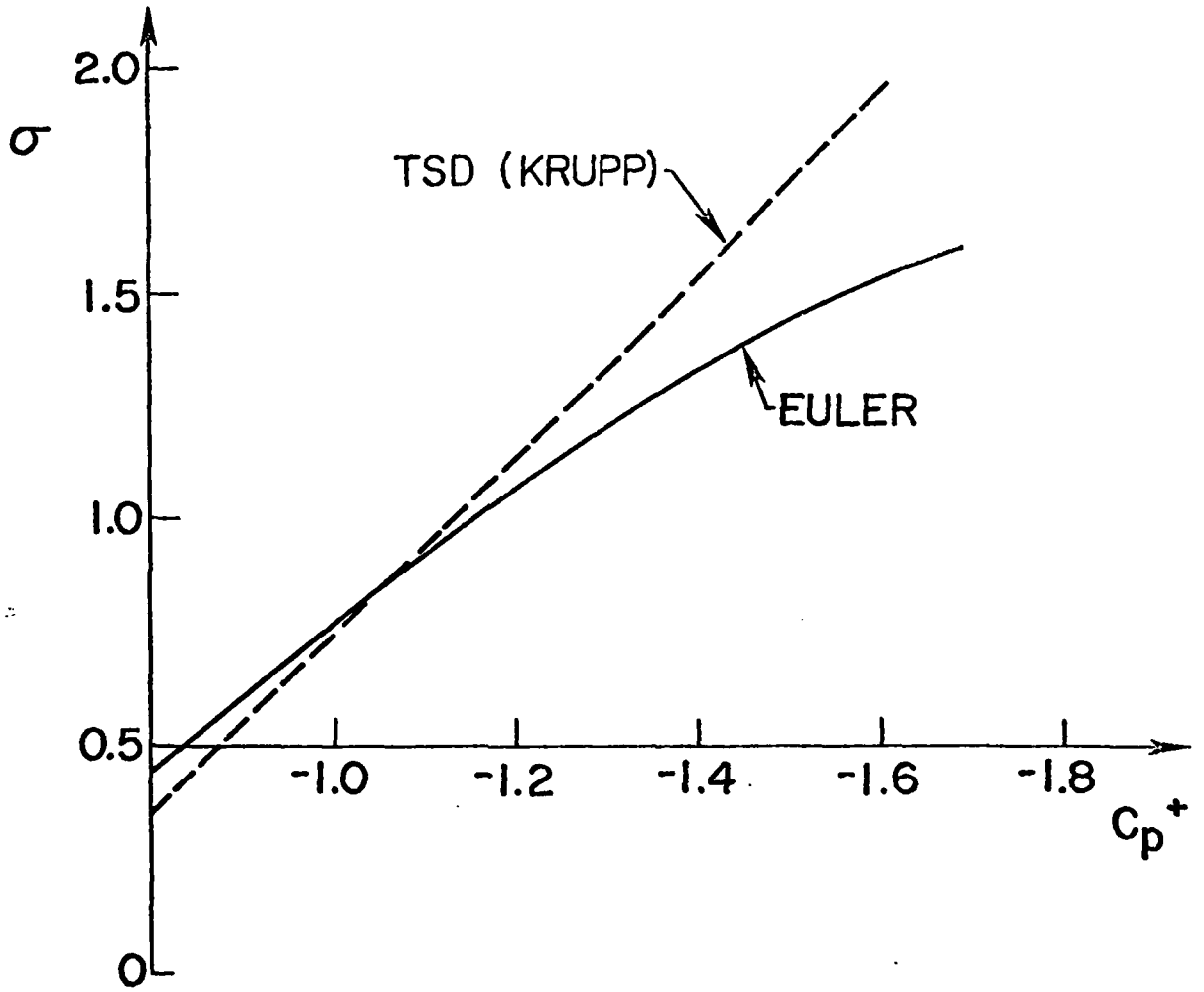

David Nixon
Figure 1

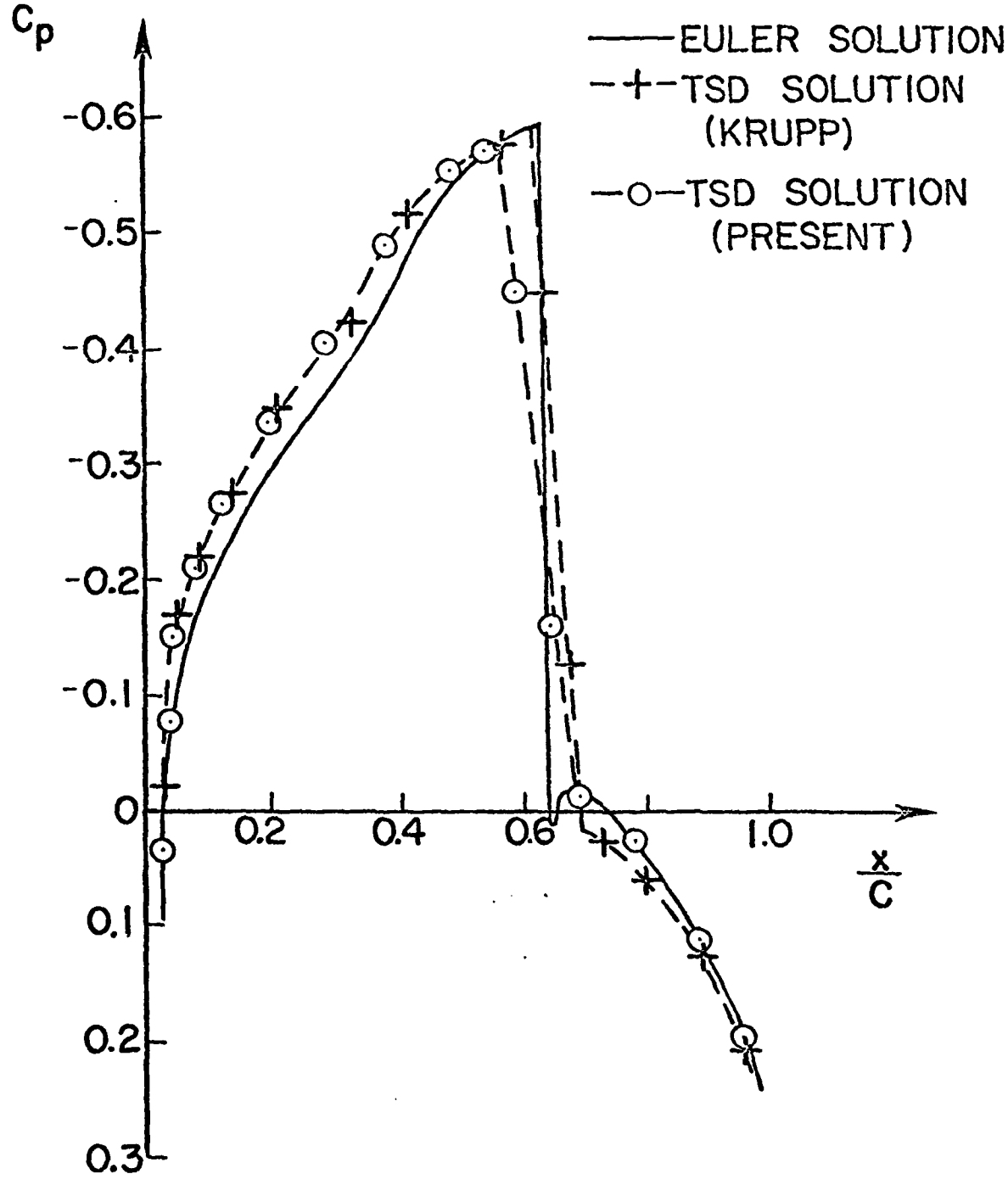

David Nixon

Figure 2

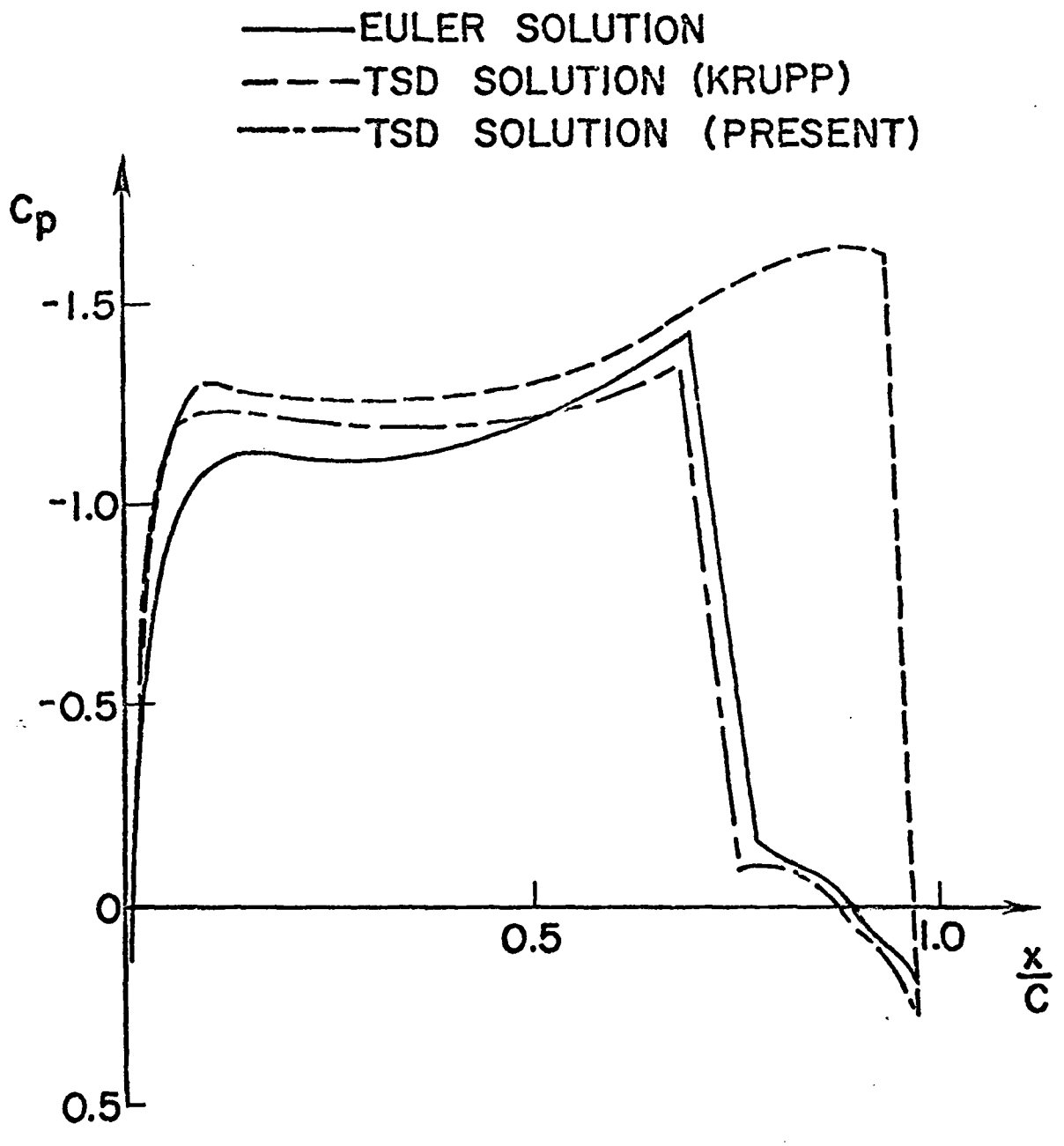

David Nixon
Figure 3